

# Multi-Spectral Analysis Of Frying Processes For Meat Products

Søren Blond Daugaard

Kongens Lyngby 2007

Technical University of Denmark  
Informatics and Mathematical Modeling  
Building 321, DK-2800 Kongens Lyngby, Denmark  
Phone +45 45253351, Fax +45 45882673  
[reception@imm.dtu.dk](mailto:reception@imm.dtu.dk)  
[www.imm.dtu.dk](http://www.imm.dtu.dk)

## Preface

---

This thesis project has been carried out at the Institute for Informatics and Mathematical Modeling (IMM), Technical University of Denmark (DTU). The thesis text documents the 30 ECTS (European Credit Transfer System) points project carried out by Søren Blond Daugaard under supervision of Ph.D. Jens Michael Carstensen and Dr. Techn. Jens Adler-Nissen.

The main goals of the project are to analyze properties in relation to the frying process of various meat products, using multi-spectral imaging. The frameworks for the analyses performed are multivariate statistics and conventional digital image analysis.

Kgs. Lyngby - June 2007

---

Søren Blond Daugaard



# Acknowledgements

---

I would like to express my sincere gratitude to my supervisor Ph.D. Jens Michael Carstensen for introducing me to the field of multi-spectral imaging, and for his support and contribution of ideas throughout the project period. Likewise it would like to thank Dr. Techn. Jens Adler-Nissen for his support, commitment and show of enthusiasm for the project and the results obtained.

Also I would like to thank Rene Thrane and Preben Bøje Hansen for help and guidance in the pilot plant and laboratory.

Lastly a special thanks to family, friends and inhabitants of kitchen 19 for their support, and contributions to the project.

# Summary

---

This project examines the possibility to assess a number of quality parameters of the frying process for meat using multi-spectral vision technology. The project examines the possibility of creating measures for the frying-treatment of minced beef and diced turkey, and the agglutination of minced beef.

## **Frying-Treatment Assessment**

It is extremely important to provide adequately processed minced beef and diced turkey to the end customer, among others since under processed meat comes with several health risks. Furthermore it is important to be able to assess the frying-treatment not only as raw and fried, but also based on the quality of the fried meat. E.g. it is important for turkey diced to have an attractive fried surface, but also still to have a juicy kernel.

This project proposes a method for assessment of frying-treatment of the meat contained in a multi-spectral image, based on conventional image analysis and multivariate statistics. This method provides a measure, not only concerning raw or fried meat, but just as well the quality of the fried meat as evaluated by experts. Furthermore the thesis proposes a visualization method, which transforms a multi-spectral image to a RGB image, clearly showing the frying degree of each meat piece / granule contained in the image.

### **Agglutination of minced beef**

When frying minced beef using the continuous wok, a specially developed method is used to prevent agglutination. This method requires the meat to be frozen, when entered into the wok; if the meat fails to meet this requirement agglutination occurs. Agglutination in fried minced meat is unwanted as high quality minced beef should contain somewhat homogenous sized granules and no large meat lumps. Apart from the visual effects the large lumps can also lead to them being under processed, which obviously is unwanted.

Using the images from each spectral band, a method is proposed creating a number of measures of agglutination from each image. These measures include mean meat granule size, maximum granule size encountered and number of meat granules per cm<sup>2</sup>. All of these measures have been examined and compared to the physical measure of strainer loss, from which it can be concluded that these can be used as measures of agglutination.

Generally measures are proposed for all quality parameters examined. The proposed methods are not ready for production, as each method should be re-designed for the specific application, but they surely create a basis for future work. I believe this is a step towards the automated frying-process, eliminating the need for constant monitoring by an experienced process operator.

# Résumé

---

Dette projekt undersøger muligheden for at fastsætte en række kvalitets parametre for stegeprocessor af kød, ved hjælp af multi-spektral billedanalyse. Projektet undersøger muligheden for at, opsætte mål for graden af stegningen af hakket oksekød og kalkun i tern, samt agglutinationen af hakket oksekød.

## **Graden af stegning**

For både hakket oksekød og kalkun i tern, er det ekstremt vigtigt at kunden får kød der er gennemstegt, bl.a. fordi understegt kød kan medføre risiko for sygdomme etc.. Endvidere er det vigtigt at kunne vurdere det stegte kød ikke blot som rå og stegt, men baseret på kødets kvalitet. F.eks. er det vigtigt for en kalkun tern, at den har en tiltrækkende stegt overflade men stadig har en saftig kerne.

I dette projekt er foreslået en metode der ved hjælp af konventionelle billedanalyse teknikker og multivariant statistik kan give et mål for stegningen af kødet indeholdt i et billede. Denne metode kan give et mål, der adskiller kød ikke blot på baggrund af rå eller stegt, men baseret på kvaliteten af kødet vurderet af eksperter. Endvidere er der foreslået en visualiserings metode, der transformere et multi-spektral billede til et RGB billede, hvor kød stykkerne tydeligt er markeret efter hvilken grad af stegning der er opnået.

### **Agglutinationen af hakket oksekød**

Ved stegning af hakket oksekød i den kontinuerte wok bruges en speciel udviklet metode, der forebygger agglutination af kødet. Denne metode kræver at kødet er frossent når det indføres i wokken, hvis dette ikke er tilfældet opleves der agglutination af kødet. Agglutination af kødet er uønsket da godt stegt hakket oksekød, bør have en nogenlunde homogen sammensætning af størrelsen af kød granuler og ikke indeholde store klumper af kød. Udover den visuelle effekt kan store klumper også medføre at de ikke bliver gennemstegt, hvilket selvfølgelig er uønsket.

Ved hjælp af billederne af de forskellige spektrale bånd, er der foreslået en metode til at udtrække en række mål for agglutination fra hvert billede. Disse mål inkluderer den gennemsnitlige størrelse af kød granulerne i billedet, størrelsen af den største granule fundet samt kød stykker pr. cm<sup>2</sup>. Alle disse mål er blevet undersøgt nærmere, og det kan konkluderes at disse kan bruges som mål for agglutinationen.

Generelt set er der foreslået metoder til at estimere alle kvalitets parametre undersøgt. De foreslået metoder er ikke klar til produktion, da alle metoder bør tilpasses den specifikke applikation de er tiltænkt. Dog er det et skridt på vejen mod en automatiseret stegeproces, uden behov for konstant overvågning af en erfaren procesoperatør.

# Table of Contents

---

Preface	iii
Acknowledgements	v
Summary	vi
Résumé	viii
Chapter 1 Prologue	14
1.1 Motivation .....	15
1.2 Overview - a Readers Guide.....	16
I Domain Description	17
Chapter 2 Terminology Listing	18
2.1 Abbreviations .....	19
Chapter 3 Involved Actors	20
3.1 BioCentrum .....	21

---

3.2	Institute of Informatics and Mathematical Modeling.....	21
Chapter 4	Equipment Used	22
4.1	VideometerLab 2.....	23
4.2	Matlab.....	24
4.3	The continuous wok.....	25
II Theory		27
Chapter 5	Multi-spectral Imaging	28
5.1	Multi-spectral images.....	29
5.2	Spectrum measurements.....	30
5.3	False color composition.....	31
Chapter 6	Digital Image Analysis	32
6.1	Enhancement filters .....	33
6.2	Mathematical morphology .....	35
Chapter 7	Multivariate Statistics	41
7.1	Principal Component Analysis.....	42
7.2	Canonical Discriminant Analysis.....	45
7.3	Regression Analysis .....	47
7.4	Analysis of Variance .....	50
Chapter 8	Meat Chemistry	53
8.1	Stir frying .....	54
8.2	Meat pigments.....	54
8.3	The Millard reaction .....	56
8.4	Fibrous Tissue.....	56
III Data Analysis		57
Chapter 9	Assessment of Frying Treatment for Minced Beef	58
9.1	Sample preparation.....	59
9.2	Chemical experiment.....	60
9.3	Pre-Processing.....	61
9.4	Preliminary spectrum comparison.....	64
9.5	Multivariate analysis.....	65
9.6	Visualization.....	71
9.7	Discussion.....	72
Chapter 10	Agglutination of Minced Beef	73

10.1	Sample preparation .....	74
10.2	Physical / chemical experiments .....	75
10.3	Pre-processing .....	77
10.4	Assessing agglutination .....	77
10.5	Analyzing results .....	84
10.6	Discussion .....	87
Chapter 11	Assessment of Frying Treatment for Diced Turkey	88
11.1	Sample preparation .....	89
11.2	Chemical experiment .....	90
11.3	Pre-processing .....	91
11.4	Preliminary analysis .....	93
11.5	Multivariate analysis .....	94
11.6	Visualization .....	99
11.7	Discussion .....	100
Chapter 12	Assessment of Frying Treatment for Sliced Diced Turkey	102
12.1	Sample preparation .....	103
12.2	Chemical experiments .....	103
12.3	Pre-processing .....	103
12.4	Preliminary analysis .....	105
12.5	Multivariate analysis .....	106
12.6	Visualization .....	111
12.7	Discussion .....	112
Chapter 13	Reducing Spectral Bands	114
13.1	Reducing for Frying Treatment Assessment .....	115
13.2	Reducing for Agglutination Assessment .....	122
13.3	Discussion .....	123
IV	Epilogue	125
Chapter 14	Conclusion	126
Chapter 15	Putting into perspective	129
	Bibliography	130
	Table of figures	132
V	Appendix	135
Appendix A	VideometerLab 2 – Wavelength table	136

---

Appendix B	Experiment Design January (Danish)	138
Appendix C	Results Moisture Contents January Experiment	140
Appendix D	Visualization Results – Minced Meat	142
Appendix E	Experiment Design March (Danish)	145
Appendix F	Results Moisture Contents March Experiment	148
Appendix G	Results measures of agglutination	150
Appendix H	Experiment Design April (Danish)	153
Appendix I	Results Moisture Contents April Experiment	157
Appendix J	Visualization results – Diced Turkey	159
Appendix K	Visualization results – Sliced Diced Turkey	162
Appendix L	Poster and presentation for 2007 Vision Day	165
Appendix M	A Method for Frying Treatment Assessment of Minced Meat Using Multi-Spectral Imaging (Article)	168
Appendix N	New Vision Technology for Multidimensional Quality Monitoring of Continuous Frying of Meat (Article) Draft	173
Appendix O	DVD	187

# Chapter 1 Prologue

---

This thesis concerns multi-spectral image analysis of frying processes in meat products. The main focus of the thesis is to assess various quality parameters for the meat frying process, using multi-spectral vision technology. The estimation of the quality parameters is thought to replace or be a supplement to the experienced process operators.

The analysis presented throughout this thesis is based on multi-spectral images of food products, processed with state-of-the-art reproducible frying methods, developed at the centre for Food Production Engineering at BioCentrum. The images are acquired using the VideometerLab 2 multi-spectral camera, recording images in bands from 405[nm] to 970[nm], thereby covering the ultra blue, the visible and the near-infrared (NIR) bands.

The use of multi-spectral imaging for quality assessment of food product has been proven possible in various different contexts. In [8] multi-spectral imaging is used for determination of oxidation in minced turkey patties, in [9] multi-spectral imaging is used for meat color evaluation of salami, water barrier estimations for biscuits and water contents estimation in bread and in [12] multi-spectral imaging is used for detection of oxidation in cheese.

## 1.1 Motivation

This section provides an overview of the products examined and the motivation for examining these products.

### **Minced beef**

BioCentrum at DTU has developed a patented, state-of-the-art method for industry scale frying of minced meat. In connection with developing this method, and the continuous wok, BioCentrum wants to explore possibility of monitoring certain properties using vision technology, minimizing the use of experienced process operators to continuously monitor the process. Furthermore vision technology has obvious advantages over conventional chemical or visual inspection methods. Vision technology provides a non-destructive and reproducible way of continuously examining a product; this compared to a conventional sample method saves both time and money and increases the quality of end product.

The basic idea is for the vision technology to be able to replace or be a supplement to an experienced process operator. The properties examined for minced beef are the degree of frying treatment and the agglutination of meat.

### **Diced turkey meat**

The continuous wok, developed at BioCentrum DTU, also enables high quality frying of turkey meat in a sliced or diced form, as known from various oriental stir-fried dishes. In this context BioCentrum wants to explore the possibility of monitoring a continuous production of diced turkey using vision technology.

The process parameter to examine for turkey meat is the frying treatment. Compared to minced beef, the diced turkey meat however has some different properties and requirements. As the turkey meat is in dices and not minced, the meat might be at different frying stages down the meat lump, meaning the internal kernel might be under-processed at same time as the external layers are adequately processed. To examine this the diced turkey forms the basis for two types of examination, namely frying treatment assessment of diced turkey based on images of the surface, and frying treatment assessment based on sliced diced turkey, meaning the dices have been physically preprocessed before imaging, by slicing them into two pieces. This will enable us to examine, if the images of the surface are able to assess the frying treatment as well as by using images of the interior, thereby enabling a continuous monitoring without any physical interaction.

## 1.2 Overview - a Readers Guide

The readers guide will provide an overview of the document structure. Here the various parts of the document are described, thus giving the reader a quick introduction to the various parts and providing a tool for effective reading the document.

### **I - Domain Description**

The domain description is setting the scene for the project. It includes a description of all involved actors in this project, their goals, interest and involvement with respect to the project. Furthermore it describes the equipment and tools used throughout the project, to obtain and analyze the multi-spectral images.

### **II - Theory**

The theory part will populate the scene set; describing the relevant theory used in the analysis of the multi-spectral images and introduces the relevant chemistry of meat in order to create a foundation for analyzing and interpreting the results of the multi-spectral analysis.

As the intended audience of this thesis text has different backgrounds ranging from biotechnologists to vision experts, the theory part tries to cover the areas from the basics and up. This means vision experts are able to skip to chapters explaining the basics in image analysis without losing continuity, whereas biotechnologists might gain insight from reading those.

### **III - Data Analysis**

The data analysis part of the report performs the act using the scene populated by the theory. This part includes five chapters, the first four each describing one of the analyses performed in the thesis project, and the last examining the possibility to optimize the analyses by reducing the input data needed.

The first four chapters can be read in random order, but it is advised to read them in chronological order to get continuity. The first four must be read before reading the last chapter in order to fully understand the methods and purpose.

### **IV - Epilogue**

The epilogue evaluates the act; it contains the final conclusion and discussion of the results gained throughout the thesis project. Furthermore it contains a section where the project is put into perspective, commenting on the results gained and suggesting areas for further work.

Lastly the epilogue contains reference to the literature used for the project, and a table of figures included in the thesis text.

I

# Domain Description

## Chapter 2      Terminology Listing

---

This chapter includes a list of the terminologies and abbreviations used throughout the thesis text. The table is included to increase similarity and consistency throughout the different chapters.

## 2.1 Abbreviations

The abbreviations used throughout thesis text are given below in lexicographical order.

ANOVA	ANalysis Of VAriance
CDA	Canonical Discriminant Analysis
CDF	Canonical Discriminant Function
CV	Cross Validation
DTU	Technical university of Denmark.
ECTS	European Credit Transfer System
FPE	The Food Production Engineering Centre at BioCentrum
FTS	Frying Treatment Score
HIPS	Hyper-spectral Image Processing System
IACG	The Image Analysis and Computer Graphics group at IMM
IMM	Department of informatics and mathematic modeling, at the technical university of Denmark
LOO	Leave One Out Cross Validation
LSE	Least Squares Estimator
MB	Mega-Byte
MSE	Mean Squared Error
MSI	Multi-spectral imaging
NIR	Near-Infrared Reflectance
OLS	Ordinary Least Squares
PC	Principal Component
PCA	Principal Component Analysis
RGB	Red Green Blue
RMSE	Root Mean Squared Error
ROI	Region-Of-Interest
SS	Sum of Squares

## Chapter 3      Involved Actors

---

This chapter briefly describes the institutes and centers at DTU which have been involved in this thesis project. Their contribution to the project is lined up as well as the goals of their involvement.

## 3.1 BioCentrum

BioCentrum, the largest institute at DTU, provides research and education in area of sustainable, environmentally friendly and competitive processes for the biotechnical industry and the food production industry.

This thesis was done in cooperation with the research centre of *Food Production Engineering (FPE)* at BioCentrum. The FPE's main research interest areas are heat treatment processes and their effect on food quality. The FPE is contributing to this project by providing access and guidance to the continuous work, and providing expert knowledge in food processing and food quality parameters. FPE is supporting this project, to gain increased knowledge of the possibilities of using vision technology for continuously monitoring of frying processes.

## 3.2 Institute of Informatics and Mathematical Modeling

The institute of *informatics and mathematic modeling (IMM)* at DTU provides research and educations in the areas of mathematical modeling and computer science. IMM mainly focus their research on specific problems in the production industry and financial world.

The thesis work was carried out in cooperation with the *Image Analysis and Computer Graphics (IACG)* group at IMM. The IACG group has a wide range of research area from geo-informatics to medical image analysis. The IACG contributes to this project by providing expert knowledge and tools related to multi-spectral image analysis and industrial vision control. Furthermore IMM provides office space and technical equipment. IMM is supporting this project in order to gain increased knowledge about the application areas of multi-spectral vision technology.

## Chapter 4      Equipment Used

---

This chapter will describe the equipment used to carry out the thesis work. This includes describing the equipment used for acquiring and analyzing image data, as well as describing the relevant equipment used to process the various meat products.

All equipment for image analysis has been provided by IMM, and all equipment for meat processing has been provided by BioCentrum.

## 4.1 VideometerLab 2

VideometerLab 2 is a combination of a multi-spectral camera for laboratory analysis, and the accompanying software for image acquisition and analyses.

### 4.1.1 Camera

The VideometerLab 2 camera was used to acquire all image data used in the thesis. The camera is able to measure light intensity of an object in wavelengths spanning from the Ultra-blue to the Near-Infrared spectrum (NIR). The complete listings of wavelengths are given in Table 4.1, for examples of application areas please refer to the full listing in Appendix A.

Band	Wavelength [nm]	Color	Band	Wavelength [nm]	Color
1	430	Ultra Blue	10	700	Red
2	450	Blue	11	850	NIR
3	470	Blue	12	870	NIR
4	505	Green	13	890	NIR
5	565	Green	14	910	NIR
6	590	Amber	15	920	NIR
7	630	Red	16	940	NIR
8	645	Red	17	950	NIR
9	660	Red	18	970	NIR

Table 4.1 - VideometerLab camera 2 - Wavelength

To ensure a total diffuse illumination of the object without shading and reflection, the camera is equipped with an Ulbricht sphere. The Ulbricht sphere is hollow sphere, internally painted with a diffuse reflecting paint, and an opening in the top and underside of the sphere. The top hole is used for placing the camera, whereas the bottom hole is used to place the image object. The camera with the characteristic Ulbricht sphere is shown in Figure 4.1.



Figure 4.1 - VideometerLab 2 Camera

When acquiring an image the sphere is run down encapsulating the object, thereby ensuring no false light is illuminating the object. Following diodes of different wavelengths, placed in the rim of the sphere, will illuminate the object in turn while the camera is acquiring images.

As the entire camera setup is quite complex, it requires calibration in order to ensure reducibility of the images. The VideometerLab 2 software can be used to calibrate the camera.

## 4.1.2 Software

Accompanying the VideometerLab 2 camera is the VideometerLab software package. This software is primarily used for calibrating the camera and acquiring images. However an upgrade of the license can be purchased, transforming the software package into a powerful image analysis tool.

The upgraded software package not only includes conventional image analysis tools for segmentation and enhancing features in greyscale images. The tool also includes a *transformation builder*, which enables the use of well-known multi-spectral transformations as principal component analysis, maximum autocorrelation factor and canonical discriminant analysis. Furthermore the software package includes tools to apply segmentation procedures or transformations batch wise to a large number of images, reducing the time needed having to apply them manually on each image.

### 4.1.2.1 Camera calibration

To ensure the highest possible reproducibility of images, it is important to calibrate the camera before acquiring images. The calibration is a crucial part of using the camera since small variations in physical conditions, such as temperature, can cause the camera to lose calibration.

Calibrating the camera uses three different plates fitting into underside opening of the sphere, a black, white and patterned plate.

In addition to the camera calibration, the illumination should also be setup when changing the image object. This is needed to prevent saturation of pixels thereby ensuring high quality images of any object calibrated with.

## 4.2 Matlab

Along with analyzing the images in the VideometerLab software, Matlab is used for custom designed procedures, analyses which are not available in the VideometerLab software and for batch processing larger amounts of images.

Matlab is short for Matrix Laboratory, and provides an excellent platform for working with matrixes. As images and multivariate statistics are easily defined in matrix form, Matlab is the obvious choice. Furthermore Matlab provides an image processing toolbox, including a large variety of well-known image processing procedures. In addition to the Matlab image processing toolbox, Videometer provided a Multi-spectral image processing package, including procedures to perform transformations and visualizations.

One of Matlabs drawbacks is poor memory management. This is especially a problem when working with multi-spectral images, as they usually take up more than 80mb per image. The memory problems can be overcome by regular reboots.

### 4.3 The continuous wok

Developed at BioCentrum-DTU to enable the scale-up of the stir frying process, the continuous wok has shown to be a powerful tool in industry scale food production. One of the main advantages of the continuous wok is the large numbers of application areas, such as stir-frying of numerous types of vegetables and meat products for industry scale production. Other advantages of the continuous wok are low fat contents in the end-product, preservation of vitamins and abilities to re-heat frozen products on a normal frying pan, while preserving the nice properties introduced by the continuous wok process.

The principle of the continuous wok as shown in Figure 4.2 is a horizontal placed thick-walled tube containing a helix with scrapers attached. The scrapers prevent the product being fried from sticking to the surface, resulting in increased heat treatment and increasing the risk of being burned. The helix is connected to an electric motor with adjustable speed, enabling regulation of the frying time. The tube is heated by gas burners placed with regularly spacing below the tube, thus ensuring equal temperatures over the entire tube. The gas burners are regulated to obtain a constant frying temperature.

When frying a product, it is being entered into the wok in the inlet funnel, from where it is continuously transported to the outlet port by the helix. Beneath the outlet port is a conveyor belt from where it can be collected. The wok prototype used in the pilot plant, measures 1.6 meter in length and 0.2 meter in diameter.

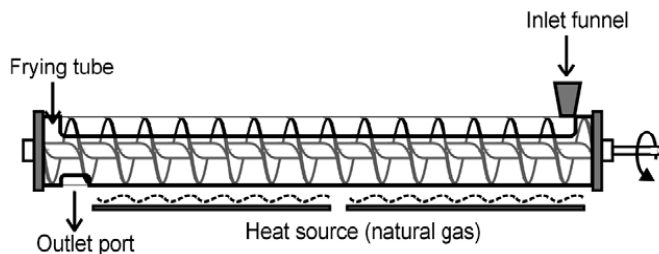


Figure 4.2 - The continuous wok



II

Theory

## Chapter 5      Multi-spectral Imaging

---

This chapter contains an introduction to multi-spectral imaging and the basic concepts and methods. The chapter will further introduce the notation and notion of images and concepts used throughout the thesis text.

This chapter is intended for persons without specialized knowledge of multi-spectral imaging; professionals should however skim the chapter in-order to capture the notation and notion used.

## 5.1 Multi-spectral images

Multi-spectral, or hyper-spectral images, are images acquired in a range of different wavelengths. Wavelengths often ranging from the visible to non-visible wavelengths, compared to conventional imaging only capturing information in the visible spectrums. The obvious advantage of multi-spectral images is the ability to detect properties, which are not usually visible for the human eye. Examples of such properties could be water and fat contents, and oxidation level. As multi-spectral images are different from conventional RGB images, this chapter will introduce the notion and notation used for such images.

### 5.1.1 Notation

A multi-spectral image can be perceived as a 3D matrix, where the two first axes represent the well known geometric image axes in an image (row and columns), and the third axis represents the number of bands the image consists off. This essentially means having a single grayscale image for each band available in the image.

Let  $\underline{I}$  denote the entire image matrix,  $r$  and  $c$  represents the rows and columns in the image and  $b$  the spectral bands, thus giving a size of the matrix to be  $r \times c \times b$ . A specific item in  $\underline{I}$  can then be referred to as  $i_{r,c,b}$ ; this concept is illustrated in Figure 5.1.

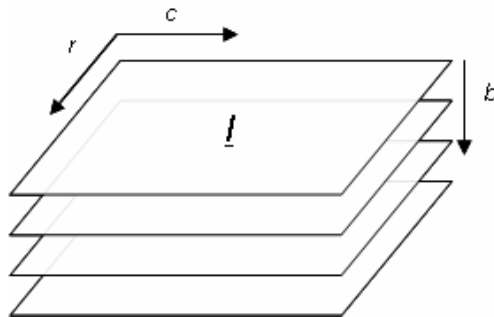


Figure 5.1 - Matrix storage concept

### 5.1.2 Transforming for statistics

Having defined the image matrix, it comes clear it cannot be directly applied to conventional multivariate statistics, since conventional multivariate statistics requires the data to be transformed into a two dimensional matrix.

This is since a statistical variables are usually not presented in a two dimensional space, but rather as a vector of observations of a variable. For multi-spectral images each band is thought as a variable, making the transformation of the entire image matrix into a two dimensional

matrix straightforward. This is done by simply combining the rows and columns keeping the division into spectral bands (variables). Thus giving a resulting matrix with the dimensions  $r \times c$  and  $b$ .

Obviously this transformation removes the spatial information from the bands, making the analysis only dependent on spectral variables. If needed it is however straightforward to reconstruct the spatial information, as long as one of the geometrical dimensions of the image is known. This concept is illustrated in Figure 5.2.

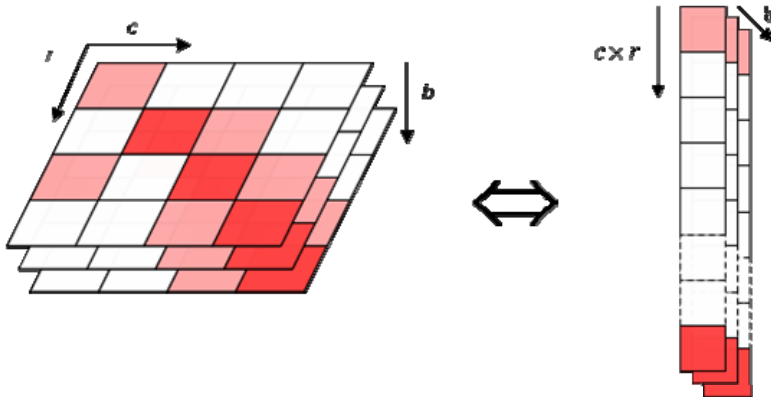


Figure 5.2 - 2D transformation concept

## 5.2 Spectrum measurements

Having a multi-dimensional image with wavelengths associated with each dimension, makes it possible to plot a spectrum for interesting parts of image. A spectrum is normally plotted as the values of a single pixel, or as the mean values of a region-of-interest. For a region-of-interest the standard deviation can be plotted as well, thereby given an impression of the deviation over the region. In Figure 5.3 is shown an example spectrum of a single meat pixel and a region-of-interest (ROI) plotted with the mean value and the standard deviation.

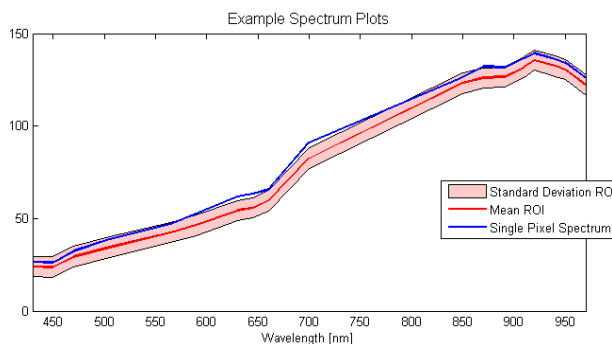


Figure 5.3 - Example spectrum plot

## 5.3 False color composition

The nature of a multi-spectral image makes it difficult to interpret by the human eye, if it were to perceive all available wavelengths at once. Instead false color composition can be used to display features otherwise not-visible for the human eye.

The basic idea in false color composition is to extract specific bands or results from an analysis and assign a color to each band or feature extracted, thus giving an RGB image illustrating the results, such that it is easier for the human eye to perceive the features not normally visible.

In Figure 5.4 a combination of regular RGB and false color composition is used to illustrate the frying degree of sliced diced turkey squares. The blue areas represent under processed meat and the red areas over processed meat, from the image it is clear that these samples contains an under-processed kernel, but has a somewhat adequately processed external layer.

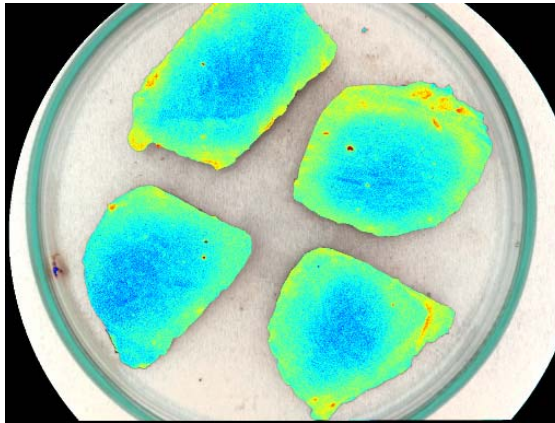


Figure 5.4 - False color composition for identifying frying treatment

Using false color composition often comes with the problem of having different intensities in each band resulting in one band dominating the others. This problem can be overcome by scaling each band thereby getting a somewhat equal contributing from each band/analysis result.

## Chapter 6      Digital Image Analysis

---

This chapter will introduce some basic image analysis tools and methods used throughout the thesis. This chapter is included for readers without prior knowledge of digital image analysis; it can be skipped for readers with basic knowledge of digital image analysis without losing continuity.

These methods presented are general image analysis methods for 2 dimensional images, but are easily performed on 3 dimensional multi-spectral images by simply applying them to either one spectral band at a time or applying them on selected spectral bands.

## 6.1 Enhancement filters

This section will describe enhancement filters as they are presented in [13]. The section starts by introducing the basics in filters, from where it moves on to describe a number of relevant and commonly used filters. The section focuses on enhancement filters, which, as the name implies, are used to enhance features in an image in order to clarify these for human or machine interpretation.

### 6.1.1 Filter basics

A digital filter for image processing can be described as a linear system  $S$ .  $S$  is considered a black box, which when applied with an input  $f(x)$  produces an output that is described as  $g(x) = S(f(x))$ . For simplicity the image is, for now, represented in one dimension, thus giving:

$$f(x) \rightarrow S \rightarrow g(x) \quad (6.1)$$

From this definition as a linear system, certain properties are inherited namely that it is linear and shift invariant. Having the linear system the description of the output can be expanded using the following integral:

$$g(x) = \int f(t)h(x-t)dt \quad (6.2)$$

This integral is called the convolution integral and can be expressed as  $g = f * h$ . For the digital form we are dealing with, it is described as a summarization instead of an integral.

$$g(i) = \sum_{k=\infty-}^{\infty+} f(k)h(i-k) \quad (6.3)$$

For 6.2 and 6.3 the function  $h$  is called the impulse response. Although the borders of the function  $h$  are defined to be infinite, it usually is set to zero outside a defined range. Having this in mind, and expanding  $h$  to be two-dimensional (as an image), the equation can now be expanded to:

$$g(i, j) = \sum_{k=i-w}^{i+w} \sum_{l=j-v}^{j+v} f(k, l)h(i-k, j-l) \quad (6.4)$$

From the equation it can now be derived that the value of  $g(i, j)$  becomes a weighted sum of the pixels surrounding within a certain distance. The weight of each pixel is defined by  $h$ , which also can be referred to as the filter weights, filter mask or filter kernel. The size and weights of  $h$  varies from filter application to filter application. Figure 6.1 is illustrating an example of equation 6.4 in use.

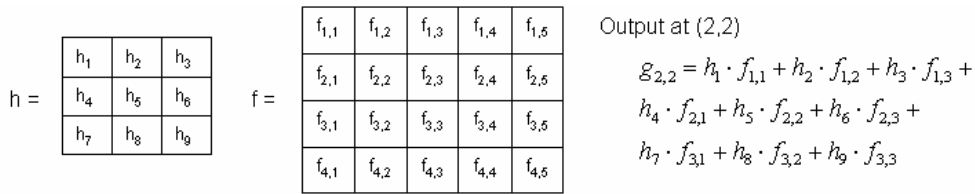


Figure 6.1 - Basic filter operation

Using this basic notion of a filter, it can be further expanded for filters in image processing. Since images are not blocked by physical properties,  $h$  can be defined arbitrarily and even changed over the image, thus resulting in a large flexibility and a large amount of useful filters.

### 6.1.2 Example filters

This section will describe a number of typical filters, along with their typical kernels, used in digital image processing.

#### Mean filter

The mean filter is a simple filter calculating the mean over a selected area. The size of the filter can be chosen to fit the application.

<i>Square shaped</i>	<i>Plus shaped</i>
$\frac{1}{9} \quad \frac{1}{9} \quad \frac{1}{9}$	$\frac{1}{5}$
$\frac{1}{9} \quad \frac{1}{9} \quad \frac{1}{9}$	$\frac{1}{5} \quad \frac{1}{5} \quad \frac{1}{5}$
$\frac{1}{9} \quad \frac{1}{9} \quad \frac{1}{9}$	$\frac{1}{5}$

#### Weighted Mean filter

A weighted mean filter is a mean filter with varying weights often related to the distance from the center pixel.

<i>Square shaped</i>	<i>Plus shaped</i>
$\frac{1}{16} \quad \frac{1}{8} \quad \frac{1}{16}$	$\frac{1}{6}$
$\frac{1}{8} \quad \frac{1}{4} \quad \frac{1}{8}$	$\frac{1}{6} \quad \frac{1}{3} \quad \frac{1}{6}$
$\frac{1}{16} \quad \frac{1}{8} \quad \frac{1}{16}$	$\frac{1}{6}$

#### Mode filter

The mode filter replaces the pixel by its most common neighbor. This can be useful for classification purposes, where a mean filter doesn't make sense. E.g. the average of two pixels of the class *poultry meat* and four pixels of the class *beef* would not make sense, but

---

classifying it as beef most likely would.

---

### Median filter

---

The median filter replaces the pixel by the median of the neighborhood pixels. The size can be defined as it is found suitable. It should be noted that unlike most of the other filters this needs a sorting mechanism in implementation and can therefore prove to be slow with large kernel sizes and large images.

---

### $K$ nearest neighbor filter

---

The nearest neighbor filter replaces the pixel with the average of the  $k$  pixels, which values are closest to the pixel in question. E.g. having a  $3 \times 3$  filter with 6 nearest neighbors, means taking the average of the 6 pixels which value are closest to the pixel in question, discarding the remaining three pixel values.

## 6.2 Mathematical morphology

Morphology is said to be *the study of forms and structure*; mathematical morphology is an approach for the study of spatial forms and structures in digital images. This section focused on mathematical morphology of binary images, and from there moves the presented methods into the gray scale domain.

### 6.2.1 Binary morphology

As claimed in [13], an image can be considered a set  $S$  having the objects of the image as the subset  $X \subset S$ . Using the set definition, it enables the use of set concepts and modifiers such as union, intersection, translation etc. and enables us to identify the properties of transformations such as anti-extensive, increasing, idem-potency and homo-topic. This section will not focus on the mathematical theory, since this is out of the thesis texts scope. Instead it will introduce the most common operations and concepts, starting with the simple translation. The translation is introduced since this forms a basis for understanding the other concepts introduces. Translating the set  $X$  with a vector  $h$  can be defined as:

$$X_h = \{z \in S \mid \exists x \in X : z = x + h\} \quad (6.5)$$

As it is observed the translation simply move the objects in an image based on the translation vector  $h$ .

In order to define further operations the *structuring element* ( $B$ ) is introduced, for the translation in equation 6.5, the structuring element can be said to be translation vector. However normally

the structuring element is a set of points centered on an origin. The use and importance of the structuring element will become apparent when introducing the common operators, but generally it is said that *the structuring element is to morphology what the filter kernel is to filtering*.

### 6.2.1.1 Dilation

One of the basic operators in morphology is *dilation*. Dilation of the set of objects  $X$  with the structuring element  $B$  is defined as:

$$X \oplus B = \bigcup_{b \in B} X_b \quad (6.6)$$

Meaning dilation enlarges the image  $X$  depended on the structuring element in use. An example is given below.

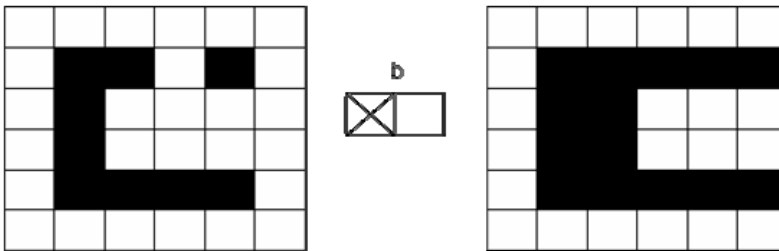


Figure 6.2 - Dilation example

### 6.2.1.2 Erosion

Intuitively introduction of the dilation, motivates the introduction of an opposite operation, namely the *erosion*. Erosion of a set  $X$  with the structuring element  $B$  is defined as:

$$X \ominus B = \bigcap_{b \in B} X_{-b} \quad (6.7)$$

Erosion causes the image to shrink depended on the structuring element in use. An example of erosion is shown below.

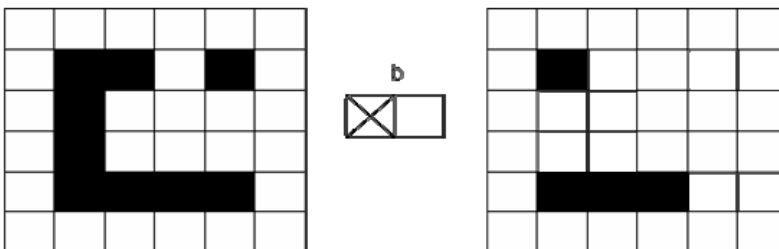


Figure 6.3 - Erosion example

Having defined these two basics operations, they enable the introduction of two other useful operations opening and closing.

### 6.2.1.3 Opening and Closing

Opening and closing are defined using the basic operators of *erosion* and *dilation* introduced in the prior section.

*Opening* is defined as:

$$X \circ B = X_B = (X \ominus B) \oplus B \quad (6.8)$$

First image is eroded with B and the resulting image is then dilated with B. It can be hard to envision the outcome from the definition above, but generally opening is said to separate the particles in the image.

An example is given here:

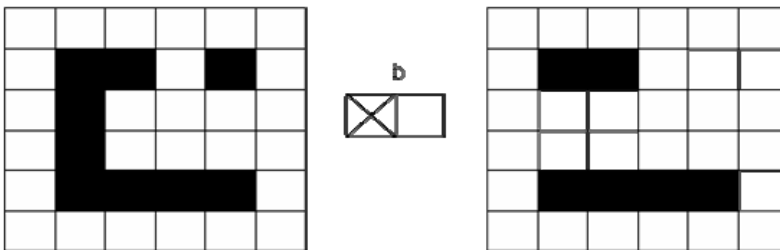


Figure 6.4 - Opening example

*Closing* is defined as:

$$X \bullet B = X_B = (X \oplus B) \ominus B \quad (6.9)$$

First the image is dilated with B, which is followed by erosion with B. Again it can be hard to envision the effects of this, it is normally said that closing connects the objects, and fills holes.

An example is given here:

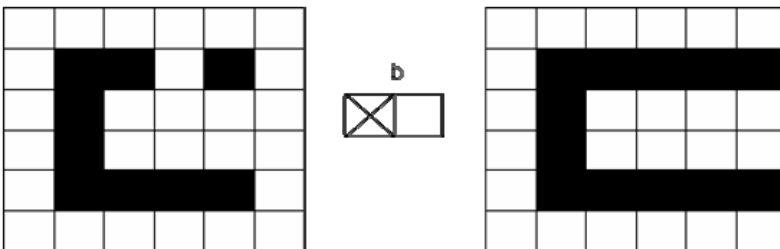


Figure 6.5 - Closing example

### 6.2.1.4 Reconstruction

The reconstruction transformation is quite different from others introduced, in the sense it does not directly use a structuring element. Reconstruction instead uses two images of the same size (a marker ( $J$ ) and a mask ( $I$ )) to generate the resulting image.

The resulting image consists of the connected components in the mask, which is marked in marker image. A component is said to be marked if one of the pixels in the component is marked with a 1 in the marker.

The reconstruction transformation is defined in [14] as “the union of components in  $I$  which contain at least one pixel in  $J$ ”.

$$\rho_I(J) = \bigcup_{J \cap I_k = \emptyset} I_k \quad (6.10)$$

An example is given here:

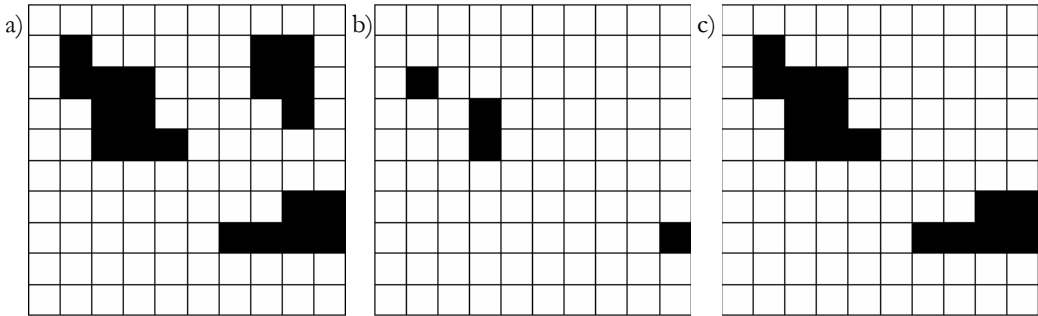


Figure 6.6 – (a) The mask, (b) The marker, (c) Result of reconstruction

## 6.2.2 Grayscale morphology

Moving binary morphology into the grayscale domain proves to create useful tools, not only for the already defined binary operators, but also opens for new operations that prove to be powerful when analyzing the profile of grayscale image.

### 6.2.2.1 Dilation and Erosion

To move the first four of the introduced operations into the grayscale domain, is simply a matter of defining dilation and erosion. Before being able to do this, a definition of the grayscale structural element is needed.

One of the approached is to simply keep the structural element in a binary form, or as it is also called having a *flat* structural element. This makes the transition into grayscale straight forward, since the OR operation will be equivalent to maximum and AND will be equivalent to minimum. Thus leading to the following definition of dilation

$$X \oplus B = \max_{[i,j \in B]} (x[m-i, n-j] + b[i, j]) \quad (6.11)$$

And the following for erosion:

$$X \ominus B = \min_{[i,j \in B]} (x[m-i, n-j] - b[i, j]) \quad (6.12)$$

It should be noted here that erosion and dilation on grayscale images, visually will have the opposite effect than on binary images. This is since 1 in a binary image means black and 0 means white, which is opposite to grayscale images. In grayscale images large values means white and small values indicate black. Below is included an example of applying erosion and dilation to a grayscale image.

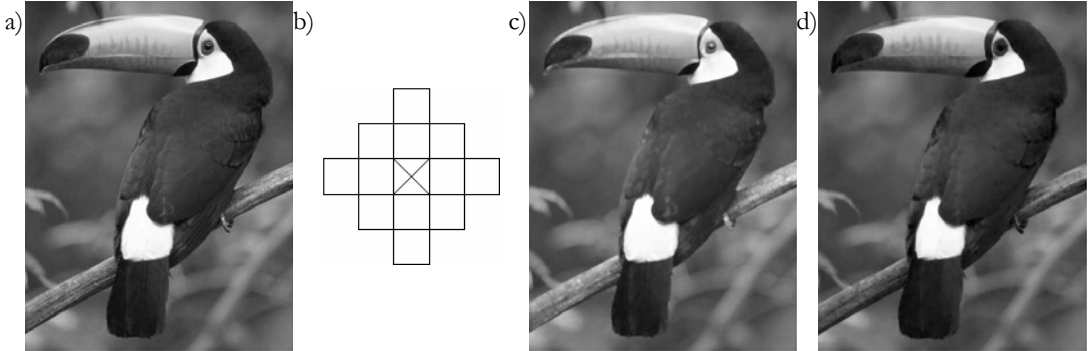


Figure 6.7 - (a) Original image, (b) Structural element, (c) Dilated image, (d) Eroded image

The example images clearly show a brighter image after dilation and a darker after erosion, this is especially apparent around the eye. Moving opening and closing into the grayscale from here is straightforward and will therefore not be examined further.

### 6.2.2.2 Reconstruction

Recalling the reconstruction transformation it was said to “*extract the connected components in the mask, which were marked in the marker*”. This raises some questions when moving into a grayscale domain, when is components connected in a grayscale image? One obvious approach could be to state that if the pixel values are higher than a certain value  $k$ , the components are connected. This motivates the definition of a *threshold* function. The threshold function  $T_k$  for an image  $I$  is defined as:

$$T_k(I) = \{p \in D_I \mid I(p) \geq k\} \quad (6.13)$$

Moving reconstruction into the grayscale domain can be done thereby be done, by saying it is to *extract the peaks from the mask which are marked in the marker*.

Using this it is now possible to define grayscale reconstruction for a mask  $I$  and a marker  $J$  both defined in the discrete set  $D = \{0, 1, \dots, (N-1)\}$  such that  $J \leq I$ , meaning each pixel in the marker must not exceed the corresponding pixel value of the mask. The reconstruction transformation  $\rho_I(J)$  can then be defined as: ([14])

$$\forall p \in D_I \quad \rho_I(J)(p) = \max\{k \in [0, N-1] \mid p \in \rho_{T_k(I)}(T_k(J))\} \quad (6.14)$$

The principle is illustrated in Figure 6.8.

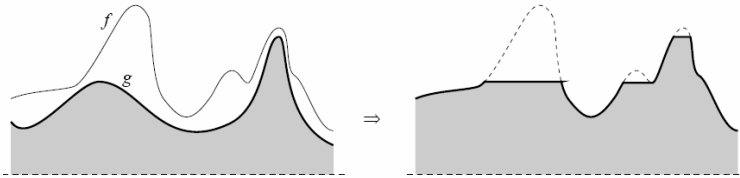


Figure 6.8 – Reconstruction of the mask  $f$  from the marker  $g$  (Figure from [14])

### 6.2.2.3 H-Domes

As mentioned in the introduction text of the section, greyscale morphology turns out to be a powerful tool for examining the profile of the image; this is due to the nature of the greyscale reconstruction transformation introduced. It turns out that using reconstruction it is possible to easily find the maximal structures or regional maximums in the images using a method called H-Domes.

The H-Domes transformation creates the marker to use in reconstruction, directly from the mask and a value  $h$  by simply subtracting this value from the mask. Having created the marker h-domes performs a reconstruction using the marker, and creates the resulting h-domes image by subtracting the reconstructed image from the original image leaving only the regional maximums in the image. This concept is illustrated in Figure 6.9.

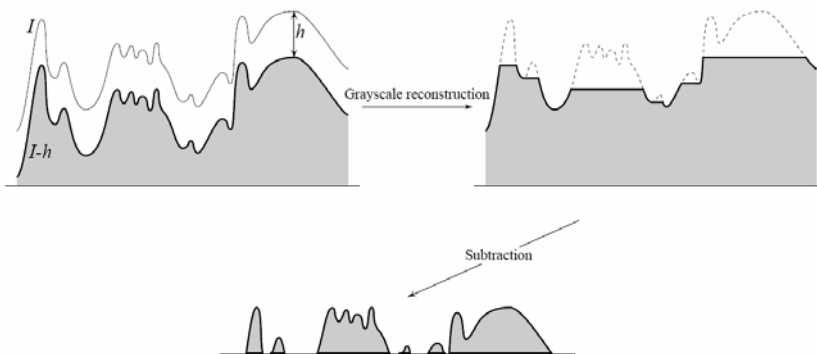


Figure 6.9 - H-Domes concept (From [14])

Formalising the concept gives the following definition.

$$D_h(I) = I - \rho_I(I - h) \quad (6.15)$$

It becomes obvious from Figure 6.9, that it is extremely important to select an appropriate  $h$  value, in order to get a useful result.

## Chapter 7      **Multivariate Statistics**

---

This chapter introduces the multivariate statistical tools used through out the thesis. For each tool the mathematical background is reviewed and its application in multi-spectral image analysis is discussed.

This chapter can be skipped by experts in multivariate statistics, and their application for multi-spectral images. It is however advised to at least skim the chapter in order to capture the notation and notions used.

## 7.1 Principal Component Analysis

One of the main challenges when examining multi-spectral images is the massive amount of data contained in the images. Most of the uninteresting data can be removed using clever pre-processing techniques, but these still leaves multiple dimensions of interesting data to be examined. To assist in this examination the Principal Component Analysis (PCA) proves to be a very useful tool.

PCA is essentially a method for re-expressing the multivariate data in a number of principal components, reorienting the data such that the first principal components (PC's) account for the larger part of the variation present in the data. Or put in another way, the PCA creates a number of new variables, each a linear combination of the original variables, such that each new variable accounts for the largest part of the variation possible. The remainder of this section lines up the mathematics behind the PCA, provides a small example and discusses how it can be applied to multi-spectral images.

### 7.1.1 Mathematics

The goal of PCA is to find a projection  $\mathbf{u}$  of the standardized multivariate input data  $\mathbf{X} = [\mathbf{x}_1, \mathbf{x}_2, \dots, \mathbf{x}_p]$  (normalized to zero mean and unit variance), such that the resulting data  $\mathbf{z}$  covers the maximum variance possible.

To maximize the variance, let's examine how the variance of  $\mathbf{z}$  can be described:

$$\text{var}(\mathbf{z}) = \frac{1}{(n-1)} \mathbf{u}' \mathbf{X}' \mathbf{X} \mathbf{u} \quad (7.1)$$

We notice that since the input is standardized,  $1/(n-1) \mathbf{X}' \mathbf{X}$  is the sample correlation matrix or the covariance matrix. This is denoted  $\mathbf{R}$ , and can be substituted giving:

$$\text{var}(\mathbf{z}) = \mathbf{u}' \mathbf{R} \mathbf{u} \quad (7.2)$$

From this definition it is clear that  $\mathbf{u}$  can be chosen to be arbitrary large, and thereby drive the variance towards infinity if there are no further constrains imposed. To prevent this, we require for  $\mathbf{u}$  to be a unit vector such that  $\mathbf{u}' \mathbf{u} = 1$ , leaving the problem of maximizing equation 7.2, such that  $\mathbf{u}' \mathbf{u} = 1$  is fulfilled. This problem is solved by forming the Lagrangian, and settings its first derivative to zero, this yields the following conditions to be met.

$$\mathbf{R} \mathbf{u} = \lambda \mathbf{u} \quad \text{or} \quad (\mathbf{R} - \lambda \mathbf{I}) \mathbf{u} = 0 \quad (7.3)$$

Thus leaving an eigenvector problem, where  $\mathbf{u}$  is the eigenvector and  $\lambda$  is the eigenvalue. The solution to this problem yields  $p$  eigenvectors and eigenvalues. Solving the eigenvector

problem will not be described further, as is rarely done by hand but often left up to one of the numerous computer programs created for the purpose.

Having solved the eigenvector problem, the eigenvectors  $\mathbf{U} = [\mathbf{u}_1, \mathbf{u}_2, \dots, \mathbf{u}_p]$  can now be used, by multiplying them with the input values  $\mathbf{X} = [\mathbf{x}_1, \mathbf{x}_2, \dots, \mathbf{x}_p]$ , to obtain the resulting principal components scores  $\mathbf{Z} = [\mathbf{z}_1, \mathbf{z}_2, \dots, \mathbf{z}_p]$ . A discussion of how many of the eigenvectors to include is given in section 7.1.2, before moving to this lets examine the eigenvalues found.

The eigenvalues obtained through the analysis, can be used to determine the amount of variance each projection includes. This can be proved since knowing  $\mathbf{R}\mathbf{u} = \lambda\mathbf{u}$  and  $\mathbf{u}'\mathbf{u} = 1$ , the following substitution can be done:

$$\text{var}(\mathbf{z}) = \mathbf{u}'\mathbf{R}\mathbf{u} = \mathbf{u}'\lambda\mathbf{u} = \lambda\mathbf{u}'\mathbf{u} = \lambda \quad (7.4)$$

Showing that the eigenvalues expresses the amount of variance accounted for by the associated principal component.

## 7.1.2 Determining the appropriate dimension reduction

As one of the main purposes of the analysis is to reduce the dimensions of data, the next obvious step is to determine how many components should be retained. For this purpose a number of rules of thumb exist, some of which are explained below.

### 7.1.2.1 Kaiser's rule

The commonsense of choosing which principal component to retain, would be to keep the components which represents at least as much variance as any of the original variables. In the case of standardized variance this means keeping the components with an eigenvalue above 1. This approach seems somewhat reasonable, but cases exists where the cut-off value might need to be changed to a value higher than 1 because it is found that the lower components only contains noise. Or the value is set to lower than 1 to retain a certain amount of original variance. As with the other rules one should remember these are only guidelines and not the ground truth.

### 7.1.2.2 Scree plot

Propose by Cattell (1966), this is a graphical approach to the problem. The idea is to plot the eigenvalues of each component, and detect the *elbow* of the resulting curve, keeping the values higher than the detected elbow point. By the *elbow* Cattell means the point where the lower components decrease in a linear fashion. This approach has the apparent disadvantage of being quite ambiguous, since the elbow point rarely is clearly identifiable.

### 7.1.2.3 Visual selection for image analysis

For the application of image analysis, choosing the relevant components can be done by simply visually examine the transformed data. By visually examining all the components, it becomes very obvious which components contain actual useable data, and which contains only noise enabling us to disregard these. As an example all components of PCA transformed image is given in Figure 7.1.

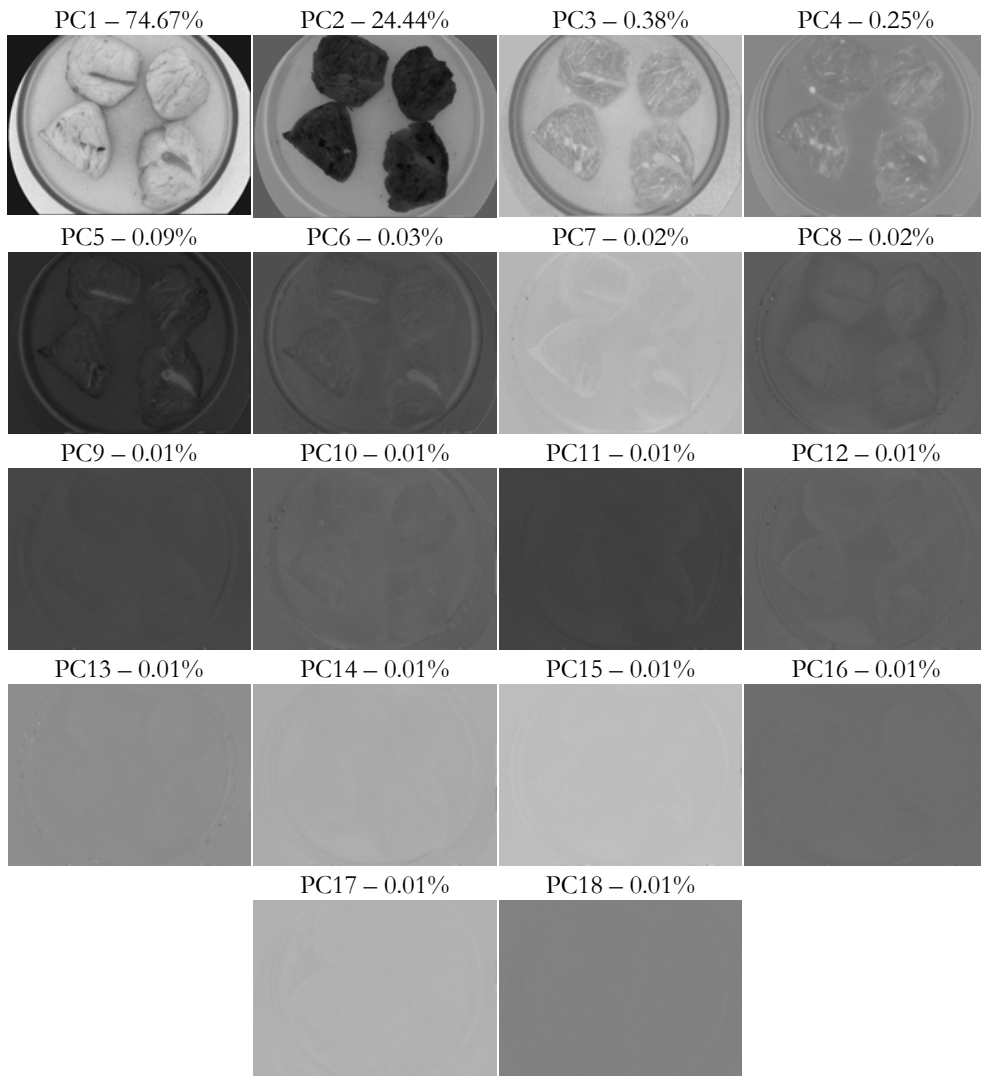


Figure 7.1 - Principal component and accounted variance

From the visualization of the components, it is clear that all below the third component contain a large amount of noise, and it will hardly make sense to include these in any kind of analysis. This is also expressed in the amount of variance the lower components account for.

Generally the best approach is common sense applied along with one of the rules presented above. It is normally easy to make out which components to include when the purpose of the data is known. E.g. if the purpose of the analysis is to distinguish between what is meat and what is surrounding objects from the image used in Figure 7.1. The best solution would clearly be to use the second principal component, since this clearly outlines the meat present in the image.

### 7.1.3 PCA for multi-spectral image analysis

Numerous examples shows that PCA is widely used technique in multi-spectral imaging. It is used in [9] for separation of meat and fat in salami and in [10] where it is used as a tool for classifying species of fungi.

Even though PCA is a widely used tool in multi-spectral images, it does have some properties that one needs to be aware of before applying it blindly. The first important thing to notice is that the image data needs to be transformed in order to fit the form required by PCA. PCA needs an input matrix as  $\mathbf{X} = [\mathbf{x}_1, \mathbf{x}_2, \dots, \mathbf{x}_p]$ , meaning a two-dimensional matrix of variables.

As an image is normally represented in a three dimensional matrix a transformation is needed, this transformation is explained in section 5.1.2. From 5.1.2 it is worth noticing the loss of the spatial information. Loosing spatial information is usually not a large problem, since in most analysis the spectral information is the interesting part, and since the spatial information can be easily recovered.

Another important property of PCA is that it is a statistical method analysis of interdependence. Meaning it will enhance any patterns found in the supplied data, but will not necessarily find the pattern one is looking for based on a dependent variable. This calls for caution when determining the data to use in a PCA. An example is the transformed image from Figure 7.1. The image given to the PCA included both meat and surrounding objects, such as the Petri dish and the metal sheeting. It is clear that the results of the analysis, found a way of distinguishing between the unwanted object and the meat, but other than that the results does not say much about the frying degree of meat or other important meat properties. To investigate these it will be an advantage, to supply data only from areas containing meat, since it is here it the analysis should search for patterns.

The last property mentioned motivates the introduction of the next analysis, namely a member of the “Analysis of Dependence”-family the Canonical Discriminant Analysis.

## 7.2 Canonical Discriminant Analysis

The Canonical Discriminant Analysis (CDA), is a member of the “Analysis of Dependence”-family, meaning it is way of finding a pattern in a number of independent variables based on a

dependent variable given. The CDA specifically is said to find the largest possible separation of the classes given, using the information provided in the independent variables.

### 7.2.1 Mathematics

Using Fishers approach the objective of the analysis is to find the linear combination of the given variables, which leaves the highest separation of the given groups. In order to provide a measure of the separation a discriminant score is introduced. Meaning the goal of the analysis is to obtain a linear combination of the independent variables, giving the *maximum* different discriminant scores for each of the given groups.

To formalize this let  $\mathbf{k}$  denote the linear combination,  $\mathbf{X} = [\mathbf{x}_1, \mathbf{x}_2, \dots, \mathbf{x}_n]$  denote the input variables where each group of values are split into the groups  $\mathbf{X}_1, \mathbf{X}_2, \dots, \mathbf{X}_i$ . The discriminant scores are then be given as:

$$\mathbf{t} = \mathbf{Xk} \quad (7.7)$$

To optimize the difference between the groups Fisher proposed, maximizing the ratio of the across-groups sum-of-square matrix ( $\mathbf{A}$ ) to the within group sum-of-squares matrix ( $\mathbf{W}$ ) of the discriminant scores  $\mathbf{t}$ . Resulting in the following problem:

$$\text{Find } \mathbf{k} \text{ to maximize } \lambda = \frac{\mathbf{k}'\mathbf{A}\mathbf{k}}{\mathbf{k}'\mathbf{W}\mathbf{k}} \quad (7.8)$$

Taking the first derivative of Equation 7.8 and solving for  $\mathbf{k}$ , results in the following eigenvector problem:

$$\mathbf{W}^{-1}\mathbf{A}\mathbf{k} = \lambda\mathbf{k} \quad (7.9)$$

Solving the eigenvector problem for a two group problem results in one linear combination (eigenvector), for a three group problem two linear combinations are found and so forward. Apart from the linear combinations the solutions also contains a number of associated eigenvalues, these are an expression of the functions ability to separate the groups.

### 7.2.2 CDA for multi-spectral images

As with the principal components analysis, the canonical discriminant analysis also has some issues to consider of when applying it to multi-spectral images.

The canonical discriminant analysis requires, just as the principal component analysis, the data to be transformed into two dimensions. This leads to the same loss of spatial information as mentioned for the PCA, and is performed as illustrated in Figure 5.2.

As CDA is an analysis of dependence, it sets out to find a linear combination which separates the classes given. The analysis will always find a combination that separates the classes in some way; it is therefore important to examine the solution found in order to verify that the linear

combination is reasonable with respect to the expected separation. As with the principal component analysis it is important to use common sense, and do a critical evaluation of the results found.

## 7.3 Regression Analysis

Often one of the main objectives of multi-variant statistics, and also image analysis, is the ability to make predications based on the observations available. Introducing regression analysis provides a tool to create a prediction model based on observations.

To solve the problem of predicting a dependent variable based on a number of independent variables, the first step is to setup an appropriate model. In lower dimensional case it is often possible to plot the observations available and from the plot determine which model to use, this is however not always possible for higher dimensional cases where model validation techniques can be used as discussed in section 7.3.2.

### 7.3.1 Least Square Regression

Having determined an appropriate model, the next step is to use the available observations to make an estimation of the model parameters based on regression analysis, for this least square regression is introduced.

For simplicity least squares is introduced for a linear model, but can be easily extended with more terms. An optimal linear model has the following well-known form:

$$y = \alpha_0 + \alpha_1 x \quad (7.11)$$

From this the estimated model can be defined as:

$$\hat{y} = a_0 + a_1 x \quad (7.12)$$

And the error in the predicted value of  $y$  can be described as:

$$e_i = y_i - \hat{y}_i \quad (7.13)$$

Meaning the objective of the regression is to optimize  $a_0$  and  $a_1$  in order to minimize the summarized error term for all observations  $n$ . Using the measure of error introduced above will introduce a large number of suitable lines, since the negative error terms cancel positive error terms. To prevent this, the principle of *least squares* is applied defining the summarized error term as a squared error, thus insuring an always possible contribution to the error term:

$$e^2 = \sum_{i=1}^n (y_i - (a_0 + a_1 x_i))^2 \quad (7.14)$$

Having defined the rules for estimating the model, it is now possible to define the *goodness of fit* for a model. Meaning the amount of variance accounted for in the depended variable using model of the independent variables. This is defined as:

$$R^2 = 1 - \frac{\sum_i (y_i - \hat{y}_i)^2}{\sum_i (y_i - \bar{y})^2} \quad (7.15)$$

Having laid down the ground rules, we are now able to move on estimating the actual parameters. This calculation is eased and enables an expansion of the model with multiple independent variables by introducing a matrix notation, giving the new optimal model as:

$$\mathbf{Y} = \mathbf{X}\mathbf{b} \quad \text{where} \quad \mathbf{Y} = \begin{bmatrix} y_1 \\ \vdots \\ y_n \end{bmatrix}, \mathbf{X} = \begin{bmatrix} 1 & x_{1,1} & \dots & x_{1,p} \\ 1 & x_{2,1} & \dots & x_{2,p} \\ \vdots & \vdots & \ddots & \vdots \\ 1 & x_{n,1} & \dots & x_{n,p} \end{bmatrix}, \mathbf{b} = \begin{bmatrix} b_0 \\ \vdots \\ b_{p+1} \end{bmatrix} \quad (7.16)$$

Where  $n$  is number of observations and  $p$  is the number of terms in the model. This leads to an estimated model defined as:

$$\hat{y} = \mathbf{X}\hat{\mathbf{b}} \quad (7.17)$$

It can then be showed that the most accurate fit can be obtained by estimating the parameters by:

$$\hat{\mathbf{b}} = (\mathbf{X}'\mathbf{X})^{-1} \mathbf{X}'\mathbf{y} \quad (7.18)$$

This line is also called the *least square estimator* (LSE), proving Equation 7.18 will not be included in this text since it is not in the scope of this thesis text.

### 7.3.2 Cross validation

Cross validation is a method which can be used to verify if the appropriate model was chosen, or to select the appropriate model among a number of models. Choosing a model blindly by optimizing for best squared error and increased  $R^2$ -value introduces the risk of over-fitting the model. Having an over-fitted model means it adjusts to the training set values with expense of not generalizing.

To prevent an over-fitted model, cross validation separates the available observations  $k$  into  $n$  sets. It then proceeds by, in turn, using one set of testing and the remaining for estimating the model parameters until all sets have been used for testing. For each turn the *mean squared error* (MSE) is recorded, this can then be used directly to select the appropriate model. This type of cross validation is called  $n$ -fold cross validation.

A special case of cross validation is when  $k = n$ ; meaning only one observation is left out for testing at each step. This is naturally called *Leave-One-Out* (LOO) cross validation. LOO is good

when having a small dataset, but when having a large datasets a  $n$ -fold cross validation is preferable.

### 7.3.3 Stepwise regression

Having a depended variable and a number of independent variables, it is often an advantage to examine the influence of the independent variable on the model before including it. This can be used to examine if the independent variable has a noticeable effect on the depended variable, in order to decrease the complexity of a model by not including the least influential variables or even to try to estimate the best model allowing only a certain number of the independent variables.

The basics in stepwise regression is to build a model, in steps by examining the available independent variables on at a time, including the ones that have the large influence (forward regression), and excluding the ones with lowest influence (backward regression).

A step in the stepwise regression can decomposed into the following tasks:

- Calculate the  $\hat{\mathbf{b}}$  for the variables already in the model
- For each variable not in model calculate the  $\tilde{\mathbf{b}}$  and corresponding F-ratio by:

$$F = \frac{RSS(\hat{\mathbf{b}}) - RSS(\tilde{\mathbf{b}})}{RSS(\tilde{\mathbf{b}})/(N - k - 2)} \text{ where } RSS(\mathbf{b}) = (\mathbf{y} - \mathbf{Xb})' (\mathbf{y} - \mathbf{Xb}) \quad (7.19)$$

- Add the variable producing the largest F
- For each variable included in the model calculate the corresponding F-ratio
- If the ratio between the largest F-ratio for exclusion and the largest for inclusion is more that one, exclude the variable. (The ratio used can be changed to fit the application)

The steps continue until a certain stop condition is encountered such as a maximum subset size or an F-ratio resulting in a certain significance level etc.

### 7.3.4 Best-sub regression

The stepwise method for including and excluding variables does not insure that the optimal subset of variables is selected. To insure the optimal subset is selected, it is possible to calculate the regression statistics for all possible subset, sorting them after the mean squared error.

This approach will ensure the best subset is selected, but is very time consuming since the number of subsets to investigate increases very rapidly.

## 7.4 Analysis of Variance

A special case of linear regression analysis is the analysis of variance (ANOVA). ANOVA is a tool for determining if a certain factor has a significant influence, on a dependent variable of an experiment. An example of use is to determine if the temperature in a frying process has a significant influence on the water contents in the end product.

The basic idea behind ANOVA can be formulated as: *“We will make an inference about differences among group means by comparing different estimates of variance associated with these observations”* [6].

### 7.4.1 One factor ANOVA

As the goal of ANOVA is to determine if a factor/treatment has an influence on a dependent variable, the analysis sets out to compare different estimates of variance, using a statistical test to determine if there is a significant difference between the estimates, thus yielding an influence.

In order to continue, the notation of the one-factor ANOVA is introduced:

$$\begin{aligned}
 Y_{ij} &= \text{the } i\text{th observation in treatment group } j \\
 \bar{Y}_{.j} &= \frac{1}{n_j} \sum_i Y_{ij} = \text{mean of treatment group } j \\
 \bar{Y}_{..} &= \frac{1}{n} \sum_i \sum_j Y_{ij} = \text{overall mean}
 \end{aligned} \tag{7.20}$$

Where  $n$  is the number of observations and  $m$  is the number of treatment groups. The basic model of the one factor ANOVA is given as:

$$Y_{ij} = \mu + \tau_j + \varepsilon_{ij} \tag{7.21}$$

Meaning an observation is made up by the mean value plus a treatment effect ( $\tau_j$ ) and an error term. The analysis is now to test for the existence of the treatment effects, meaning the difference in the mean value across treatment groups. In order to do so, a *null hypothesis* is setup, saying all mean values are equal:

$$H_o : \tau_1 = \tau_2 = \dots = \tau_m = 0 \tag{7.22}$$

To test this hypothesis the ratio between two estimates of the with-in group variance ( $\sigma^2$ ), the across group estimate ( $S_A^2$ ) and the with-in group estimate ( $S_W^2$ ), is used. This ratio is distributed as an F-statistic, meaning if the *null hypothesis* is true the ratio is close to one, whereas the ratio will be larger than one if the hypothesis is false. The with-in and across group estimates are given as:

$$S_A^2 = \frac{\sum_j n_j (\bar{Y}_{.j} - \bar{Y}_{..})^2}{m-1} \tag{7.23}$$

$$S_w^2 = \frac{1}{m} \sum_j \frac{\sum_i (Y_{ij} - \bar{Y}_{.j})^2}{n_j} \tag{7.24}$$

The results of the ANOVA are most often presented in a so-called ANOVA table, for the one-factor example the tables looks like:

Source	Sum of Squares	Degrees of Freedom	Mean Square	F-Ratio
Across	$S_A^2$	$(m - 1)$	$MS_A = S_A^2 / (m - 1)$	$MS_A / MS_W$
Within	$S_W^2$	$(n - m)$	$MS_W = S_W^2 / (n - m)$	
Total	$S_T^2 = \sum_i \sum_j (Y_{ij} - \bar{Y}_{..})^2$	$(n - 1)$		

Table 7.1 - One factor ANOVA table

### 7.4.2 Two factor ANOVA

Expanding the one-factor model to a two-factor model; means having two different kinds of treatments testing each for influence. An example could be testing if time and temperature in frying process has an influence on the water content in the final product. In addition to testing the two kinds of treatment for influence, one also tests the effects of the so-called *interaction effect*. This is the differences encountered, not accounted for by the main effects of the treatments.

Expanding the notation from Equation 7.20 to the two factor model gives:

$$\begin{aligned}
 Y_{ijk} &= \text{the } i\text{th observation in level } j \text{ of factor 1 and level } k \text{ of factor 2} \\
 \bar{Y}_{.j} &= \text{mean for level } j \text{ of factor 1} \\
 \bar{Y}_{.k} &= \text{mean for level } k \text{ of factor 2} \\
 \bar{Y}_{.jk} &= \text{mean for level } j \text{ of factor 1 and level } k \text{ of factor 2 and} \\
 \bar{Y}_{...} &= \text{overall mean}
 \end{aligned}
 \tag{7.25}$$

When  $n$  is the total number of observations and  $m_a$  is the number of treatment groups of factor 1 and  $m_b$  is the number of treatment groups of factor 2. This gives the following model of an observation  $Y_{ijk}$  :

$$Y_{ijk} = \mu + \alpha_j + \beta_k + \alpha\beta_{jk} + \varepsilon_{ijk} \tag{7.26}$$

As for the one-factor model the observation is made up by the mean value ( $\mu$ ), the effects of the treatments ( $\alpha_j, \beta_k, \alpha\beta_{jk}$ ) and an error term. To the test for the effects of the treatment three *null hypotheses* is setup, one for each factor suggesting it is not contributing.

$$\begin{aligned}
 H_o : \alpha_1 = \alpha_2 = \dots = \alpha_{m_a} &= 0 \\
 H_o : \beta_1 = \beta_2 = \dots = \beta_{m_b} &= 0 \\
 H_o : \alpha\beta_1 = \alpha\beta_2 = \dots = \alpha\beta_{m_a m_b} &= 0
 \end{aligned}
 \tag{7.27}$$

As for the one-factor model an ANOVA table is setup, using F-statistics to accept or reject the null hypothesis.

Source	Sum of Squares	Degrees of Freedom	Mean Square	F-Ratio
Across	$SS_a$	$(m_a m_b - 1)$	$MS_A = \frac{SS_a}{(m_a m_b - 1)}$	$\frac{MS_A}{MS_W}$
Factor 1	$SS(\alpha)$	$(m_a - 1)$	$MS(\alpha) = \frac{SS(\alpha)}{(m_a - 1)}$	$\frac{MS(\alpha)}{MS_W}$
Factor 2	$SS(\beta)$	$(m_b - 1)$	$MS(\beta) = \frac{SS(\beta)}{(m_b - 1)}$	$\frac{MS(\beta)}{MS_W}$
Interact	$SS(\alpha\beta)$	$(m_a - 1)(m_b - 1)$	$MS(\alpha\beta) = \frac{SS(\alpha\beta)}{(m_a - 1)(m_b - 1)}$	$\frac{MS(\alpha\beta)}{MS_W}$
Within	$SS_W$	$(n - m_a m_b)$	$MS_W = \frac{SS_W}{(n - m_a m_b)}$	
Total	$SS_T$	$(n - 1)$		

Table 7.2 - Two factor ANOVA table

Where the sum of squares as given as:

$$\begin{aligned}
 SS_a &= SS(\alpha) + SS(\beta) + SS(\alpha\beta) \\
 SS(\alpha) &= \sum_j n_j (\bar{Y}_{.j} - \bar{Y}_{...})^2 \\
 SS(\beta) &= \sum_k n_k (\bar{Y}_{..k} - \bar{Y}_{...})^2 \\
 SS(\alpha\beta) &= \sum_j \sum_k n_{jk} (\bar{Y}_{.jk} - \bar{Y}_{.j} - \bar{Y}_{..k} + \bar{Y}_{...})^2 \\
 SS_W &= \sum_i \sum_j \sum_k (Y_{ijk} - \bar{Y}_{.jk})^2 \\
 SS_T &= \sum_i \sum_j \sum_k (Y_{ijk} - \bar{Y}_{...})^2
 \end{aligned}
 \tag{7.28}$$

## Chapter 8      Meat Chemistry

---

This chapter will introduce the relevant chemistry needed to perform a qualitative analysis of the processed meat. This includes describing what generally happens in stir frying, what makes up the color of meat, how and why the color changes over time and due to processing of the meat, also including other aspects that are crucial and / or interesting for the later analysis.

This chapter can be skipped by professionals with expert knowledge in meat chemistry and frying processes of meat.

## 8.1 Stir frying

A hypothesis of the mechanisms in the stir-frying process has been proposed in [2], in which a process model is formulated based on observations made during stir-frying. The hypothesis suggest that the stir-frying process can be divided into four phases each having their specific impact on the product. The process is illustrated on Figure 8.1.

In the first phase the food product undergoes a rapid heat up, until reaching the temperature gradient established in phase 2. [2] Suggest the average temperature in the food product piece is about 80°C and around 90°C on the surface, this temperature is held down by the cooling resulting from evaporation.

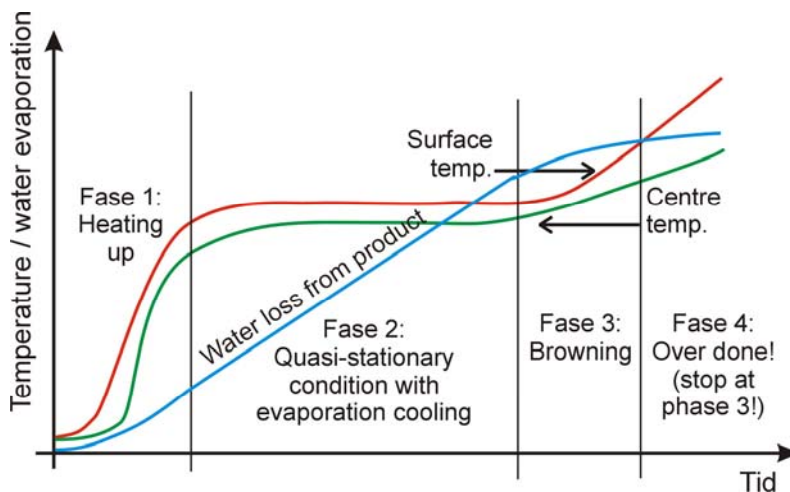


Figure 8.1 - Phases of the stir-frying process [2]

In phases 3, the evaporation wears off and the food product forms crust, this crust has a large influence on the look, taste and feel of the product. It is in this phase the product forms the well-known fried taste and look. Over doing the heat treatment results in going into phase 4, producing an over processed product. The characteristics of over-processed products are low water contents and the well known burned black-brown colour.

## 8.2 Meat pigments

Meat contains a variety of meat pigments each contributing to the look and color of the meat product. This section examines some of the basic and important pigments, when it comes to color evaluation of meat.

One of the basic pigments in meat is the meat fat. The pigments contained in meat fat varies considerable in both type and quantities, therefore it is very hard to explain the exact pigments in meat fat [11]. It can however generally be concluded that visually the age of the animal has a direct effect on the color of the fat, as the animal grows older the fat darkness in color from the white cream color, to a more yellowish color.

A much more interesting pigment in meat with regards to the frying process is the muscle pigments. The muscle pigments basically consist of myoglobin and small quantities of haemoglobin. These pigments, is of special interest in this context, since this determines the color of the meat in different stages, also relating to the frying process.

Myoglobin consists of the protein globin, enclosing a so-called heme group. The heme group is an iron atom with six bounding points, one of these is bound to the protein, and four is bound to nitrogen atoms, leaving one open to bind to either water or oxygen.

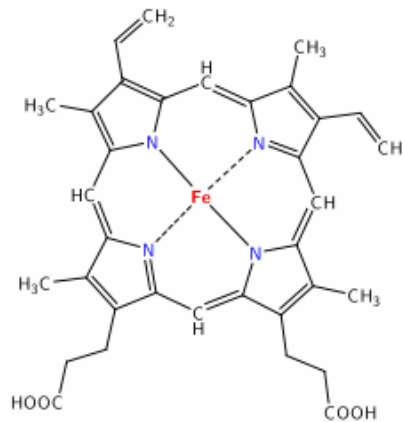


Figure 8.2 - Heme group

This open bind is enabling myoglobin to be an oxygen holder / transporting pigment in the muscle. The atom bound to the 6<sup>th</sup> binding is a determining factor of the color of the pigment. In addition to the binding, the oxidation state of the iron atom also determines the color of myoglobin. In the living state of the tissue, the iron is in a ferrous state (Fe<sup>2+</sup>) but the oxidation state may change to a ferric state (Fe<sup>3+</sup>) in the dead tissue due to various processing of the meat. The last factor determining the color of the pigment is the state of the protein. When stress (such as extreme heat) is applied to the protein, the protein gets de-naturated resulting in an irreversible change in the molecular structure. These changes in the pigments can be summed up in the following table, showing the color in each state.

Pigment	Oxidation step	The 6 <sup>th</sup> bind	Protein state	Color
Reduced Myoglobin	Ferrous (Fe <sup>2+</sup> )	H <sub>2</sub> O	Native	Purple
Oxy-myoglobin	Ferrous (Fe <sup>2+</sup> )	O <sub>2</sub>	Native	Red
Met-myoglobin	Ferric (Fe <sup>3+</sup> )	H <sub>2</sub> O	Native	Brown
De-natured globin	Ferric (Fe <sup>3+</sup> )	H <sub>2</sub> O	De-Naturated	Gray-brown

Table 8.1- Muscle pigment colors

When cooked the myoglobin is changing to one of these states depending on the temperature. Rare meat cooked to 60°C keeps the dark red color of oxy-myoglobin, if cooked to over 75°C it gets the gray-brown color of the de-natured met-myoglobin.

As myoglobin, haemoglobin is used as an oxygen carrier in an animal. Where myoglobin is the muscle oxygen carrier, haemoglobin is the blood oxygen carrier. Since haemoglobin is mostly present in blood, it is clear that muscles contains only small quantities of this compared to amount of myoglobin. Having this in mind and since the two pigments are structurally very alike haemoglobin will not be discussed further in this chapter.

### 8.3 The Millard reaction

When meat is exposed to temperatures around 150°C further reactions related to browning, taste and odor occurs, one of these is the Millard reaction. In the Millard reaction glucose and the amino acid glycine reacts forming, the brownish melanoid pigments. These pigments give the meat the distinctive look of roasted meat.

### 8.4 Fibrous Tissue

An important part of the meat structure is fibrous tissue. In muscle fibrous tissues forms a three-dimensional network, which supports the muscle cells, and therefore is of big importance for the feel of the meat. Fibrous tissue mainly consists of the protein collagen. As an animal grows older the weak bindings in collagen is replaced with harder bindings thus making the meat non-tender.

When the meat is heated the collagen protein, starts to de-nature at 60°C, thus making the meat more non-tender until 80°C. From 80°C the meat will start to get tender due to the break of the harder cross-bindings and peptide-bindings. The de-naturation of the collagen protein furthermore has the property, that it expels water and fat due to contraction. These effects of the de-naturation are of special interest for since the water and fat absorbs in the NIR bands available.

III

# Data Analysis

## Chapter 9      Assessment of Frying Treatment for Minced Beef

---

Adequate frying treatment of minced meat is crucial, not only to ensure extermination of microorganisms, but also to ensure high quality and well tasting meat. This chapter examines the possibilities to assess the frying treatment of minced meat using non-destructive multi-spectral vision technology.

The methods and results obtained in this chapter have been presented in the following publications:

***A Method for Frying Treatment Assessment of Minced Meat Using Multi-Spectral Imaging.***

The article is to be submitted to the 3<sup>rd</sup> International Symposium on Recent Advances in Food Analysis.

***A Method for Frying Treatment Assessment of Meat Using Multi-Spectral Vision Technology***

The poster was presented on the 2007 Industrial Vision Day, the 23<sup>rd</sup> of May at the Technical University of Denmark.

***New Vision Technology for Multidimensional Quality Monitoring of Continuous Frying of Meat***

The article is to be submitted to Elsevier's international journal *Food Control*.

## 9.1 Sample preparation

Using the continuous wok and the method developed in [5] for frying of minced meat, a number of samples were prepared in accordance with the experiment design included in Appendix B.

Frozen minced meat with a fat percentage of 15-18% purchased from the wholesale supplier Inco Denmark Amba. Copenhagen was used. The meat was crushed using a hammer into pieces of 150[g]. These pieces were then chopped using a meat chopper (Kilia 57cm diameter). 1[kg] of meat was chopped at a time, until it was finely divided into pieces of approximately 5[mm]. Exaggeration of the chopping should be avoided due to the forming of heat during chopping.



Figure 9.1 - Meat pieces before and after meat chopper

After chopping the meat was contained in plastic cups each containing 100[g], and cooled down using ice to prevent the meat from thawing until it was to be fried.

### 9.1.1 Wok-frying

The samples were prepared by feeding 800[g] of the still frozen meat to the wok, for each sample regulating parameters for time and temperature. The temperature was altered using the steps 200°C, 225°C and 250°C, for each temperature step four samples were prepared varying the frying time from 120[s] to 240[s] in 40[s] intervals.

This combination of temperature and time, following [4], results in samples that have characteristics of under- and adequate-processed meat. It can be argued that some of the samples can have characteristics of over-processed meat. These samples are in this context perceived as adequately-processed, since the by far largest part of the meat granules are adequate-processed, containing only a few over-processed granules which are easily identified by the human eye due to the very characteristic black-brown color. It is important to note that the under-processed meat does not contain raw-meat, but instead is used as a term for meat with

high moisture and fat content, thereby having a lower frying quality. The meat samples are divided into processing classes in accordance with Table 9.1.

Temp / Time	120[s]	160[s]	200[s]	240[s]
200°C	Under	Under	Under	Under
225 °C	Under	Adequate	Adequate	Adequate
250 °C	Adequate	Adequate	Adequate	Adequate

Table 9.1 - Processing degree of meat samples

### 9.1.2 Image acquisition

For each combination of time and temperature, three sub-samples were taken out for imaging, giving triple determination of the results. For each sub-sample a Petri dish was filled and a finger was run over removing excess particles, leaving a somewhat homogenous surface for image acquisition. The images were acquired using the VideometerLab software, and saved in the hips format. For details of storing refer to Appendix B.

## 9.2 Chemical experiment

To examine the water contents of the meat, water determination was performed. Water contents are examined since it can be argued, that it to some degree can be used as an indicator of the frying treatment.

The experiments are done by taking 20[g] meat of each sample and making it homogeneous in a liquidizer. From the homogeneous 20[g] of meat, three samples of approximately 2[g] are taken out and dried at 105°C for 24 hours. The difference between the weights before drying and after makes up the water content.

### 9.2.1 Results water determination

The results of the water determination are given in Appendix C and summarized in Table 9.2.

Water contents	120 [sec]		160 [sec]		200 [sec]		240 [sec]	
	Mean	$\sigma$	Mean	$\sigma$	Mean	$\sigma$	Mean	$\sigma$
200°C	54.3%	0.217	52.7%	0.440	51.5%	0.212	51.2%	0.425
225°C	53.4%	0.150	54.0%	0.136	52.5%	0.411	51.3%	0.240
250°C	51.0%	0.185	46.3%	0.206	49.7%	0.273	48.3%	0.226

Table 9.2 - Water contents - Minced Meat

Generally the results show a low deviation within the sub-samples. The results further shows, as expected, that the under processed meat same to have higher water contents than the adequately processed meat.

From Table 9.2 it is hard to conclude if both the frying time and temperature, has an effect on the water contents of the end product. To examine this further a two-factor ANOVA is performed, the results are presented in Table 9.3.

	Sum of Squares	df	Mean Square	F-Ratio	Pr > F
Across	177.44	11	16.13	135.38	0.0000
Time	29.42	3	9.81	83.29	0.0000
Temperature	111.69	2	55.85	468.71	0.0000
Time x Temperature	36.33	6	6.05	50.81	0.0000
Within	2.86	24	0.12		
Total	181.59	35			

Table 9.3 - ANOVA table water content - Minced Meat

The ANOVA clearly shows that both the frying time and temperature, has a large influence on the water contents of the end product, furthermore it shows that the interaction effect is very influential.

## 9.3 Pre-Processing

Despite the attempt to create a homogenous surface, the nature of the meat granules results in the forming of dents, which leads to a large variation over the image parts consisting of meat. This and the fact that the images also contains other objects than meat (Petri dish, metal plate from imaging device) stress the need for pre-processing of the images.

The pre-processing procedure is to isolate the tops of the meat granules, removing all other objects, thereby ensuring less variation over the image data and a reduction in the data to analyze. It should be noted that there will still exists some variation due the natural variation as a results of frying minced meat, it is not the purpose of the pre-processing algorithm to remove this.

### 9.3.1 Eradicate non-meat objects

In the first step of the pre-processing procedure the goal is to eradicate all non-meat objects found in the image. Examining the spectrum of the objects in the images (Figure 9.2a), it shows the lower bands of the image shows a clear separation of the objects. This will allow of a simple threshold operation to remove the un-wanted objects. The histogram curves of various interesting bands shown in Figure 9.2b further supports this proposition.

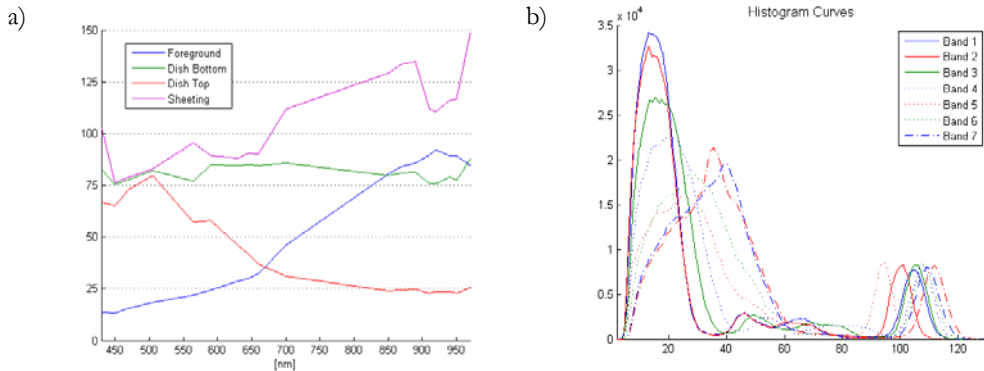


Figure 9.2 - a) Spectrum Background / Foreground, b) Histogram curves

Using a score based technique to select the optimal band and threshold value, will enable an optimal eradication of the non-meat objects for every picture, regardless of intensity and distribution of the objects. The score parameter defined is based on the following features:

#### ValueFirstPeak

The height of the first peak found in the histogram. This would represent the foreground of the image.

#### ValueSumLastPeaks

The sum of the peak values of the last peaks; this is used to calculate the ratio between the first and the last peaks. This ratio is useful since a low ratio could imply noise peaks, instead of actual background peaks.

#### DistanceFirstSecond

The distance between the first and the second peak. A large distance implies it a good separation of the background and foreground, whereas a low distance implies low separation.

#### WidthFirstAtHalfMax

The width of the first peak at half of the maximum value, this is an expression of the variance of the peak. A too large variance might imply more than one distinct feature.

From these features the best score is calculated using the following equation. The equation has been derived from a number of experiments.

$$\text{score} = \frac{\text{ValueSumLastPeaks}}{\text{ValueFirstPeak}} \times (\text{DistanceFirstSecond}) \times \frac{1}{\text{WidthFirstAtHalfMax}^3} \quad (9.1)$$

From the equation it can be derived that narrow peaks far from each other will get large score, whereas low and wide connected peaks will get a low score as intended for the separation. The scores are only calculated for bands lower than 650[nm], calculating for higher bands would not make sense due the nature of the spectrums.

Experience shows that the resulting region-of-interest masks still include a thin line originating from Petri dish. In order to remove the line, a 5x5 median filter applied to the ROI. The filter

not only removes the thin line, but also creates a smoother border around the isolated meat area. The ROI before filtering, the resulting ROI and the difference image is shown in Figure 9.3.

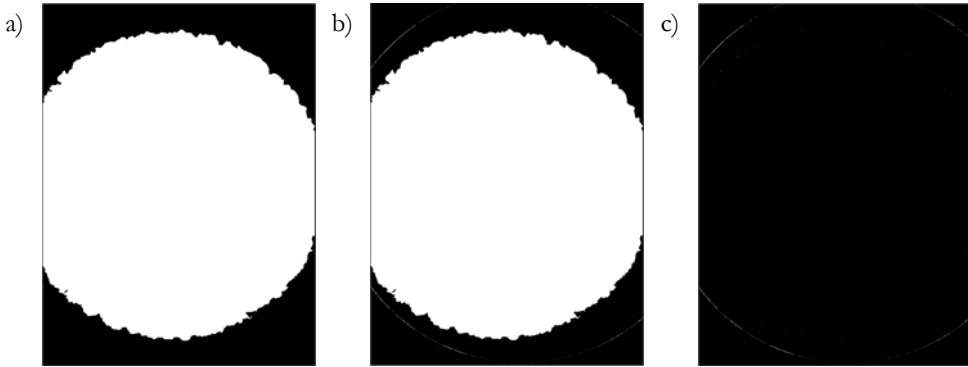


Figure 9.3 - a) ROI before filtering, b) ROI after filtering, c) a-b

### 9.3.2 Isolate meat tops

Having removed the non-meat objects, there still is a large variation over the meat left in the image. This is due to the granule structure of the meat, creating dents in surface. The next step of the pre-processing procedure is to isolate the top of the granules, to ensure less variation over the granules.

In-order to isolate the granule tops the h-domes segmentation technique is used, along with a threshold on the resulting h-domes image. To get the optimal results of the h-domes segmentation profiles of the image has been examined, concluding that band 10 (700 [nm]) with an h-value of 35 and a threshold value of 7 is an appropriate choice.

Below is shown an example image along with the image after removing non-meat objects and the mask obtained using the h-domes transformation.

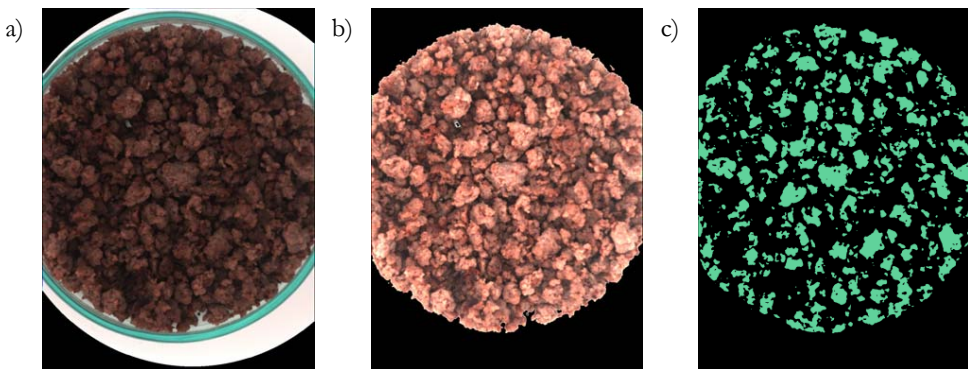
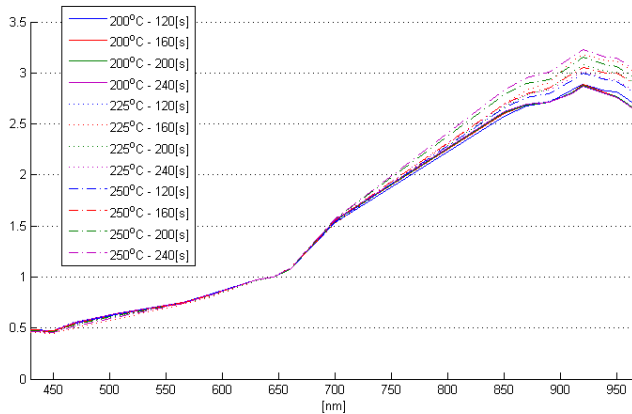


Figure 9.4 – a) Example image, b) After eradication of non-meat objects, c) Resulting pre-processing mask

## 9.4 Preliminary spectrum comparison

To stress the relevance of further analysis a preliminary spectrum comparison is performed. This comparison will outline the changes observed in the spectra due to heat treatment of the meat. For each meat sample a mean spectrum is derived from the image area consisting only of meat, these spectra form the basis for the comparison.

It is found that the differences introduced are best visualized by normalizing the spectrums around band 8.



**Figure 9.5 - Preliminary spectra comparison**

Figure 9.5 clearly shows differences introduced by the heat treatment. The main difference is observed in the upper bands where protein, fat and water have absorption. This is expected since meat expels water and fat, due to contraction as a result of the de-naturation of the proteins. The changes in this part are mainly observed as an introduction of a “break” on the curve around 950[nm].

Furthermore it is a general tendency is that the more heat applied the larger is the ratio to band 8 is in the higher bands, this is clearly observed in Figure 9.5 where the under-processed samples all are grouped together below the other spectra.

Further interesting is the minor differences in lower bands; especially band 4 and 6 was expected to have larger differences due to met-myoglobin and oxy-myoglobin. This is however not the case, most likely since the all samples have undergone sufficient heat treatment, such that the myoglobin is transformed into de-naturated met-myoglobin.

## 9.5 Multivariate analysis

To further enhance the differences found in the preliminary spectra comparison, in-order to provide an assessment of the frying treatment, various multivariate analyses are applied.

### 9.5.1 Principal Component Analysis

Recalling the principal component analysis (PCA) it will extract the patterns in the images, accounting for the largest part of the variation. The PCA was performed on the pre-processed images, to insure that it only takes the variation introduced by the meat applied with different heat treatment into account.

It was found that the first two PCA components accounts for 96.7% of the total variance (85,26% and 11,67% respectively), examining the lower components, accounting for very small amounts of variation, they mainly show noise and are therefore not examined further. To examine the first two components further, histograms of the pre-processed and transformed images are plotted.

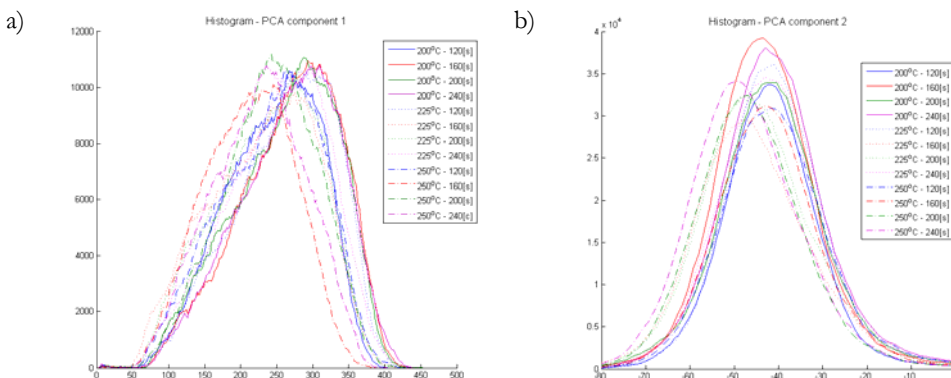


Figure 9.6 – a) Histogram curves PCA component 1, b) Histogram curves PCA component 2

From the histograms it is observed that different heat treatments results in different displacements of the top of the histogram curves. This displacement is generally more apparent in first component than in the second, but cannot be used directly from any of the components since the variation is very small. Instead one can use the combination of the two components to investigate the results further. To examine the combination the mean of the first and second component for each frying degree is plotted in a scatter plot.

The scatter plot is given in Figure 9.7. The plot shows two groupings of observations, which almost corresponds to the under- and adequately-processed division of meat samples however with some exceptions. To further enhance these groupings and their similarity to the under/adequate treatment classes, the border line between the under- and adequately processed observations is calculated and plotted using their classes discriminant functions. The

border line shows that the top right grouping, corresponds to the under-processed meat, with the exceptions of two measurements namely 250°C 120[s] and 225°C 240[s], and the bottom left grouping corresponds to the adequately-processed meat.

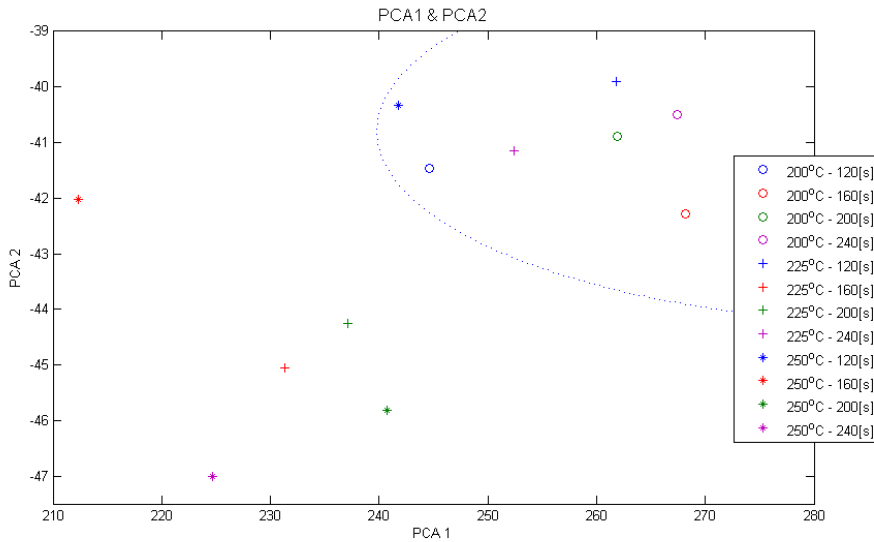


Figure 9.7 - PCA1 and PCA2 scatter plot

Generally it seems like it is possible to do an assessment of the heat treatment using PCA, however it does not seem completely accurate. The inaccuracy is not only observed in the scatter plot, but also the histograms plotted since they show little division between the different frying degrees.

## 9.5.2 Canonical Discriminant Analysis

In addition to the PCA, a canonical discriminant analysis is also applied to the images to see if it is able to separate the classes better than the PCA.

The images were preprocessed as described in 9.2, and divided into the classes described in Table 9.1. The canonical discriminant analysis was then performed, deriving the optimal linear combination of the 18 bands separating the data into the two processing classes.

To examine the separation of the data, a histogram curve for a transformed image from each frying degree is derived and plotted in Figure 9.8.

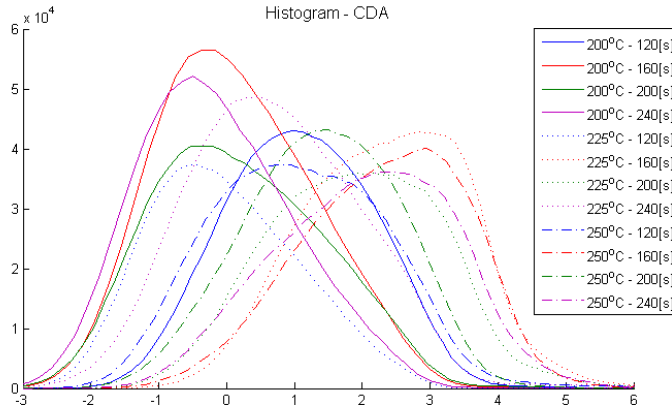


Figure 9.8 - Histogram – CDA

The histogram curves show a good separation of the different frying degrees, based on the top of the histogram curves. The under-processed samples seem to have their tops from 1 and down, whereas the adequately-processed samples seem to have their tops from 1 and up. The curves however seem to be somewhat wider, than the ones derived from the PCA. The wider curves indicate the image contains a variety of different frying degree, having such a range of different frying degrees seems inevitable in a process like this.

From the projections of the first CDF it seems like CDA is able to separate the frying degree using only one projection, and therefore it is decided to continue the heat treatment assessment using CDA.

Examining the derived linear combination, also called the canonical discriminant function, gives an impression of which bands are the most important in separating the frying degrees.

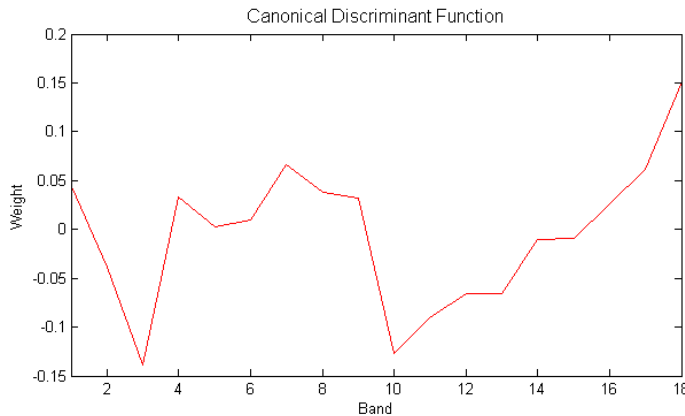


Figure 9.9 - Loadings Canonical Discriminant Function

The loadings of the CDF show that the most influential bands to the CDF seem to be 3, 10, 17 and 18. This is in accordance with the preliminary spectrum analysis, in which it was

concluded that higher values in the upper bands implies longer heat treatment, also it was found that most of the lower bands had little or no effect on the heat treatment.

### 9.5.3 The Frying-Treatment Score

As concluded in the prior section, the CDF derived from the CDA can be used to give an assessment for the frying degree in the images. The next step is to define a measure of the frying treatment based on that linear combination.

The measure of frying treatment will be denoted the Frying-Treatment Score and abbreviated FTS. Recalling the CDF function, the results of applying it to a multi-spectral image is a projection of the 18 bands, thereby essentially creating a grayscale image. The grayscale images can be compared, and one will find an intensity difference between the meats at different frying degrees. However since we, for now, are not interested in a visual inspection of the meat, but rather a measure for the entire image, it is decided that the FTS for minced beef is to be defined as:

*The Frying-Treatment Score (FTS) for a multi-spectral image containing minced beef, is the mean value of the pixels in the pre-processed image, containing only meat, projected with the CDF derived in 9.5.2*

Having this definition of the FTS for minced beef images, it is now possible to plot the scale of the FTS. Meaning plotting the FTS for the various images, thus giving an impression of how the FTS is distributed. Furthermore using the values from the images, it is possible to examine from which FTS value the images are categorized as adequately-processed, this is simply the mean value of the two groups (under and adequately processed) mean values. This cut-off point is found to be at a FTS value of 0.95. The mean of the three sub-sample images for each frying degree, and the cut-off point is plotted on the Frying-Treatment Score scale in Figure 9.10.

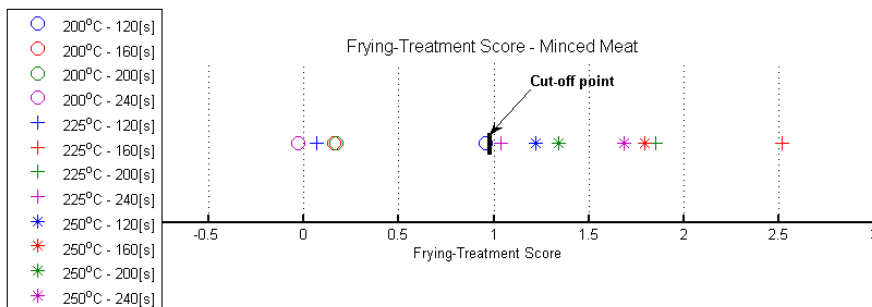


Figure 9.10 - Frying-Treatment Score - Minced Meat

From the points on the scale, one observes that the no samples seems to be placed on the wrong side of the cut-off point. Furthermore it is observed that the Frying-Treatment Score seems to be increasing along with the frying treatment. Having defined the FTS the next parts will show some applications of use.

### 9.5.4 Regression analysis

To investigate the relation between temperature, frying time and the FTS factor, the relation is fitted using least square regression. The model is created such that it gives an estimated time based on the measured FTS and frying temperature, this is done since this will give an estimation of a value for which the ground truth is known.

To find the optimal degree of the regression model a 3-fold cross validation is used, dividing the dataset in three subsets. This is done by having one value for each combination of time and temperature in each subset; this is possible since triple determination was used when acquiring the images.

From the cross validation the root mean square error and the  $R^2$  value is determined; this can be used to select the appropriate model. The results are shown in Table 9.4.

Polynomial degree	RMSE <sub>T<sub>test</sub></sub>	RMSE <sub>T<sub>train</sub></sub>	R <sup>2</sup>
1	44.78	44.71	0.00
2	39.58	32.97	0.43
3	30.97	26.85	0.62
4	120.34	24.10	0.67
5	122.51	23.57	0.68

Table 9.4 - Cross Validation Results

From the validation results of the various models, it can be concluded that the optimal relationships is the cubic relationship. Furthermore the results show that the cubic relation accounts for 62% of the variance in time. From the cubic relation contours are drawn as shown in Figure 9.11.

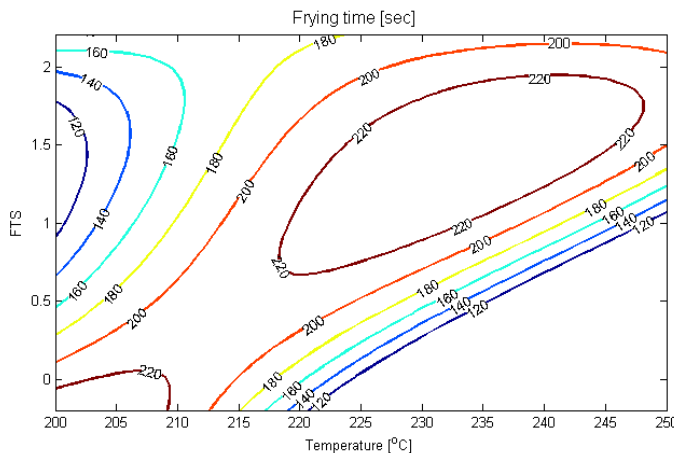


Figure 9.11 – ISO lines frying time

The inaccuracy which occurs in regression clearly shows in the contours drawn. For example are the contours suggesting that a high frying treatment score can be achieved at 200°C using a

relatively short frying time, this is of-course incorrect and suggest that the top-left-most part of the plot is invalid.

As the modeling of frying time suggests the optimal relation is cubic, it can be assumed that this is also the case for modeling the FTS based on time and temperature. By doing so the parameters are estimated with a goodness of fit of  $R^2 = 0.65$ , meaning 65 percent of the variance in FTS is accounted for by the temperature and frying time. This is an acceptable result, but it also shows that factors beyond the time and temperature have a significant impact on the FTS. Some of these effects can be the known varying quality parameters of minced beef, an example is the fat percent in minced meat, in [22] it is found that in one batch (from the same wholesale supplier as used for this experiment) the fat percentage can vary from 9% to 14% in meat said to contain 15-18%.

Having estimated the parameters for the polynomial using regression, it can now be used to further model the relationship between frying time, temperature and frying-treatment. This is done by deriving the contour lines for the FTS at various interesting FTS values. The contours are plotted in Figure 9.12.

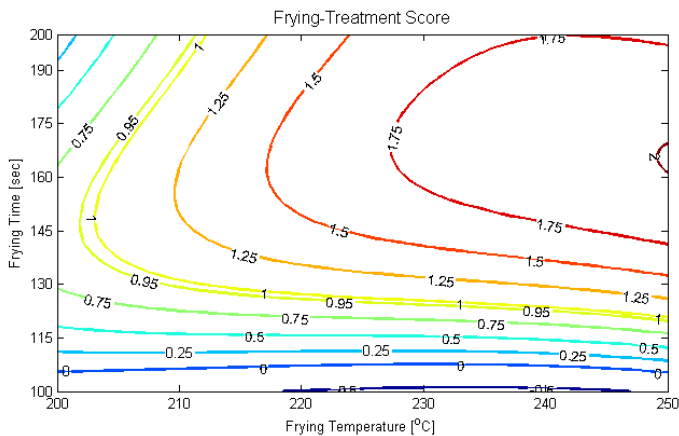


Figure 9.12 - FTS Contours, Time vs. Temperature

The model of FTS values implies that meat prepared at 120[sec] or less regardless of temperature (from 200°C to 250°C) does not seem to reach the frying degree of adequate-processed meat, which to some extent can be a fair approximation for the range plotted. It further shows that meat prepared at 200°C regardless of frying time, does not reach the adequate-processed frying degree either.

## 9.6 Visualization

The prior section in this chapter presents a method for evaluation the frying degree of an image using the Frying-Treatment Score. This section will examine a way of visualizing the results, by creating a false RGB image enabling an easy way of examining the frying degree.

Recalling the CDF derived, it is creating a projection of the 18 band multi-spectral image, which essentially is a grayscale image changing in insensitivity based on the projected value of each pixel. However since the changes in the intensity is rather small, it is decided to scale the grayscale change over series of RGB values. This will create a false RGB image of the original image, assigning a certain color to a specific FTS value. The FTS values will be scaled to the RGB values as shown in Figure 9.13.

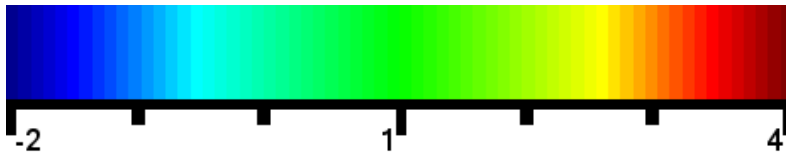


Figure 9.13 - FTS values to RGB

To further enhance the ease of visualization, only the parts of image containing meat, meaning the part isolated by the pre-processing, is converted using the false color composition, the remaining parts of the image are shown as if they were acquired using a regular camera. Examples of images converted are shown in Figure 9.14. All the resulting images are included in Appendix D.

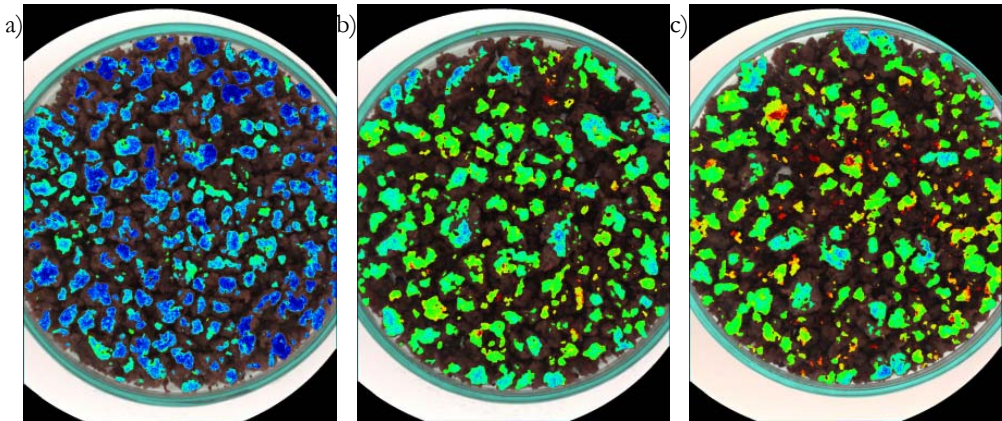


Figure 9.14 - a) 200°C - 160[s], b) 225°C - 200[s] c) 250°C - 160[s]

These examples clearly show how the visualization is able to show which meat granules are adequately processed and which are under-processed.

## 9.7 Discussion

This chapter shows how it is possible to assess the frying-treatment of minced beef using multi-spectral images and multivariate statistics. By using canonical discriminant analysis to derive the optimal linear combination, separating the images at different frying degrees, a Frying-Treatment Score (FTS) is defined based on the result of the projection. It is found that the defined FTS gives an assessment of the frying treatment, such that increased frying treatment results in an increased FTS. Using the FTS of all the images in the dataset, it is possible to define the FTS cut-off point, from where meat can be categorized as adequately processed; this point is found to be at 0.95.

Using the Frying-Treatment Score a model is created, to estimate the FTS based on the frying time and temperature. The model created is able to account for 65% of the variance in the FTS values, based on frying time and temperature. This relatively low amount of variance is most likely due the fact that some parameters with-in the minced meat, such as fat percentage, can vary within a batch making it harder for the analysis to generalize for a specific type of minced meat. Also other factors such a temperature when entered into the wok, and time from frying to imaging can create inaccuracies.

Along with the defining FTS, an example of how it could be used to visualize the frying treatment is given. The visualization transforms a multi-spectral image into a RGB image, in which the meat objects are colored based on the FTS values. The entire dataset converted to these false RGB images are given in Appendix D.

## Chapter 10      Agglutination of Minced Beef

---

The frying process described in [5] requires the minced meat to be frozen when it enters the continuous wok; if the process fails to comply with this requirement the resulting meat has a tendency to agglutinate. It is important for fried minced meat that the meat has a uniform size, and that it does not include large lumps. This chapter examines the possibility to detect such agglutination using vision technology.

The methods and results obtained in this chapter have been presented in the following publications:

*New Vision Technology for Multidimensional Quality Monitoring of Continuous Frying of Meat*  
The article is to be submitted to Elsevier's international journal *Food Control*.

## 10.1 Sample preparation

The meat samples used in this experiment was prepared in accordance with the experiment design included in Appendix C, using the method briefly described in section 9.1.

After chopping the meat it was contained in plastic cups, without cooling to thaw for the time specified in the experiment design. After thawing the meat was placed on ice to prevent further thawing before frying. The time on ice was held to a minimum to prevent the meat from freezing.



Figure 10.1 - Meat contained in plastic cups without cooling, and tray to use for cooling during frying

The experiment design specifies three thaw times namely 30, 90 and 150 minutes.

### 10.1.1 Wok frying

When the thaw time elapsed samples were fried in the continuous wok, at different temperatures and times to examine the frying treatments effect on agglutination. The temperatures used was 200°C and 225°C, and for each of these temperatures a sample was created with the frying times 160[s] and 240[s]. This provides us with samples having characteristics of both under- and adequate processed.

### 10.1.2 Image acquisition

For each combination of thaw time, frying time and temperature, 3 sub-samples were taken out for imaging. The sub-samples taken out for imaging were selected such that it ensured a somewhat representative selection of the entire sample. Meaning it was ensured that large particles were present in the sub-samples, if they were present in the entire sample production. The sub-samples were placed in a Petri dish and a finger was run over to remove excess

particles. The images were acquired using the VideometerLab software and saved in the hips format.

## 10.2 Physical / chemical experiments

To examine some of the physical and chemical properties of the fried meat, two experiments were made. One to determine the amount of large particles and one to determine the water content of the meat.

### 10.2.1 Strainer loss

In order to examine the amount of large particles in the meat sample, the meat was run through a strainer and the amount of meat kept in the strainer was measured. The strainer used had square holes with a side length of 1.1-1.2 cm.



Figure 10.2 - Strainer

Thaw time / Temperature	Frying time [s]	Before strainer [g]	After strainer [g]	Loss [g]	Loss %
<b>30 min</b>					
200°C	160	162.4	160.7	1.7	1.04
200°C	240	208.2	208.2	0.0	0.00
225°C	160	240.3	239.8	0.5	0.21
225°C	240	317.7	314.7	3.0	0.94
				<i>Ang.</i>	<i>0.55</i>
<b>1h 30 min</b>					
200°C	160	264.2	259.2	5.0	1.88

Thaw time / Temperature	Frying time [s]	Before strainer [g]	After strainer [g]	Loss [g]	Loss %
200°C	240	487.7	462.9	24.8	5.09
225°C	160	457.7	446.7	11.0	2.40
225°C	240	352.1	544.2	7.8	2.22
				<i>Avg.</i>	<i>2.90</i>
<b>2h 30 min</b>					
200°C	160	310.5	290.0	20.5	6.59
200°C	240	350.3	327.0	23.3	6.65
225°C	160	371.3	349.0	22.3	6.01
225°C	240	287.9	268.8	19.1	6.63
				<i>Avg.</i>	<i>6.47</i>

Table 10.1 – Strainer loss

The results of the strainer loss experiment shows a loss of <1% for the samples without considerable thawing, and a loss of 6-7% for meat let to thaw for 2½ hours. This clearly shows the thaw time has a significant influence on the agglutination. Furthermore the results imply that the frying treatment has no significant effect on the strainer loss, as the variance of the strainer loss over frying treatment seems to be rather sporadic. This is investigated further in a later section.

### 10.2.2 Water content determination

A water content determination was performed using the method described in the in the prior chapter. The results of the water determination is given in Appendix F and summarized in Table 10.2.

Water contents / Thaw time	200°C 160 [sec]		200°C 240 [sec]		225°C 160 [sec]		225°C 240 [sec]	
	Mean	$\sigma$	Mean	$\sigma$	Mean	$\sigma$	Mean	$\sigma$
<b>30 min</b>	50.3%	0.401	46.6%	0.245	45.3%	1.828	46.0%	0.080
<b>1h 30min</b>	43.4%	0.189	48.1%	0.672	47.5%	3.036	45.0%	0.271
<b>2h 30min</b>	48.8%	0.209	49.2%	0.117	53.8%	0.261	50.5%	0.325

Table 10.2 - Water contents - Minced Meat

The results generally seem to follow the same scheme as in the prior chapter, where water contents decrease when frying treatment increases. Since it was concluded in the prior chapter that both frying time and temperature, has a significant influence on the water contents, this will not be examined further. Instead an ANOVA is performed to examine if the thaw time has an influence on the water contents. For this purpose the frying time and temperature is combined into a factor called *treatment*. This is done to simplify the analysis to a two factor analysis; the resulting ANOVA table is given in Table 10.3.

Source	Sum of Squares	df	Mean Square	F-Ratio	Pr > F
Across	273.08	11	24.83	22.31	0.0000
Treatment	14.45	3	4.82	4.33	0.0142

Source	Sum of Squares	df	Mean Square	F-Ratio	Pr > F
Thaw time	138.39	2	69.19	62.17	0.0000
Treatment x Thaw Time	120.23	6	20.04	18.00	0.0000
Within	26.71	24	1.12		
Total	299.41	35			

Table 10.3 - ANOVA table water content - Minced Meat

The results of the ANOVA show that the thaw time is greatly influential on the water contents of the end product. From Table 10.2 it seems like the water content increase as the wait time increases. Furthermore the ANOVA results show that the interaction effect of thaw time and temperature is also significantly influential.

## 10.3 Pre-processing

As with the samples used in Chapter 9 (for frying treatment assessment), the samples used for this analysis also included unwanted objects in the images. Due to the similar process of acquiring the images the first stage of the pre-processing can be reused. For more details on separating the meat objects from the other objects refer to section 9.3.1.

Since the analysis for this chapter concentrates on the spatial properties of the image, namely the formation of lumps in the meat, a different approach than the one taken in the prior chapter is taken. To examine the formation of lumps in the image, one must carefully extract the meat granules present in the image, as opposed to the prior chapter where the main goal was to minimize the spectral information by isolating the granule tops. The approach for a carefully isolation of the meat granules is explained further in the following section.

## 10.4 Assessing agglutination

Having the preprocessed images, containing only meat, the goal of the analysis is to isolate the meat granules, using the spatial information of those to provide measures for the agglutination in the meat samples.

### 10.4.1 Optimal band selection

Since a spatial analysis is needed, it is important to select the optimal band of those available for performing the analysis. For the detection of lumps it is important that the band is able to distinguish between tops and dents in the meat sample.

To examine this property, a profile derived from a line, going through the horizontal middle, of the grayscale image of each band is created. The middle of the image is chosen, since this

contains meat granules over the entire profile, thus giving a better basis for comparison. Below is shown the profile plot, along with the corresponding grayscale image of the band.

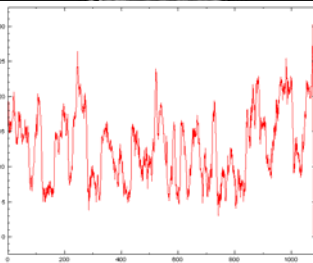
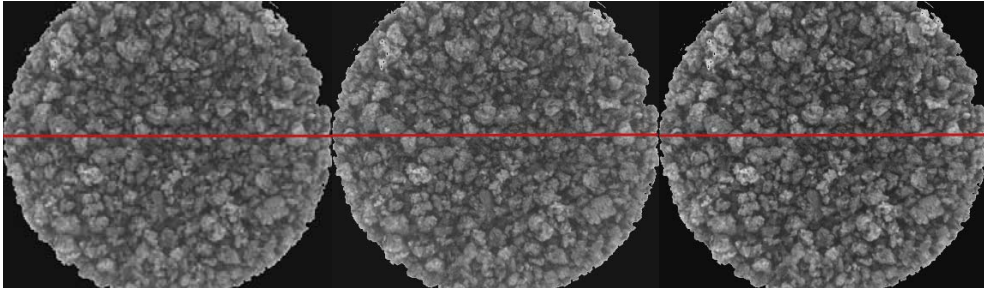


Figure 10.3 - Band 1

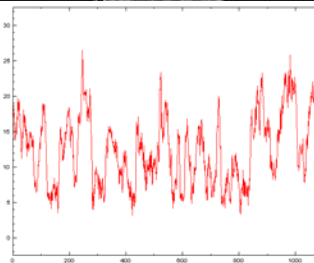


Figure 10.4 - Band 2

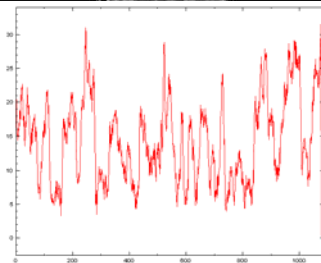


Figure 10.5 - Band 3

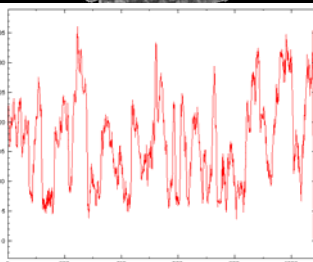
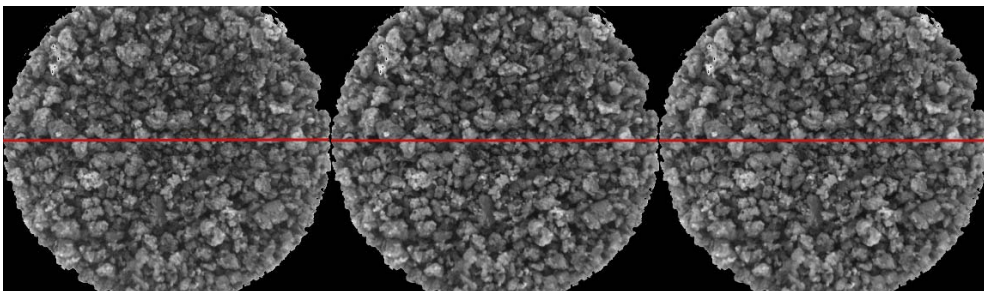


Figure 10.6 - Band 4

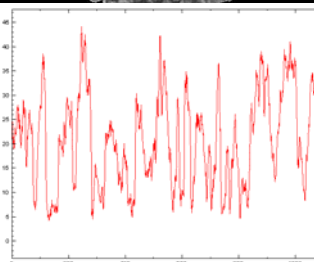


Figure 10.7 - Band 5

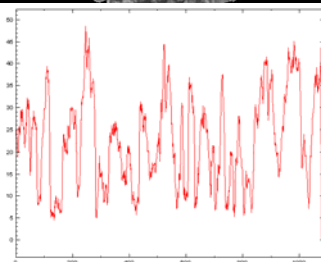


Figure 10.8 - Band 6

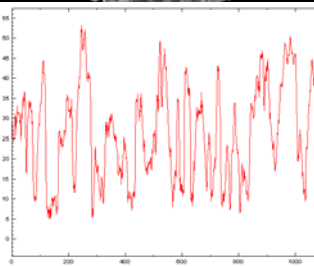
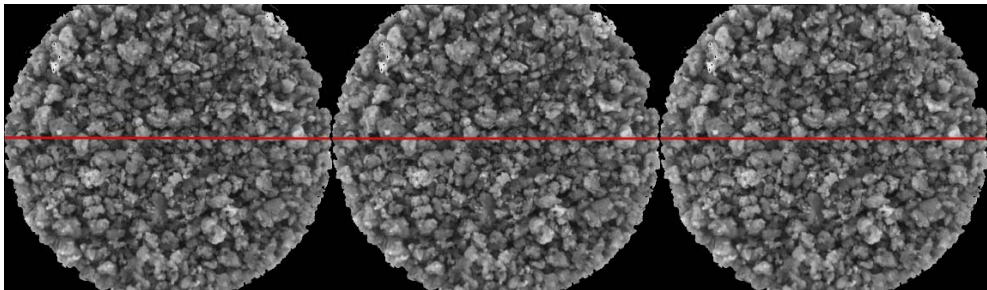


Figure 10.9 - Band 7

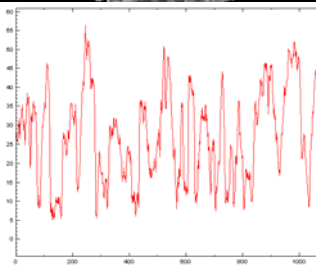


Figure 10.10 - Band 8

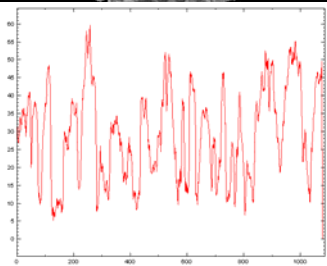


Figure 10.11 - Band 9

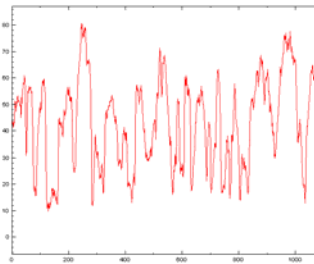
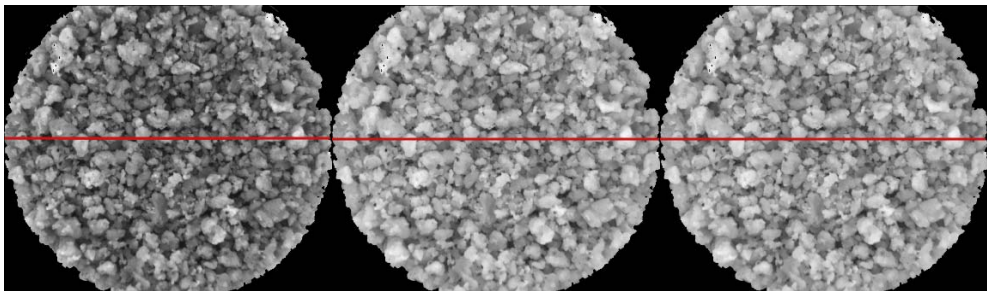


Figure 10.12 - Band 10

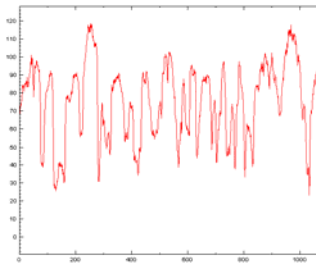


Figure 10.13 - Band 11

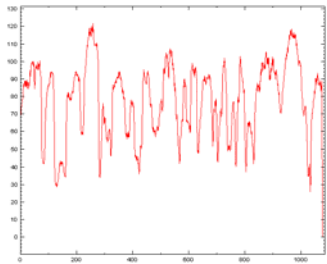


Figure 10.14 - Band 12

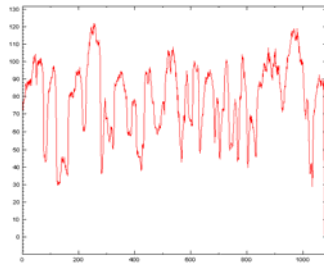
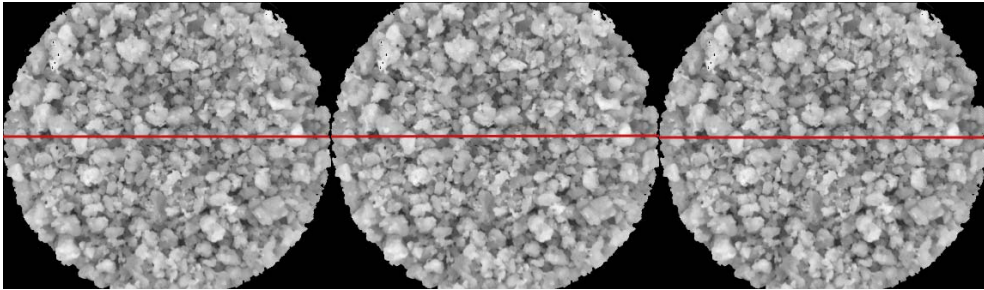


Figure 10.15 - Band 13

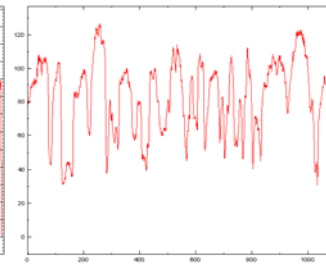


Figure 10.16 - Band 14

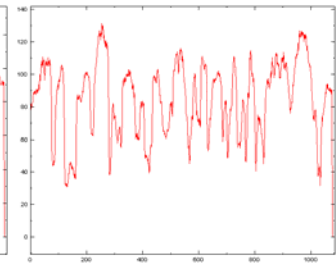


Figure 10.17 - Band 15

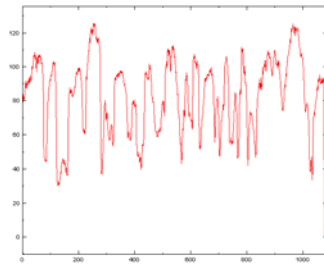
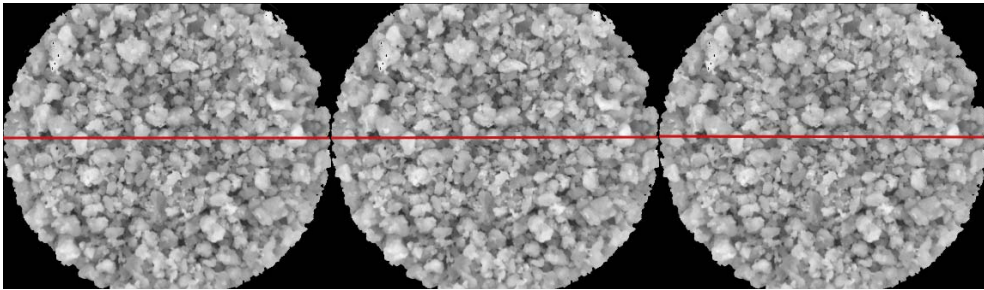


Figure 10.18 - Band 16

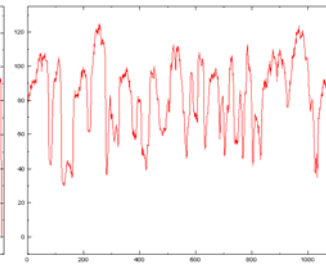


Figure 10.19 - Band 17

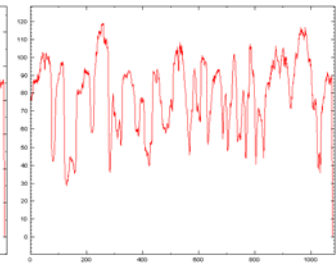


Figure 10.20 - Band 18

The profiles show that the lower bands profile is flickering a lot, and seems to be spanning over a low range of values thus making it unfit for this purpose. Around band 10 and up the curves become smoother, and the range of values used increases to a higher level, thus making them more fit for the purpose. It is chosen to use band 11 shown on Figure 10.13 for the purpose as this seems like the better fit.

### 10.4.2 Detection of meat granules and lumps

The method for detection of meat granules must be able to detect both large and small granules; and be able to separate the meat granules in the Petri dish even if they are located very close together, as it is the case with the sample images, were they are located even on top of each other.

For this purpose an h-domes segmentation technique is used, followed by a threshold and a connected component analysis for detecting meat granules. Recalling the basics of H-Domes segmentation a  $h$  value must be determined. To determine an optimal value for  $h$  the profile of band 11 can be examined again. Since the profile of meat granules is independent of orientation of the profile-line, the profile examined is again given for the horizontal line through the middle of the preprocessed image.

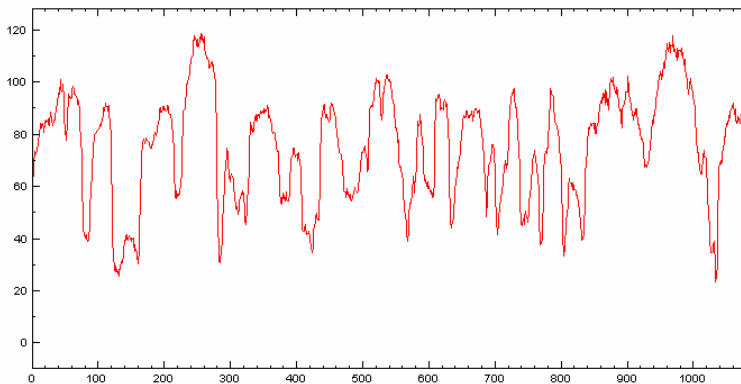


Figure 10.21 - Profile band 11

The  $h$  value must be small enough to separate all different granules, both also large enough to not create several spikes representing a single granule. Inspecting the profile shows that a value between thirty and forty, will be able to separate the granules creating only one spike for each granule. Through experiments the  $h$  value is chosen to be 35.

The next challenge is to select an appropriate threshold value for the resulting h-dome image. To assist in this selection the resulting image and the profile of this image is useful.

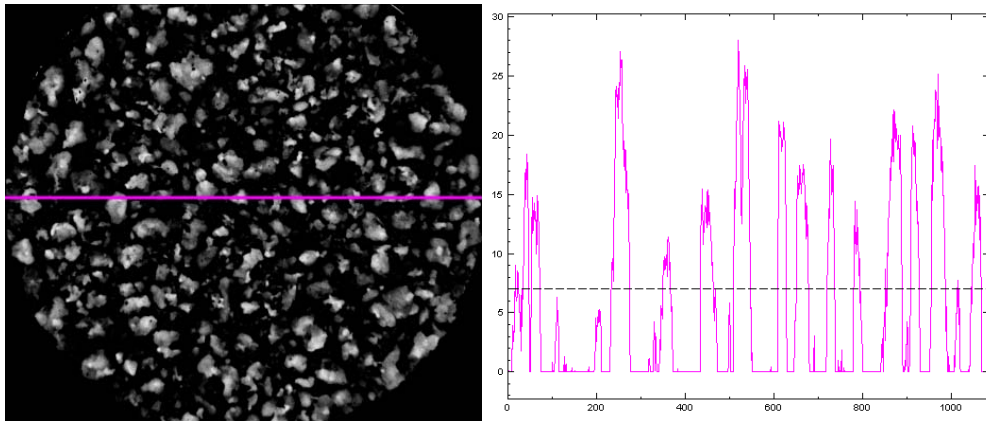


Figure 10.22 - H-Domes image & profile

Selecting a useful threshold value involves selecting a value which is small enough to include all significant granules, and large enough to avoid separating the spikes from large meat granules, thus being very similar to the section of an appropriate  $h$  value. From the profile in Figure 10.22 it can be derived that 7 seems like an appropriate threshold value. Using 7 as threshold value will result in the binary image given in Figure 10.23.

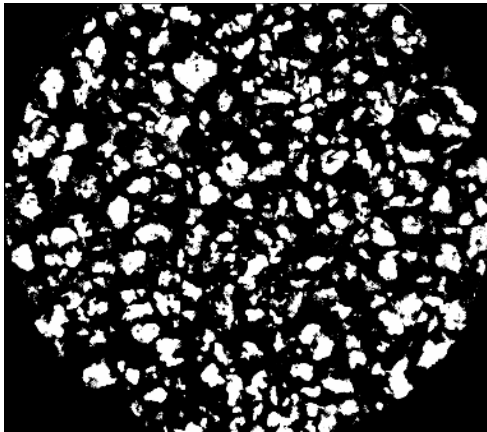


Figure 10.23 - H-Domes with threshold on 7

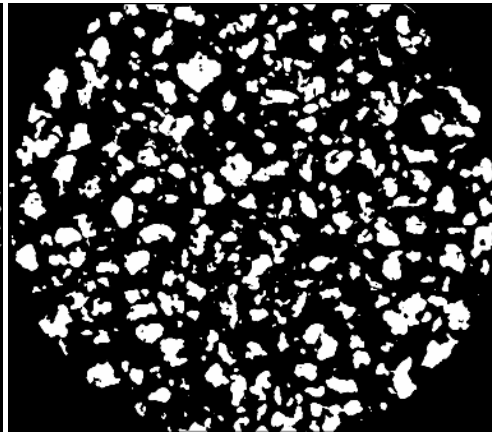


Figure 10.24 - Threshold image w. median filter

Figure 10.23 clearly shows that this technique is able to isolate the meat granules as needed; but the image still includes some noise-like elements which can disturb the connected component analysis. To remove the noise a 5x5 median filter is applied, this removes the larger part of the noise and provides a smoother image for the connected component analysis; the median filtered image is given in Figure 10.24.

The last step of the analysis is to find some measures for the agglutination. The first measure defined will simply count the number of connected components in the image, thus giving an approximation of the number of meat granules in the image. 4-connectivity is used for the connected components analysis. This is used since some of the meat granules are placed very close to each other, making 8-connectivity a better fit for the background. The second measure

defined is the mean size of the meat granules found, this measure can later be converted from pixel to  $\text{cm}^2$ , as the relation between pixels and square centimeters is known for the VideometerLab camera. Finally a third measure is defined as the maximum granule size detected in the image.

### 10.4.3 Estimation of meat area

Since all images acquired have a slightly different placement of the Petri dish, some images might include more of the Petri dish than others. Therefore a dynamic solution to the estimation of the area containing meat is needed.

First step is to crop the pre-processed images such that only the area containing meat is kept, thus throwing away the areas around the meat containing no information. Having cropped the image the dimensions can be directly used to estimate the meat area. Since the camera does not capture the entire Petri dish, the dish in the image can be assumed to be elliptic, thus easing the calculation of the meat area. This principle is shown in Figure 10.25.

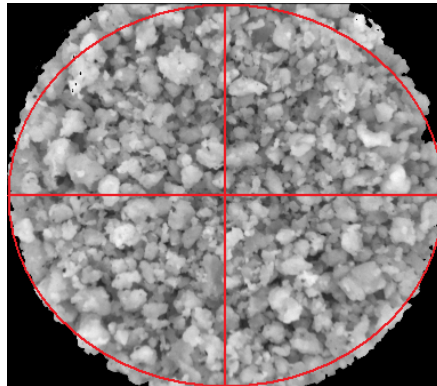


Figure 10.25 - Ellipse area estimation

The elliptic area can be calculated as:

$$Area_{\text{pixels}} = \pi \cdot a \cdot b = \pi \cdot \frac{1}{2} w \cdot \frac{1}{2} h \quad (10.1)$$

From [9] it is known that the relation between pixel and centimeter in the VideometerLab camera is given as  $0.077 \left[ \frac{\text{mm}}{\text{pixel}} \right]$ , this enables the conversion from pixels to  $\text{cm}^2$ .

$$Area_{\text{cm}^2} = \frac{0.077^2 \cdot Area_{\text{pixels}}}{100} \quad (10.2)$$

Having the meat area and the number of detected meat granules, the last measure of agglutination can be defined as meat pr.  $\text{cm}^2$ . This and the measures for mean size and maximum size is derived for all available images, and discussed further in section 10.4.4.

### 10.4.4 Results

For each sample image the estimated meat pr. cm<sup>2</sup>, mean size of granules, standard deviation of size and the maximum granule size is derived. All results are derived in square centimeters using the relation between pixels and centimeters from [9], the complete results table is included in Appendix G, and a summary is given in Table 10.4.

Thaw Time / Treatment	Meat pr. cm <sup>2</sup>	Mean granule size	$\sigma$ granule size	Maximum granule size
<b>30 min</b>				
200°C – 160[s]	6.37	0.0553	0.0949	0.5616
200°C – 240[s]	7.38	0.0476	0.0744	0.4958
225°C – 160[s]	6.18	0.0562	0.0950	0.6376
225°C – 240[s]	5.56	0.0638	0.1055	0.6901
Avg.	6.38	0.0557	0.0925	0.5963
<b>1h 30min</b>				
200°C – 160[s]	6.45	0.0535	0.0969	0.8081
200°C – 240[s]	5.91	0.0602	0.0162	0.9482
225°C – 160[s]	6.29	0.0555	0.3199	0.8489
225°C – 240[s]	5.46	0.0634	0.1119	0.7143
Avg.	6.03	0.0582	0.1588	0.8299
<b>2h 30min</b>				
200°C – 160[s]	5.55	0.0638	0.1254	1.0656
200°C – 240[s]	5.20	0.0720	0.1673	1.8337
225°C – 160[s]	5.29	0.0686	0.0892	0.9022
225°C – 240[s]	5.24	0.0677	0.1469	1.0957
Avg.	5.32	0.0680	0.1322	1.2243

Table 10.4 - Results image analysis

The results of the measures illustrate how they are able to assist in an assessment of agglutination. It is clear to see that the meat pr. cm<sup>2</sup> is decreasing as the thaw time increases, and that the meat granule size and maximum granule size increases along with the thaw time.

## 10.5 Analyzing results

This section will explore the relation between the physical method and image analysis method for measuring agglutination. The two methods have obvious differences, e.g. the physical method takes the entire meat sample into account, whereas the image analysis method only

uses the top layer of the three Petri dishes of meat, despite of the differences the results of the methods still proves to be comparable.

### 10.5.1 Initial comparison

The first action taken to compare the four measures, strainer loss, meat pr.  $\text{cm}^2$ , mean granule size and maximum granule size, is to normalize them to zero mean and unit variance. This is done to be able to plot them in the same plot, and thereby get an impression on how they relate.

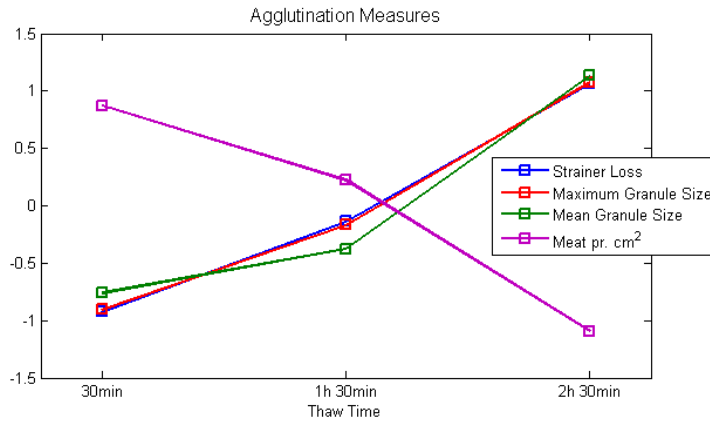


Figure 10.26 - Agglutination Measures

From the plot it is observed that the granule size measures and the strainer loss is positive correlated, and the strainer loss and meat pr.  $\text{cm}^2$  is negative correlated, this was also expected. Overall it can be concluded that there is a high correlation between the strainer loss and the measures acquired using image analysis. Thus showing these can be used for assessing agglutination.

### 10.5.2 Regression analysis

To further investigate the relation between the measures and the strainer loss, and to investigate the relation between frying degree and strainer loss, two types of regression analysis is performed. One tries to model the strainer loss based on the measures gained through the image analysis, and the second one tries to model the strainer loss based on the thaw time and the frying degree.

#### 10.5.2.1 Modelling strainer loss by spatial measures

From the image analysis results it has been chosen to use the maximum meat granule size and the mean granule size. These are selected as they are independent of the image area and therefore more realistic in a production scenario.

To determine which regression model is the optimal a 3-fold cross validation is performed dividing the dataset into three subsets, each containing one image for a combination of thaw time, frying time and frying temperature. The strainer loss is modeled using a 1<sup>st</sup>, 2<sup>nd</sup>, 3<sup>rd</sup>, 4<sup>th</sup> and 5<sup>th</sup> degree polynomial, for each model the  $R^2$  value and the root mean square error is recorded in Table 10.5.

Polynomial degree	RMSE <sub>Test</sub>	RMSE <sub>Train</sub>	R <sup>2</sup>
1	2.04	1.80	0.48
2	1.83	1.67	0.56
3	106.47	1.50	0.58
4	687.11	1.09	0.72
5	3815.52	0.68	0.83

Table 10.5 - Cross Validation Results

Based on the root mean square error it seems like the squared relation is the optimal. The relation is found to give a  $R^2 = 0.56$ , meaning 56% of the variation is accounted for using these parameters. In Figure 10.27 contours are plotted using the estimated parameters.

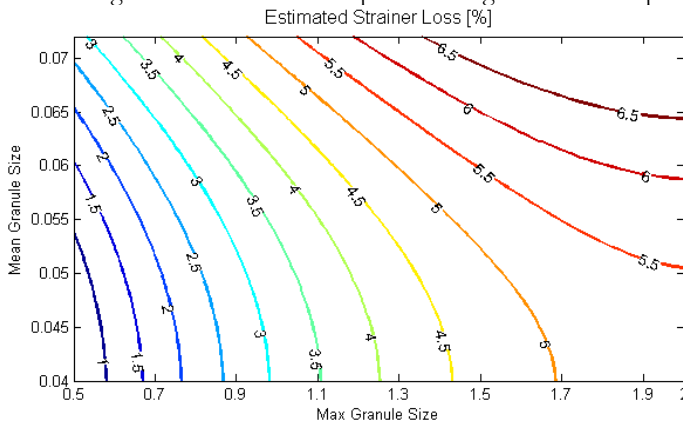


Figure 10.27 - Estimated Strainer Loss

### 10.5.2.2 Modelling strainer loss by spectral measures

Another interesting approach to the strainer loss, is to model it based on the thaw time and the degree of frying, this will help enlighten aspects of the agglutination e.g. if it can be minimized by applying a higher frying treatment. To get a measure of the degree of frying, the definition from the prior chapter is used to derive a FTS for each image used for agglutination assessment.

Again 3-fold cross validation is used and the  $R^2$  and root mean square errors are recorded resulting in Table 10.6.

Polynomial degree	RMSE <sub>Test</sub>	RMSE <sub>Train</sub>	R <sup>2</sup>
1	0.80	0.77	0.91
2	0.70	0.68	0.93
3	0.73	0.67	0.93

4	0.77	0.62	0.94
5	1.60	0.60	0.94

Table 10.6 - Cross Validation Results

The results show that the optimal model of the strainer loss based on frying treatment and thaw time is squared, this relation has the smallest error and accounts for 0.93% of the variation using these parameters. This shows a large improvement in both R<sup>2</sup> and error from the spatial properties, meaning it is easier to predict the strainer loss knowing the thaw time and frying treatment. This is also expected since the thaw time has a large influence on the strainer loss.

To illustrate the relation contour lines are plotted in Figure 10.28, the contour lines support the suggestion made in [4] suggesting that higher heat treatment results in lower agglutination. This seem to be especially significant for higher FTS values (> 1).

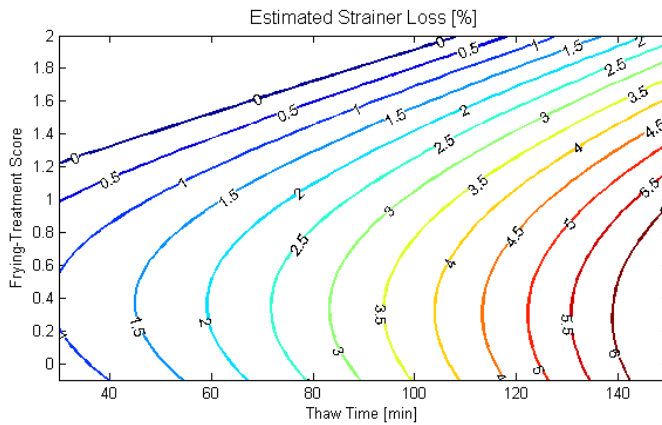


Figure 10.28 - Estimated Strainer Loss

## 10.6 Discussion

The results obtain in this chapter shows how it is possible to obtain measures from a multi-spectral image containing minced meat, which can assist in assessing agglutination for minced meat. The chapter defines the measures: meat pr. cm<sup>2</sup>, mean granule size and maximum granule size and derives these for all sample images.

From the resulting data it is found that these have a high correlation to the strainer loss, which shows that these can be used to assess the agglutination of minced meat. This relation is investigated further using regression analysis, this further supported the proposition.

Furthermore the relation between agglutination, thaw time and frying treatment is examined, concluding that the frying treatment seems to have some influence of the agglutination. Namely that increased frying treatment can decrease the agglutination of the minced meat.

## Chapter 11      Assessment of Frying Treatment for Diced Turkey

---

Adequate frying treatment is important for preparing turkey meat, not only to provide correctly tasting meat having the correct consistency, but also to ensure healthy poultry meat free of potentially dangerous microorganism. This chapter will examine how frying treatment can be assessed for turkey squares, directly from or on a conveyor belt, without use of any physical pre-processing of the meat.

The methods and results obtained in this chapter have been presented in the following publications:

***New Vision Technology for Multidimensional Quality Monitoring of Continuous Frying of Meat***  
The article is to be submitted to Elsevier's international journal *Food Control*.

***A Method for Frying Treatment Assessment of Meat Using Multi-Spectral Vision Technology***  
The poster was presented on the 2007 Industrial Vision Day, the 23<sup>rd</sup> of May at the Technical University of Denmark.

## 11.1 Sample preparation

Whole turkey breasts were purchased in the retail store *Netto*, the turkey breast was prepared in accordance with the experiment design in Appendix G. A short description of the process, the wok frying and the image acquisition processes are included here.

### 11.1.1 Wok frying

The turkey breast were cut into pieces of approximately 10[g], 20 pieces were taken out for control measurements. The result of the control measurement is given in Table 11.1. The results show that the average weight is very close to the expected 10[g], however with a noticeable deviation. This is unfortunately typical when human interaction is needed, and it is acceptable for this experiment.

Meat piece #	Weight [g]	Meat piece #	Weight [g]
1	10.60	12	10.97
2	10.31	13	6.63
3	9.77	14	10.65
4	8.67	15	9.70
5	9.32	16	7.25
6	9.01	17	8.38
7	9.53	18	10.08
8	14.02	19	6.78
9	6.81	20	13.01
10	7.19	<i>Arg.</i>	9.48
11	10.05	<i>Std.</i>	2.09

Table 11.1 – Weight distribution turkey squares

After chopping, the meat piece were scalded for 7 seconds in boiling water. The scalding coagulates the soluble meat proteins in the surface layer, thereby preventing the meat from sticking to walls of the wok.

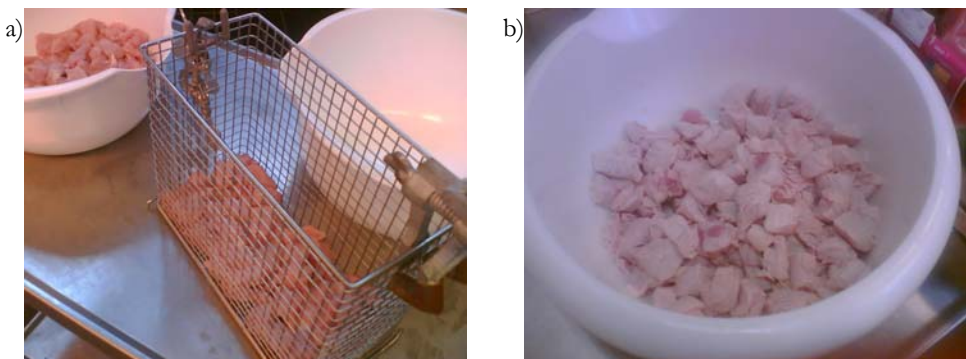


Figure 11.1 – a) Meat before lowering into boiling water, b) Meat after scalding

The basic experiment had the combinations of frying temperature and time given in Table 11.2. Table 11.2 furthermore shows the division into classes of under-, adequate- and over-processed meat.

Temp / Time	3 min	4 min	6 min	7 min	9 min
250°[C]	Under	Under	Adequate	-	-
275°[C]	-	Under	Adequate	Adequate	Over
300°[C]	-	Adequate	Over	Over	-

Table 11.2 - Temperature, time and expected frying treatment combinations

This division of meat is based on the following observations made during a test frying, conducted before the experiment, and is made in cooperation with a trained butcher. The under processed turkey meat is characteristic by having a clearly under processed core, easily identified when slicing, furthermore the surface is very bright and the meat is generally very moist. The adequately processed meat has a homogeneous looking core, the meat is moist and has a darker surface compared to the under processed meat. The over processed meat, has a homogenous core as the adequately processed meat but is generally slightly less moist and has a noticeably darker surface than the other processing degrees.

In addition to the experiments described above an experiment was conducted at 275°C and 7 minutes with non-scaled meat to investigate the effect of scalding before frying. Furthermore an experiment was made at 275°C and 300°C at 6 minutes, with a larger load of meat to investigate any effects the loading will have on the meat.

### 11.1.2 Image acquisition

For each experiment conducted three sub-samples consisting of four pieces of meat was taken out for imaging. The pieces were placed on a Petri dish with as much space as possible between them. The images were acquired using VideometerLab and saved in the hps format.

## 11.2 Chemical experiment

In order to establish a physical measure of comparison, a water content analysis was performed. The water contents were determined by taking 2-3 meat pieces of each sample, making them homogeneous with a liquidizer. From the homogeneous mass three samples of approximately 2[g] was taken out for 24 hours of drying at 105°C, the weight was registered before and after drying.

### 11.2.1 Water contents results

The complete results of the water contents experiment is presented in Appendix I, and summarized in Table 11.3.

Type / Temp.	3 min		4 min		6 min		7 min		9 min	
	Mean	$\sigma$								
250°C	66.9%	0.019	64.4%	0.318	64.9%	0.152	-	-	-	-
275°C	-	-	66.8%	0.052	65.1%	0.200	65.0%	0.060	62.8%	0.099
300°C	-	-	66.4%	0.334	63.7%	0.102	67.0%	0.310	-	-
W.o. scald. 275°C	-	-	-	-	-	-	68.2%	0.055	-	-
150g load. 275°C	-	-	-	-	65.4%	0.297	-	-	-	-
150g load. 300°C	-	-	-	-	64.2%	0.076	-	-	-	-

Table 11.3 - Water contents - Diced Turkey

To further examine the influence of frying time and temperature on the water content a two-factor ANOVA was created. The results are summarized in the ANOVA Table 11.4.

Source	Sum of Squares	df	Mean Square	F-Ratio	Pr > F
Across	67.83	14	4.84	54.19	0.0000
Time	40.13	4	10.03	112.22	0.0000
Temperature	3.99	2	1.99	22.35	0.0000
Time x Temperature	23.69	8	2.96	33.13	0.0000
Within	1.34	15	0.09		
Total	70.35	29			

Table 11.4 - ANOVA table water content - Diced Turkey

The ANOVA shows that the frying time has a very large influence on the water content, and that the temperature seems to have less influence. Furthermore the interaction effect also seems to be quite influential.

Considering the additional samples, it seems like increasing the load have no effect on the water content, and that scalding the meat might have a influence on the water contents. This however cannot be finally concluded from these results, as only a single sample without scalding was created.

## 11.3 Pre-processing

As it was the case with the other images acquired, the images contain objects which are not relevant to our analysis. Objects as the Petri dish and the metal sheeting of the camera, the pre-processing process is to eliminate these objects.

In-order to find a suitable method for eradicating the un-wanted object, the spectrums of these objects are examined and compared to the spectrum of the meat. Furthermore the histogram of selected interesting bands is investigated to assess the usefulness of a simple threshold solution. The spectra and histograms are shown in Figure 11.2.

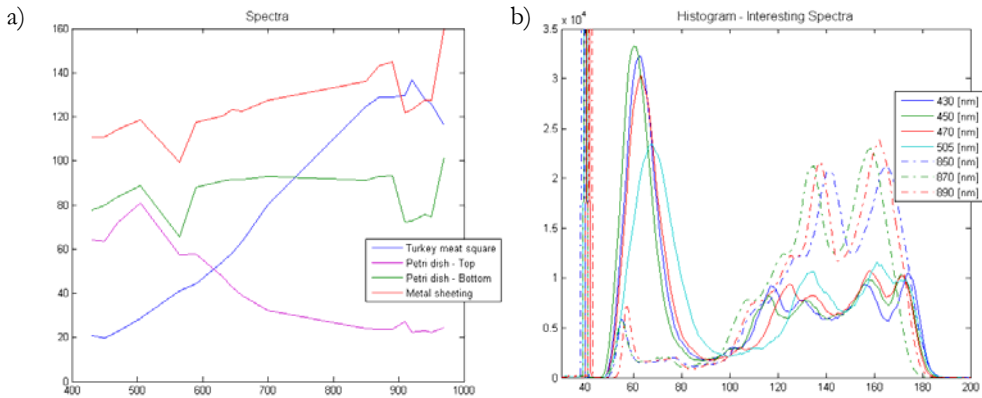


Figure 11.2 – a) Spectra of interesting objects, b) Histogram of interesting bands

As it can be observed in Figure 11.2a, the un-wanted objects has spectra that is very different compared to the meat. However when examining the histograms in Figure 11.2b, it is observed that the values are somewhat overlapping, meaning there is no zero value between the top representing meat pixel and the tops representing other objects. This can lead to undesired eradication of meat pixels and/or preservation of pixels belonging to un-wanted objects.

Instead of doing a threshold on an existing band, it is possible to take advantage of the spectrum shape. It is observed that the pixel value of un-wanted objects does not vary much throughout the bands, compared to the values of the meat. This property can be used by subtracting band 2 (450[nm]) from band 13 (890[nm]), the pixel values of meat will now be very high compared to the pixel value of the other objects. This is shown in Figure 11.3 where the difference image is shown along with histogram.

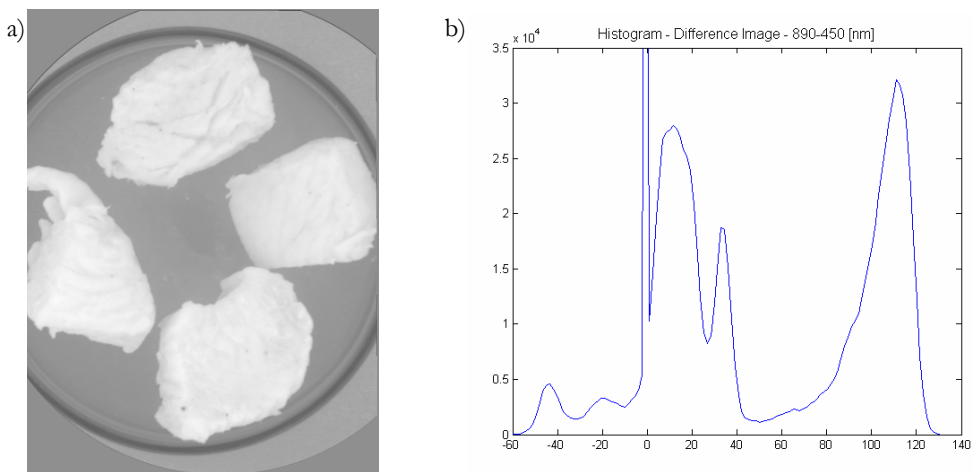


Figure 11.3 - a) 890[nm] - 450[nm], b) histogram of 890[nm] - 450[nm]

From the histogram it is clear that the low values (<40) represent the un-wanted objects, whereas the large spike around 110 is representing the meat pixels. Doing a threshold around 41, should leave us with a mask covering the meat objects only. It however is observed that

after doing the threshold, a few unwanted pixels from the Petri dish is still present. These can be removed by applying a 5x5 median filter as illustrated in Figure 11.4.

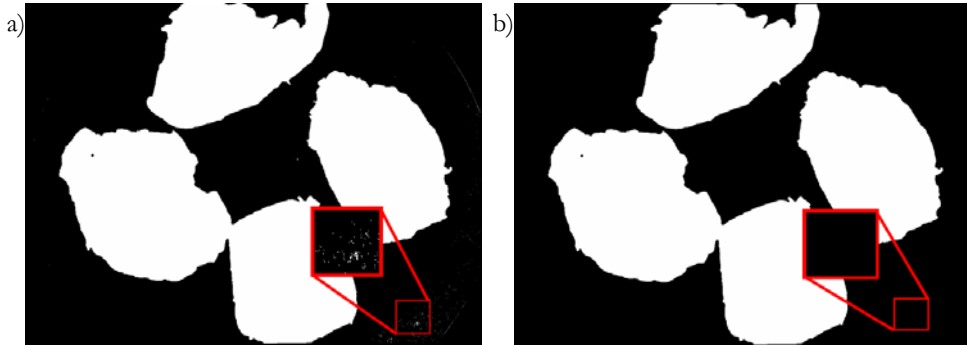


Figure 11.4 - a) Mask without median filter, b) Mask after applying median filter

Since the meat squares are cut out in an approximate cubical form, there is no need to perform further processing for isolation meat tops etc..

## 11.4 Preliminary analysis

In-order to determine if a basis exists for assessing frying treatment based on the spectral information, a preliminary analysis of spectrums from different frying degrees are examined. A random image from each combination of frying time and temperature is selected, and the spectrum is derived from a ROI containing meat and plotted in Figure 11.5

It is observed in the plot, that the differences between the different frying degrees seem to be substantial enough to continue the analysis. The plot clearly shows that there are differences over the entire spectrum, however largest in the lower visual part. This is a noticeable difference from the minced meat, where the differences were largest in the NIR spectrum.

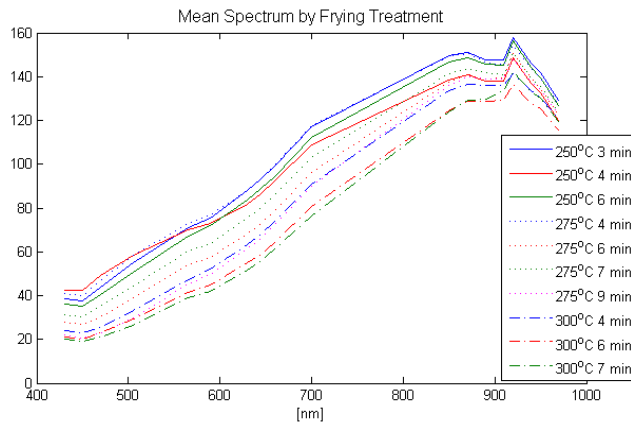


Figure 11.5 - Preliminary spectra analysis

## 11.5 Multivariate analysis

To assess the frying quality of the meat, the differences found in the preliminary analysis is to be enhanced by applying various multivariate analyses.

### 11.5.1 Principal Component Analysis

The first analysis to apply is the principal component analysis (PCA). This analysis will extract pattern found in the image, expressing it in a new multi-dimensional image.

The PCA was performed on pre-processed images, resulting in faster and more precise analysis since only differences in the meat data is examined. It was found that the two first components of the PCA accounts for 97.1% of the total variance (77.6% and 19.5% respectively), examining the remaining components shows that they were mainly containing noise, it is therefore decided to proceed examining the first two components.

For each frying degree (temperature and time combination) an image was transformed using the two first components of the PCA. From the resulting data a histogram was derived to examine the distribution over the components. The histograms are given in Figure 11.6.

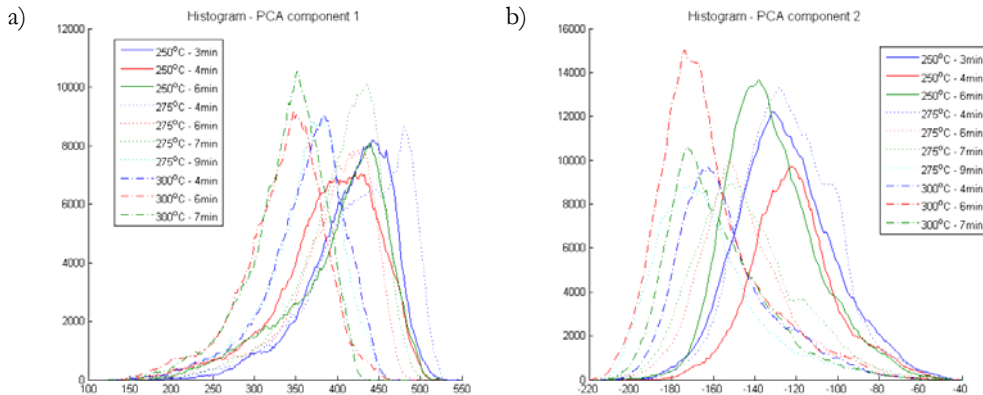


Figure 11.6 - a) PCA component 1 histogram, b) PCA component 2 histogram

From the histograms it seems like the first component creates a displacement of the histogram curves separating the over-processed meat from the other processing degree. And the second component seems to be better for separating the under-processed from the other processing degrees. Thus suggesting a combination of these could be used. This can be examined closer by plotting the mean value of the populations, into a plot where each component represents an axis.

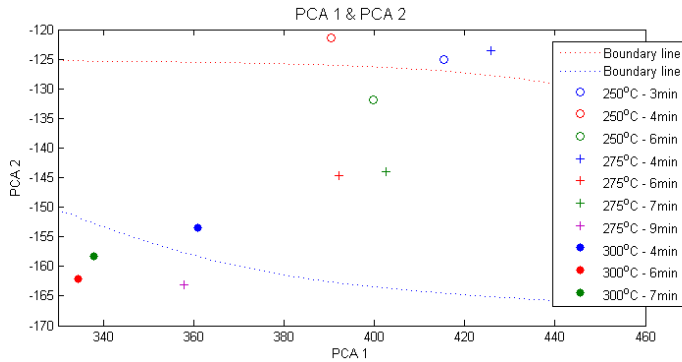


Figure 11.7 - Population means PCA1 vs. PCA2

This is illustrated in Figure 11.7, from the plot it seems like the two populations being under-processed and over-processed are gathered in two corners of the plot, thus implying the frying treatment can be assessed using these components. To illustrate this further the boundary lines, computed from the discriminant functions separating the classes, is plotted as well. The boundary line suggests that it is mainly the second principal component which is used for classification into classes. From this it can be concluded that the variations found by the PCA seem to reflect the variation in frying treatment.

### 11.5.2 Canonical Discriminant Analysis

Another obvious analysis to apply is the canonical discriminant analysis, finding a transformation separating the data from different frying degrees as much as possible. The classes used for the analysis are the ones given in Table 11.2 separating the meat into under-, adequately- and over-processed meat classes.

Separating the dataset into 3 groups results in two linear canonical discriminant functions, as with the components from the PCA, these can be used to derive histograms of transformed images. The histograms are given in Figure 11.8.

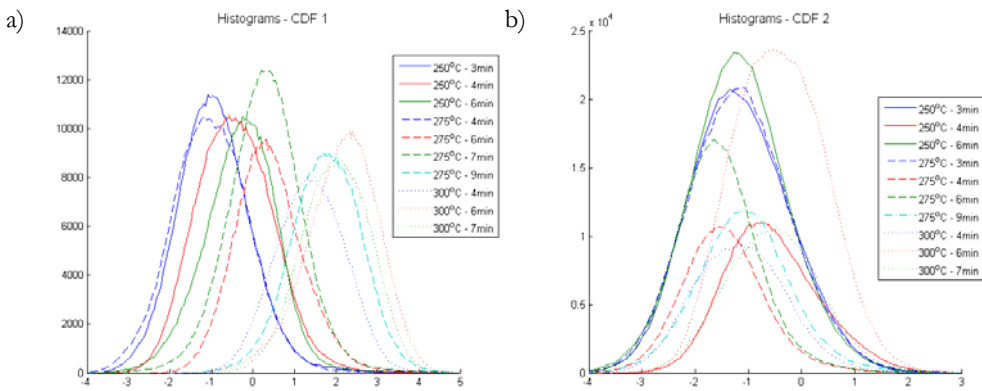


Figure 11.8 - a) CDF 1 Histograms, b) CDF 2 Histograms

The histogram shows that the first CDF seems to create a displacement of the histogram curve based on the frying treatment of the data. Furthermore it is noted that the histogram curves has a narrower bell shape, compared to the ones for the principal components. The second CDF however does not seem to create a displacement based on frying treatment.

To further examine the first CDF, the loadings is plotted thereby giving an impression of which bands are important with regard to separating the various frying-treatments of diced turkey.

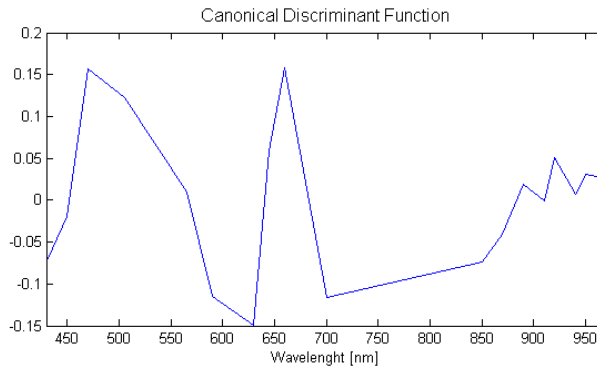


Figure 11.9 - Loadings Canonical Discriminant Function

The loadings for the CDF show that the visual part of the spectrum (<700nm) seems to play a very important role in separating the frying treatments, as compared to the minced meat where the high loadings mainly was present in the NIR bands.

### 11.5.3 The Frying-Treatment Score

To have a general base of comparison for the frying degree based on image analysis, the Frying-Treatment Score (FTS) for turkey meat is to be defined. Both multivariate analysis applied to the images, was able to separate the defined frying degrees. However the PCA needed two dimensions to separate the data into all classes, whereas the first canonical discriminant function seemed to be able to do the job on its own. Furthermore the histogram curves for the data applied with the first CDF, were smoother and had a narrower bell shape than those for the principal components, this motivates using the first CDF for defining the FTS.

Using the first CDF for defining the FTS is the same approach as used for the minced meat, however with different loadings for the CDF. This motivates a definition of the FTS similar to the one for minced meat; the definition for diced turkey is formulated as:

*The Frying-Treatment Score (FTS) for a multi-spectral image containing the surfaces of diced turkey, is the mean value of the pixels in the pre-processed image, containing only diced turkey, projected with the CDF derived in 11.5.2.*

This definition of the FTS now enables us to derive the scale of the FTS for diced turkey, giving an impression of the distribution of meat over the scale. Furthermore it enables the definition of the cut-off points, where meat is categorized as adequately-processed instead of under-processed and where meat is categorized as over-processed instead of adequately-processed. These can be found by finding the average of the two class' averages. The cut-off between under- and adequately processed meat is found to be -0.118, and the cut-off between adequately- and over-processed is found to be 1.05.

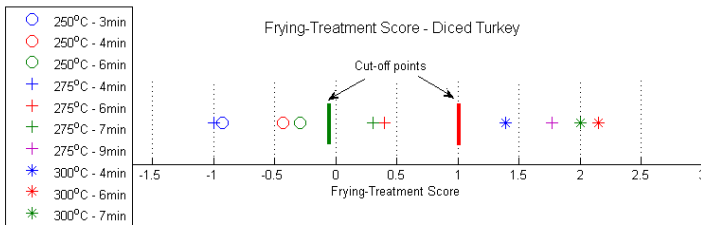


Figure 11.10 - Frying-Treatment Score - Diced Turkey

From the points plotted on the scale, one observed that the two of samples which was intended as adequately processed are not within the cut-off points. This is undesirable and could motivate another definition of the cut-off points, if they were to be used for categorization purposes.

### 11.5.4 Regression analysis

To investigate the relation between FTS, time and temperature, regression is used to try to model the frying time in seconds using the FTS and temperature. Models of 1<sup>st</sup>, 2<sup>nd</sup>, 3<sup>rd</sup>, 4<sup>th</sup> and 5<sup>th</sup> degree polynomials are tested using a 3-fold cross validation. The dataset are divided such that each contains a value of each combination of time and temperature.

The result of the cross validation is given in Table 11.5.

Polynomial degree	RMSE <sub>Test</sub>	RMSE <sub>Train</sub>	R <sup>2</sup>
1	70.75	70.09	0.55
2	47.75	41.92	0.83
3	44.62	34.22	0.88
4	48.34	32.97	0.89
5	186.45	25.16	0.92

Table 11.5 – Cross Validation Results

The cross validation results suggest the optimal model to be a cubic, this has the smallest error and a R<sup>2</sup> of 0.88, meaning 0.88% of the variance in time is accounted for by the FTS and temperature. The model gained is illustrated by drawing the contours of the interesting frying times in Figure 11.11.

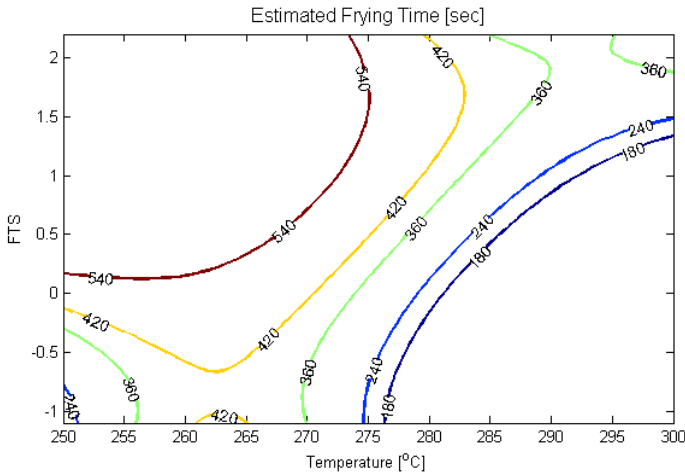


Figure 11.11 - Frying Time Contours

The model seems to be an acceptable approximation, it basically suggest higher frying times results in a higher frying-treatment score which is correct. Also it suggests that very high frying times are needed in order to obtain adequately processed meat at 250°C, which is also correct.

These results suggest that a model for the frying-treatment score, based on frying time and temperature will also have a cubic relation. Using this knowledge the model is estimated with  $R^2 = 0.98$  which means the by far largest part of the variance in the data is accounted for, this further support the FTS as useful measure of frying degree.

The resulting model is used to draw contour lines for the system.

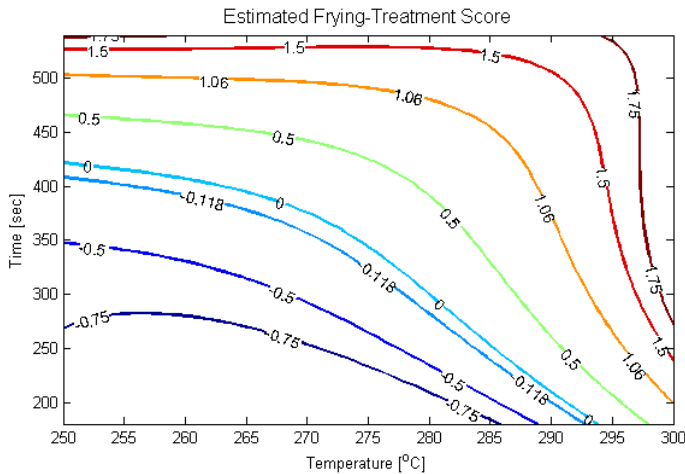


Figure 11.12 - FTS Contours Turkey Squares

The most interesting contour lines are the one at -0.118 which represents the cut-off line between under- and adequately-processed turkey squares and the one at 1.05 which represents

the cut-off line between adequately- and over-processed turkey squares. Within these lies the production window giving the optimal fried turkey diced.

From these lines it can be derived that the optimal temperature is around 285°C, as this gives the largest interval of times resulting in an adequate processing of the meat. As the temperature drop or increases the time window for adequately processed meat narrows.

## 11.6 Visualization

Having defined a way of assigning each image an FTS, another method for evaluation of the frying-treatment is proposed in this section, namely a visual approach. Visualizing the results gained via the analysis provides the process operator with a tool for visual evaluating the meat.

Recalling the CDF used for assigning a FTS value, this creates a projection of the 18 band image onto one band. The resulting band is essentially a RGB image, which intensity varies over the degree of frying-treatments. As for the minced meat, the changes in intensity are so small it is hard for the eye to interpret. To enhance the differences a scale for converting them into a RGB image is created. By examining the histogram curves from Figure 11.6a, it is found that the scale should cover FTS values from -4 to +4.

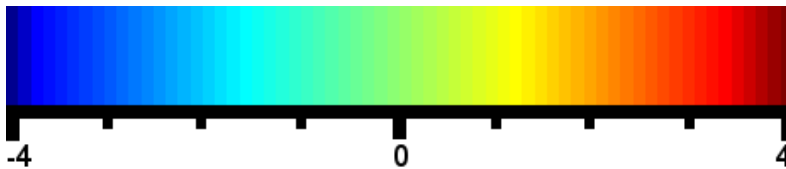


Figure 11.13 - FTS values to RGB

As for the minced meat images, only the parts of the image containing meat is converted using the scale from Figure 11.13, the remaining parts of the image is presented as if it was acquired with a regular camera. The entire data has been converted and is included in Appendix J, below is shown some samples.

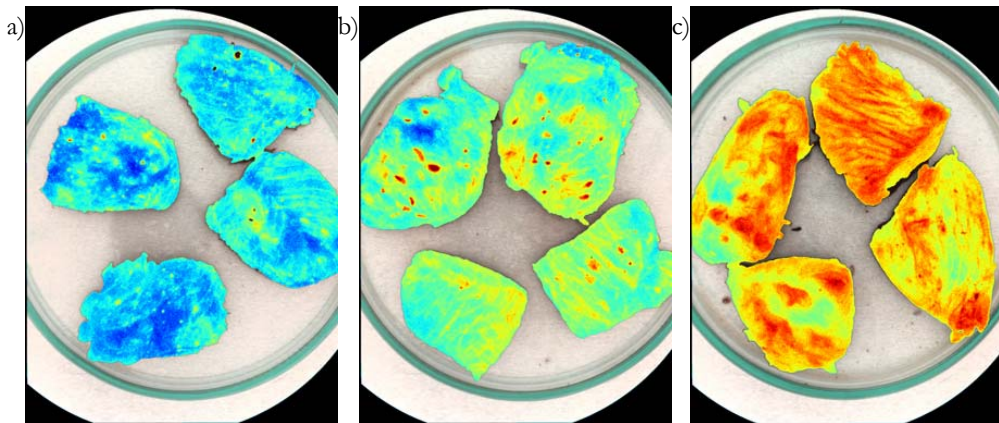


Figure 11.14 - a) 250°C - 4min, b) 275°C - 7min, c) 300°C - 6min

The sample image clearly shows the essence of the visualization, the underdone meat pieces are mainly covered by blue pixel, the adequately processed are covered by green/yellow pixels and the over processed show large red areas on the over processed meat.

## 11.7 Discussion

This chapter shows the principles used for frying treatment assessment of minced meat can be transferred to assessment of frying treatment for diced turkey meat. It is however only the principles that can be used as the meat naturally has large spectral differences a new canonical discriminant function must be computed for each type of meat. Using the CDA method the Frying-Treatment Score for diced turkey is defined.

The FTS is used to derive contours illustrating the optimal combinations of temperature and time for frying of turkey meat. The model of FTS based on frying time and temperature, proves to cover 98% of the variance in the FTS, which is an excellent result, compared to the one achieved for minced meat. This also comes to show in the contour lines, as these seem to give a very realistic illustration of the frying process. The counters can among others be used to adjust the settings of the wok in future when frying turkey squares.

Furthermore the FTS is used to create a visualization of the frying degree. This visualization creates a false RGB image, assigning colors to FTS values of the transformed image. The resulting images shows to give a very intuitive approach, to estimating the frying treatment of the meat contained in the image.

Using the FTS as defined in this chapter, it is now possible to analyze the effects scalding before frying and loading of the wok has to frying degree.

To investigate the effects of scalding the FTS is found for the samples without scalding at 275°C 7min. The mean FTS of the samples without scalding is -0.286, which actually indicates that it is under processed, compared to the normal mean FTS at 275°C 7min which is 0.356.

This indicates that scalding has an effect on the frying degree, as well as on the water contents of the meat as found in section 11.2.1, but cannot be finally concluded without further experiments.

Next the effect of increased loading is investigated using the same procedure. The mean FTS for a 150g loading at 275°C 6min is found to be 0.555, this indicates an increase in frying degree from the normal 0.220 at 275°C 6min. The same tendency is found at 300°C 6min, where the increased loading images have a mean FTS of 2.093 compared to the normal 1.982. The increased FTS was expected since blockings was observed in the frying pipe; the helix was simply not large enough to move the high loading of meat, resulting in some meat being left behind receiving additional frying treatment.

## Chapter 12      Assessment of Frying Treatment for Sliced Diced Turkey

---

In the prior chapter a method was found to assess frying treatment for turkey squares without any physical pre-processing. This chapter will investigate a method for assessment of frying treatment using sliced turkey squares, and compare this method to the assessment of frying-treatment based on the surface of turkey squares.

Slicing the turkey square intuitively gives a better domain for comparison of frying treatment, as the sliced dices of inadequately cooked meat will show areas of the meat where the proteins has not denatured yet, thus keeping the raw reddish color easily observed even for the human eye and introducing larger spectral differences.

## 12.1 Sample preparation

The turkey pieces were prepared in accordance with the description provided in section 11.1, with the exception of the image acquisition which is described beneath.

### 12.1.1 Image acquisition

For each combination of time and temperature 3 sub-samples of four pieces of meat were taken out for imaging. The meat pieces were cut into halves, and placed, with the internal part facing against the camera, in a Petri dish with appropriate spacing. The images were acquired using the VideometerLab camera and saved in the HIPS format.

## 12.2 Chemical experiments

Since the turkey squares used in this chapter are identical with the squares used in Chapter 11, there will not be performed any further physical or chemical experiments. For a recap on the results refer to section 11.2.

## 12.3 Pre-processing

Since the images were acquired using the same scheme as the images from the prior chapter, the need for removing the unwanted objects still exists. The images basically contain the same objects as in the prior chapter, but since the turkey pieces have been sliced it introduces a larger variation over the meat pieces. To examine these variations, spectra for red under-processed meat, white adequately-processed meat, Petri dish and metal sheeting have been plotted in Figure 12.1.

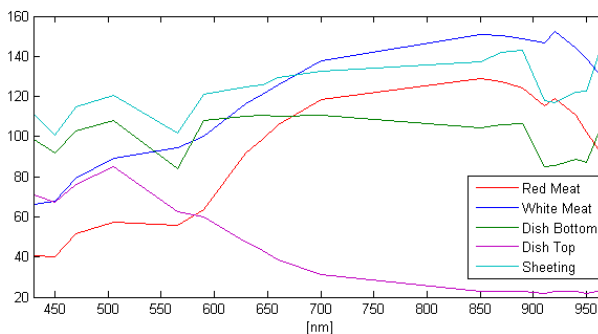


Figure 12.1 - Pre-processing spectra comparison

The spectrums show that it is not possible to perform a simple threshold operation on a single band, since there is no band with a large enough separation. Instead, the spectrums show that the unwanted items have a lower variation over the bands, than the meat spectrums. This motivates us to use the method used in the prior chapter, namely subtracting a band to gain separation. Examining the spectrums shows that a good separation would occur when subtracting the band at 430[nm] from the band at 850[nm], the histogram for the resulting image is shown below, along with the histogram obtained by using the bands used in the prior chapter.

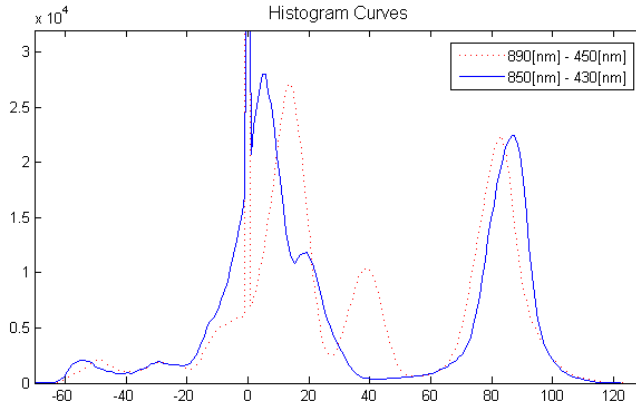


Figure 12.2 – Pre-processing histogram curves

From the histogram curves it is obvious that the 850-430[nm] subtraction, gives the by far better separation of the objects. The histogram curve can further be used to assess a good threshold value, at first sight it looks like a value between 40 and 50 would give a good separation since this is the local minima of the curve. By experimenting it is found that the optimal value is 47.

Figure 12.3 shows the results of each step of the preprocessing. From Figure 12.3c, showing the result of the threshold operation, it is observed a small amount of distortion in the image. This is removed by applying a 5x5 media filter resulting in the image shown in Figure 12.3d.



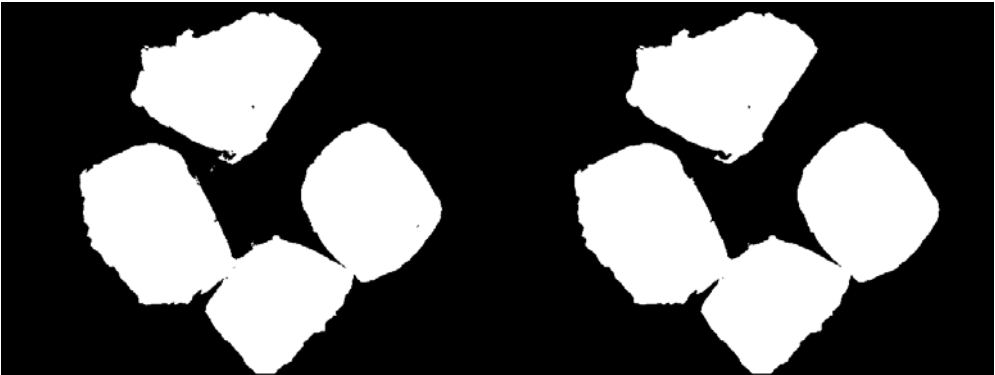


Figure 12.3 - a) Initial image (RGB), b) 850-430[nm], c) Threshold 47, d) Threshold + 5x5 median filter

Since the meat squares due the slicing have a level top, there is no need for further pre-processing to isolate the meat.

## 12.4 Preliminary analysis

To examine the differences in the spectrums based on heat treatment, a spectrum is derived for each combination of time and temperature. The spectrum is derived manually by selecting a ROI on a random meat pieces from the sample images.

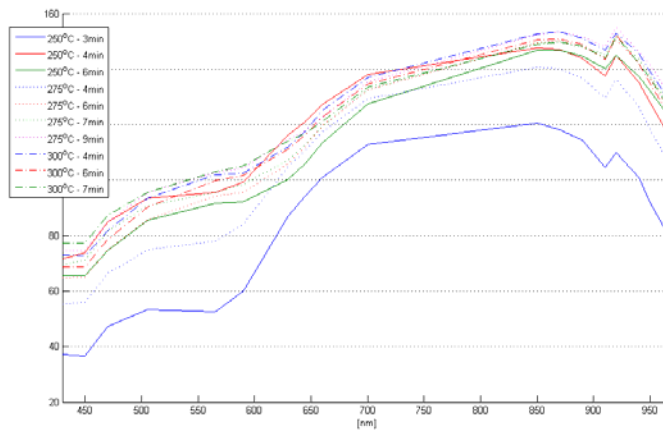


Figure 12.4 - Preliminary spectrum comparison

Figure 12.4 shows a large difference in the spectrum shape between the under-processed and the adequately/over-processed meat. Especially around the bands 500-700[nm] larger difference is shown, in this context it is worth noticing that the band at 505[nm] which shows met-myoglobin and the band at 590[nm] which shows oxy-myoglobin have large difference,

implying that the interior of the meat is not processed enough to change the state of the proteins.

Further the figure shows minor differences from adequately-cooked meat to over-cooked meat. The minor differences can imply that it might be more difficult to separate these classes, than to separate them from the under-processed.

## 12.5 Multivariate analysis

To investigate if the differences found in the spectrums can be used to assess the frying-treatment, multivariate analyses are applied to the data.

### 12.5.1 Principal component analysis

Applying the Principal Component Analysis (PCA) to the data, creates a new 18 dimension image, each new dimension a linear combination (component) of the original 18 dimensions sorted after the maximum variance accounted for.

The linear combinations have been derived using a pre-processed data set. From the derived combinations it is observed that the three first dimension accounts for 96.14% of the total variation (76.48%, 16.34% and 3.32% respectively), the remaining dimensions only seem to contain noise and is therefore not examined further. The three first principal components is applied to the pre-processed images, and histogram curves of the new dimensions are plotted.

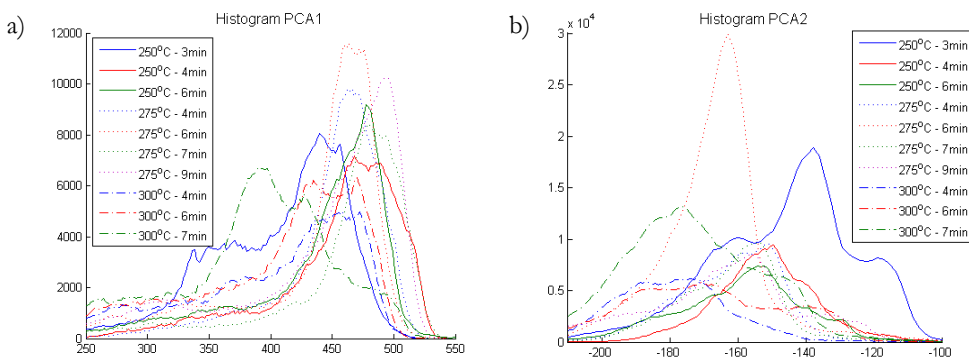


Figure 12.5 - Histogram Curves, a) First principal component, b) Second principal component

Examining the first principal component, it shows very rough curves, implying that it shows features not related to the frying degree, but rather to the differences found over the surface of the turkey square. Examining the histogram curves of the second component shows a somewhat identical same scheme. The bell shapes are generally very wide, this either because the interior of the meat dices contains a variety of different frying-treatment, or because the component captures a pattern not related to the frying-treatment.

Extracting the histogram curves of the third principal component shows a similar scheme as with the two prior components. The bell shape is very varying in width, and it is hard to conclude if the displacements of the curves are due to frying-treatment.

Having examined the first three principal components, it can be concluded that principal component analysis is unfit for the purpose of assessing frying-treatment for sliced diced turkey squares.

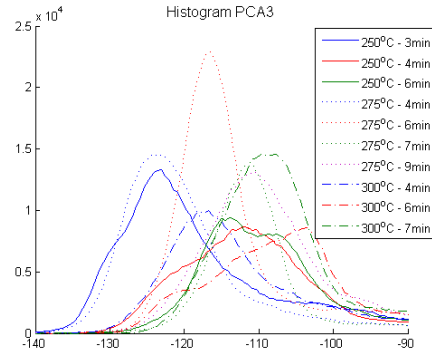


Figure 12.6 – Histogram curves third component

### 12.5.2 Canonical discriminant analysis

Finding the PCA unfit for the purpose, Canonical Discriminant Analysis (CDA) is examined. The CDA finds the linear combination separating the defined classes best possible, logically resulting in two combinations when separating 3 classes, as is the case with the diced turkey dataset.

The pre-processed images have been divided into classes according to Table 11.2, and the CDA is applied, resulting in two linear combinations or canonical discriminant functions (CDF). The two CDF's have been applied to all pre-processed images and the histogram curves are derived to examine the results.

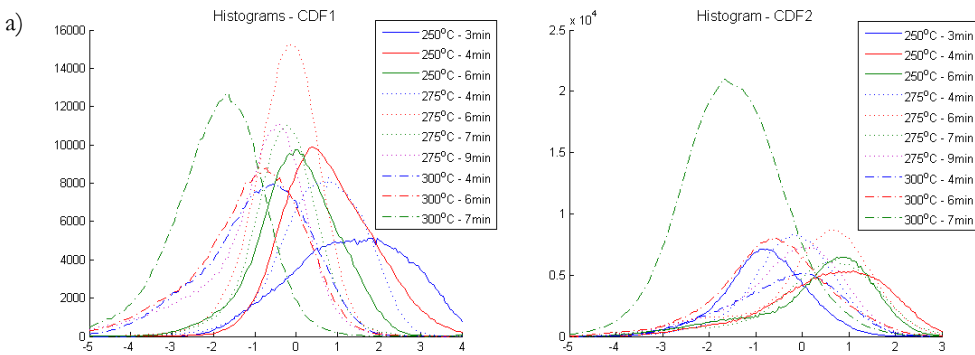


Figure 12.7 - Histogram curves, a) CDF1, b) CDF2

Examining the first discriminant function shows large improvements compared to the principal components. The histogram curves are much smoother indicating that the feature found applies to the larger part of the turkey square, and more importantly the top of the curves seems to be displaced according to frying degree, implying this is a useable tool for an assessment of the frying degree. Furthermore it is observed that the bell form of the curves, especially at the lower frying degrees, are wider compared to those from the frying-degree

examinations of minced meat and diced turkey, this can be explained by the nature of the sliced turkey dices. A sliced turkey diced which is inadequate processed, have a internal kernel of meat that has a low frying degree, surrounded by a ring of meat with a higher frying degree, thus creating an wider bell shape covering various frying degrees.

Examining the second CDF shows curves that are smooth but, there is not indication that the displacements of the tops are due to changes in the frying treatment.

To examine the findings further, and to rule out that the second canonical discriminant function has no influence when it comes to determining frying treatment, the mean value of the histograms are plotted in xy-plot with each axis representing a CDF. To further illustrate the divisions of group's, the border lines are derived using bayes classifier.

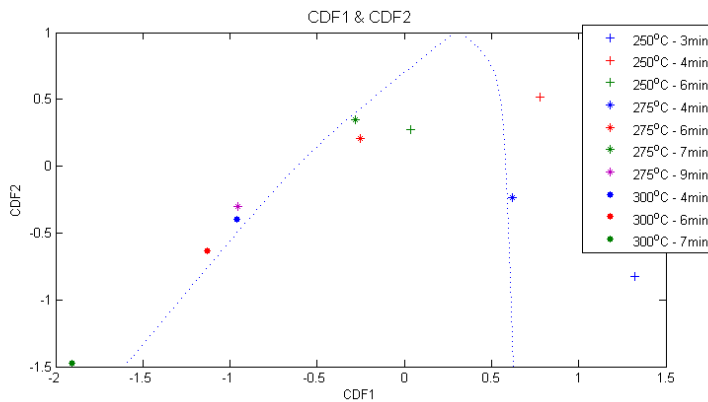


Figure 12.8 - CDF1 & CDF2 plot

The plotted values clearly show a division of classes based on the CDF 1 value, and not the CDF2 value. The border line between under- and adequately-processed meat seems to be almost vertical, which also implies that these can be separated using only the first CDF. The border second line however seems to have a screw, but when examining the data it can be seen that intuitively one would place a vertical line instead, again motivating a separation using only the first CDF. To further understand how the CDF separates the frying degrees, the loadings of the function are examined.

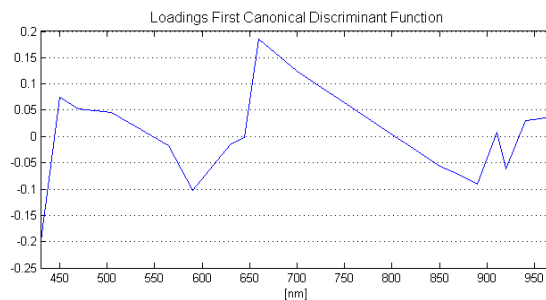


Figure 12.9 - Loadings CDF 1

The loading shows that the bands really influencing the value are the lower visual bands (<700[nm]), this fit the conclusions from the preliminary spectrum comparison. Furthermore it seems as the higher bands (<890) also has some influence on determining the frying-treatment.

### 12.5.3 The Frying-Treatment Score

The prior section shows how data can be transformed, such that their histogram value gives an impression of the frying degree of the meat in question. This method is obviously identical to the one used for minced meat and the surface evaluation of diced turkey, this motivates a similar definition of the Frying-Treatment Score.

There is however one major difference, the two definitions of FTS from minced meat and the surface of diced turkey are defined such that when the frying-treatment increases so does the FTS, Figure 12.8 shows this is not the case for the CDF derived for sliced turkey. To obtain a consistent Frying-Treatment Score scale throughout this thesis, it is decided to multiply the CDF for sliced diced turkey with -1, to obtain the regular scheme, thus defining the FTS as:

*The Frying-Treatment Score (FTS) for a multi-spectral image containing sliced diced turkey, is the mean value of the pixels in the pre-processed image, containing only the interior of the diced meat, projected with the CDF derived in 12.5.2 multiplied by -1.*

It can be argued that this definition may cause problems for the meat squares at lower frying degrees, as these contain a variety of FTS values, and the deviation is not taken into question in this definition. It is however believed that since the larger part of the meat dice is under-processed; these pixels will be able to drag the FTS down to the intended level.

Having defined the FTS, it is now possible to define the cut-off line between under-, adequately- and over-processed meat. This is defined by finding the mean between the groups mean. The cut-off value between under- and adequately-processed meats is found to be -0.276; meaning meat with values beneath this is under-processed. Between adequately- and over-processed meats the mean value is found to be 0.884; meaning values above this indicates over-processed meat, and values between -0.276 and 0.884 implies adequately processed meat. FTS value from sample images and the cut-off lines are shown in Figure 12.10.

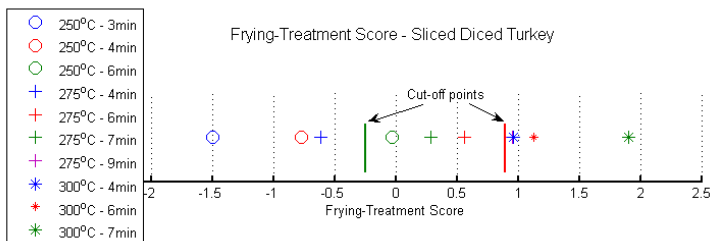


Figure 12.10 - Frying-Treatment Score - Minced Meat

### 12.5.4 Regression analysis

As with the prior definitions of FTS, the definition is used to examine the relation between FTS, frying time and frying temperature.

The first model created is modeling the frying time, based FTS and frying temperature. Using 3-fold cross validation the frying time is modeled using a 1<sup>st</sup>, 2<sup>nd</sup>, 3<sup>rd</sup>, 4<sup>th</sup> and 5<sup>th</sup> degree polynomial, the root mean square error and the  $R^2$  value is recorded, the result is given in Table 12.1.

Polynomial degree	RMSE <sub>Test</sub>	RMSE <sub>Train</sub>	R <sup>2</sup>
1	47.73	41.27	0.87
2	41.50	31.24	0.92
3	40.19	29.81	0.93
4	53.96	28.96	0.93
5	75.55	26.94	0.94

Table 12.1 - Cross Validation Results

The cross validation suggest the 3<sup>rd</sup> degree polynomial to be the best model for modeling the time based on temperature and the FTS. From this model the contour lines are drawn for the interesting frying times.

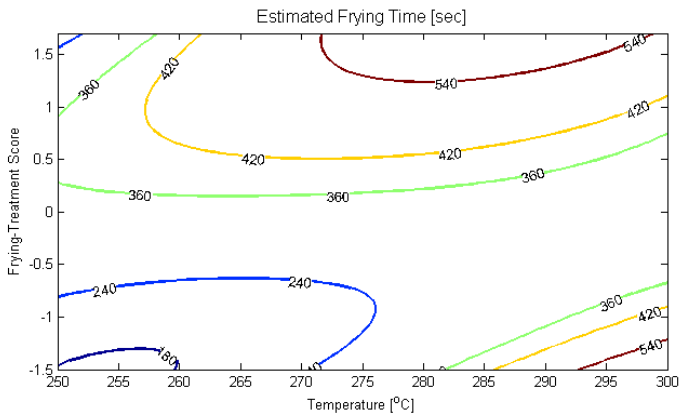


Figure 12.11 - Frying Time Contours

This model of the frying time implies that increasing time and temperature results in a higher frying treatment, which is known to be true. The model however seems to include some inaccuracy concerning long frying times at the low temperatures; this can be expected as this is based purely on a generalization, since no data exists for long frying times at low temperatures.

These results imply that the optimal model for FTS based on time and temperature also is a 3<sup>rd</sup> degree polynomial. Modeling this gives a  $R^2$  of 0.96 which shows that almost all variation of the frying-treatment score can be captured using the time and temperature. This further support the definition of FTS as a measure for the frying treatment applied. The contour lines for this model are shown in Figure 12.12.

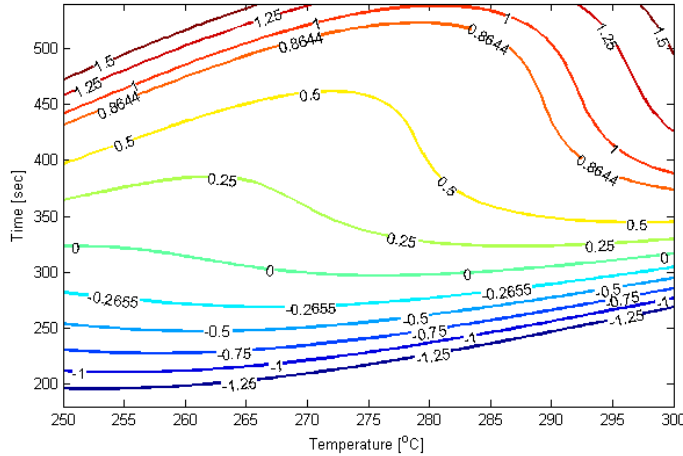


Figure 12.12 - FTS Contours Sliced Turkey Diced

The model derived from the sliced turkey dices, are quite similar to the one derived for the surface images of the diced turkey. Both suggest the production window for producing adequately processed meat is widest at the temperatures around 275°C, and narrows down for lower and higher temperatures. It is however worth noticing that the frying time for obtaining adequately processed meat at high temperature (>290°C), does not drop as significantly for the sliced model compared to the surface model. Also the time needed to obtain adequately processed meat at low temperatures, is significantly lower than for the surface model.

## 12.6 Visualization

As for the surface images of the diced turkey, a visualization method for examining the frying-treatment of entire images is proposed. The goal of the visualization is to provide a tool for visual inspection of the frying-treatment, which is better than using a conventional RGB image.

As for the visualization of the other types of meat, the FTS for each pixel containing meat is used to assign an appropriate color. Examining the histogram curves in Figure 12.7a it can be concluded that the scale should cover FTS values from -5 to 5, below is shown the scale used.

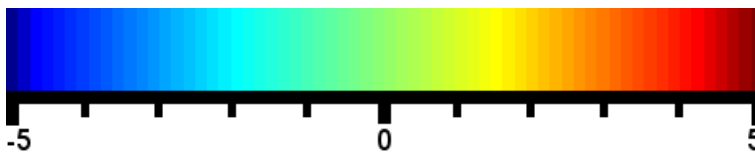


Figure 12.13 - FTS values to RGB

As for the surface images of diced turkey, the parts of the image containing other objects than meat are shown in normal RGB style. The entire dataset has been converted and is included in Appendix K; samples of the converted images are shown below.

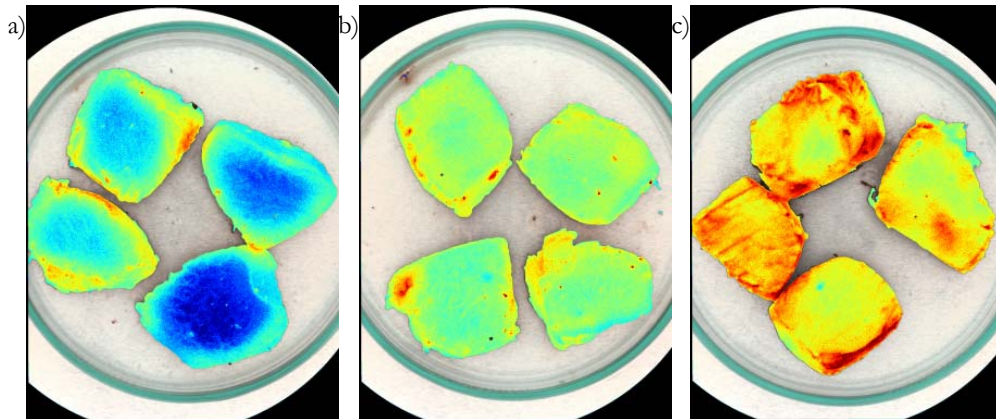


Figure 12.14 - a) 250°C - 3min, b) 275°C - 6min, c) 300°C - 7min

The samples clearly show how the under processed meat, have a under processed kernel (blue), and a shell that seems to be adequately processed. Furthermore the adequately processed meat in Figure 12.14b shows a homogenous green / yellow color as expected, and the over processed meat diced shows large red areas indicating they are over processed.

## 12.7 Discussion

In this chapter a method for frying treatment assessment of physically pre-processed diced turkey has been proposed. The method proposed is based on the same principles as used for treatment assessment of minced meat and non-physically preprocessed turkey squares, thus showing this method is applicable for various types of meat. As for the other types of meat the method defines a Frying-Treatment Score, providing us with a value representing the frying-treatment of the meat contained in the image.

The FTS values of all available sample images have been used in a regression analysis, to examine the relation between the FTS values and the frying time and temperature of the meat. The regression analysis shows that using a cubic relation, the estimated parameters are able to account for 96% of the variance in the FTS values using frying time and temperature. This is very good results and further support the use of FTS for a measure of frying-treatment.

Furthermore a visualization technique is proposed. The technique is able to take advantage of the spatial and spectral properties of the image, creating a RGB image clearly showing the frying-treatment of the various parts of the meat. This is especially clear when examining images of under processed meat, where the under-processed kernel clearly stands out from the outer ring of adequately processed meat.

The method obtained can be used to examine the effects of increased loading in the wok. The FTS for a normal loading at 275°C 6min is 0.5232, but for the higher loading it is 0.3241 thus indicating a decrease in frying treatment. For 300°C 6min the values are almost equal being 1.1062 and 1.0223 respectively, thus showing a slight increase in frying treatment. From this is cannot be finally concluded if the frying treatment increases due to higher loading of the wok.

Examining the meat sample without scalding it shows that their mean FTS is -0.4916, this is way lower than the FTS of 0.5332 for samples with scalding, and at the same time and temperature. This indicates that the scalding have a significant influence on the frying-treatment, as it was also observed in the prior chapter. It is however not possible to provide a final conclusion based on a single sample.

## Chapter 13      Reducing Spectral Bands

---

The prior part of the thesis shows how it is possible to assess quality parameters, such as frying treatment based on multi-spectral images of meat products. When applying this technique to a real life scenario, it introduces the problem of acquiring multi-spectral images on a running conveyor belt. To simplify this process, it is an advantage to be able to reduce the number of bands needed to assess the quality parameters of the meat. Reducing the spectral bands not only reduce the complexity of acquiring images, but also reduces computational times thus improving the response time of the system. This chapter will examine the possibility to reduce the bands used for each of the applications examined in the prior chapters.

Numerous approaches exist for reducing the number of spectral bands, mainly presented in area of hyper-spectral satellite images. In [17] techniques based on information entropy, spectral derivatives and contrast measures are discussed. However since we essentially need to model a linear function by removing some of the parameters, stepwise regression is selected to be used for this chapter.

## 13.1 Reducing for Frying Treatment Assessment

The main objective of reducing bands used for frying treatment assessment is essentially to examine how many bands are needed to emulate the results of the canonical discriminant function, with a reasonable error. The optimal solution to the regression problem, with respect to minimum error rate, will therefore be including all 18 bands since this will create an error of zero. The “optimal” solution can be written as:

$$\mathbf{y} = \mathbf{X} \cdot \mathbf{b} \quad (13.1)$$

Where  $\mathbf{X}$  contains all spectral bands,  $\mathbf{b}$  is the canonical discriminant function derived for the specific type of meat and  $\mathbf{y}$  is the Frying-Treatment Score for the specific pixel. The estimated solution with regards to the *minimum bands required* can be defined as:

$$\hat{\mathbf{y}} = \mathbf{X}_R \cdot \hat{\mathbf{b}} \quad (13.2)$$

Where  $\mathbf{X}_R$  contains the reduced number of spectral bands and an intercept term, and  $\hat{\mathbf{b}}$  is the weights calculated by least square regression for the reduced number of bands and the intercept term. The interpretation of “*minimum bands required*” is based on an evaluation of the mean squared error and the amount of variance accounted for by the bands, further explanation is given below when selecting the optimal reduction for each meat type.

The solutions are acquired using stepwise regression, this does not guarantee the best results, but it is an acceptable alternative to the time consuming best subset method. Tests performed shows that due to the immense amount of data and the rapid increase in complexity, calculations for a best subset regression reduction to 5 bands last over 1½ hours, whereas stepwise regression does the job in about 70 seconds.

### 13.1.1 Minced Beef

In-order to obtain an as accurate solution as possible all images were loaded, pre-processed and the canonical discriminant function for minced beef were applied. Since this resulted in a very large amount of data, making the analysis very time consuming it was chosen to reduce the data by only using every 50 pixel of an image, this can be done since after the reduction over 530000 observations were still available for the analysis.

To examine the impact of the band reduction a stepwise regression were performed, recording the root mean square error and  $R^2$  value at each step to obtain a plot of the evolution of these variables through the different reductions as shown in Figure 13.1. Furthermore the optimal subsets of bands at each step were recorded and given in Table 13.1 along with the root mean squared error and the  $R^2$  value.

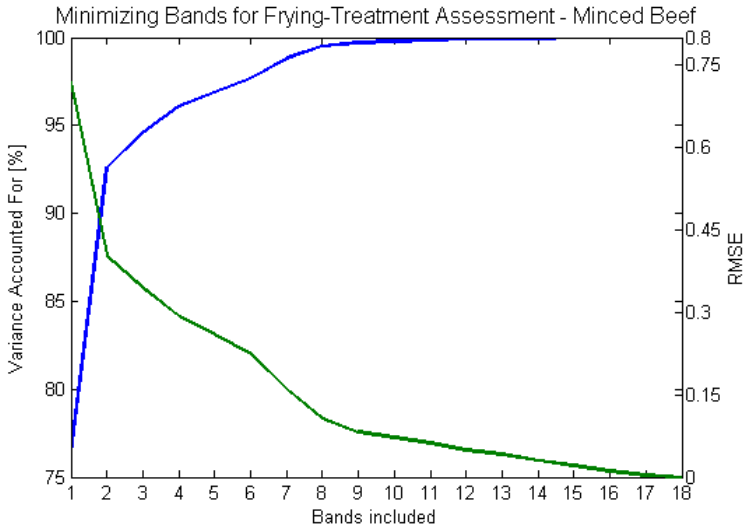


Figure 13.1 - RMSE & R<sup>2</sup> for band reduction – Minced Beef

Subset size	Bands included																		Root Mean Square Error	R <sup>2</sup>		
	1	2	3	4	5	6	7	8	9	10	11	12	13	14	15	16	17	18				
1										█										0.7199	0.7643	
2										█	█									█	0.4031	0.9261
3			█							█	█									█	0.3449	0.9459
4			█	█						█	█	█								█	0.2927	0.9610
5			█	█	█					█	█	█	█							█	0.2609	0.9690
6			█	█	█	█				█	█	█	█	█						█	0.2236	0.9773
7							█			█	█	█	█	█						█	0.1606	0.9883
8							█	█		█	█	█	█	█	█					█	0.1066	0.9948
9							█	█	█		█	█	█	█	█					█	0.0819	0.9969
10											█	█	█	█	█					█	0.0717	0.9977
11	█										█	█	█	█	█					█	0.0616	0.9983
12	█	█									█	█	█	█	█					█	0.0495	0.9989
13	█	█	█								█	█	█	█	█					█	0.0416	0.9992
14	█	█	█	█							█	█	█	█	█					█	0.0298	0.9996
15	█	█	█	█	█						█	█	█	█	█	█				█	0.0208	0.9998
16	█	█	█	█	█	█					█	█	█	█	█	█				█	0.0113	0.9999
17	█	█	█	█	█	█	█				█	█	█	█	█	█	█			█	0.0033	0.9999
18	█	█	█	█	█	█	█	█	█	█	█	█	█	█	█	█	█	█	█	█	0.0000	1.0000

Table 13.1 - Band reduction results - Minced Beef

The R<sup>2</sup> value, the measure for the variance accounted for, increases dramatically when adding the first four variables, after which it increase at a much lower rate. Also the RMSE is

decreasing at a higher rate for the first variables, than for the adding the last which is also expected. From these results it can be concluded that using four variables seems like a somewhat optimal band reduction, since this still includes 96.1% percent of the variation and an acceptable root mean square error. Including more variable will have a too large cost, compared to the increase in accuracy gained.

Examining the bands to include, namely band 3, 11, 12 and 18 at first sight shows that the NIR bands are very important thus proving the motivation for this project. When comparing to the values of the CDF function, one notices that all for these four have large weights, but are not the ones with the highest weights. An example is band 10 which has a much higher weight but seems to be excluded since band 11 in combination with band 18 covers the variance better, thus implying redundancy in the bands which were also expected.

Another interesting property of the selected bands is that it is possible to perform the pre-processing, defined for the minced beef images, using two of these bands, 3 and 11. Originally the pre-processing mechanism selected the optimal band between band 1 and 8 to separate the meat from the surrounding objects, but from the spectrum plotted in Figure 9.2a, it is observed that band 3 seems to be able to do the job on its own, if it is the only one available. For further pre-processing band 10 was used to perform a h-domes segmentation, it is however shown in Chapter 10 that band 11 is able to do an equivalently good job for the h-domes segmentation.

To further investigate the goodness of the reduction to 4 bands, a number of images are transformed using the new weights and their resulting histogram is plotted, as for the CDF transformed data in Figure 9.8.

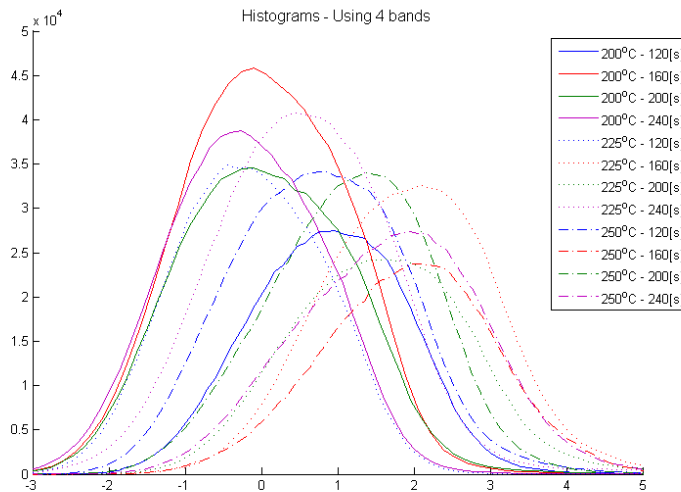


Figure 13.2 - Histograms curves - 4 bands used

Comparing Figure 13.2 with Figure 9.8 it becomes clear that they are very alike, thus implying the new projection found via band reduction actually produces similar results using 4 bands as the CDF using 18 bands. Also it can be noted that the curves in Figure 13.2 are more bell shaped not having a tail towards higher values as can be observed in Figure 9.8. This implies some of the distortion is removed, giving each image less deviation and thereby enabling a more precise FTS value.

### 13.1.2 Diced Turkey

Equivalent to the minced beef case, all images available were used in order to ensure the most accurate result. The images are loaded, pre-processed and every 25 pixel are taken out for the analysis. The increase from every 50 to every 25 pixel is possible since the turkey images contain a smaller percentage of meat in every image, thus making the observations available for the analysis approximately the same as for the minced beef.

At each regression step the RMSE and R<sup>2</sup> value was recorded along with the bands in the optimal subset found. The results are plotted in Figure 13.3 and given in Table 13.2.

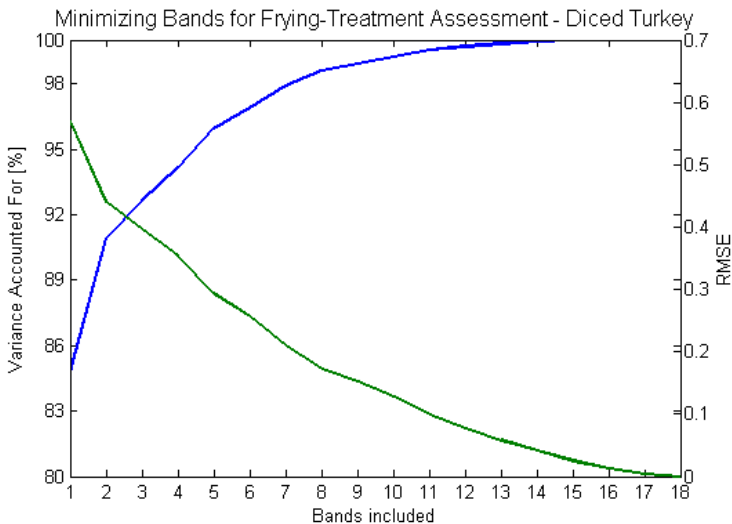


Figure 13.3 - RMSE & R<sup>2</sup> for band reduction – Diced Turkey

Subset size	Bands included																		Root Mean Square Error	R <sup>2</sup>
	1	2	3	4	5	6	7	8	9	10	11	12	13	14	15	16	17	18		
1																			0.5698	0.8475
2																			0.4404	0.9089
3																			0.3963	0.9262
4																			0.3533	0.9414
5																			0.2931	0.9596

Subset size	Bands included																		Root Mean Square Error	R <sup>2</sup>
	1	2	3	4	5	6	7	8	9	10	11	12	13	14	15	16	17	18		
6																			0.2572	0.9689
7																			0.2107	0.9791
8																			0.1727	0.9860
9																			0.1519	0.9891
10																			0.1276	0.9924
11																			0.0990	0.9954
12																			0.0780	0.9971
13																			0.0584	0.9984
14																			0.0418	0.9992
15																			0.0254	0.9997
16																			0.0126	0.9999
17																			0.0041	0.9999
18																			0.0000	1.0000

Table 13.2 - Band reduction results - Diced Turkey

From Figure 13.3 it is observed the rapid increase in variance accounted for decreases as the fifth band is added. It is therefore decided to carry on, including five bands as this gives an acceptable R<sup>2</sup> and root mean square error. Including more bands is simply not feasible as it gives a too small increase in accuracy compared to the cost.

Examining the bands to include, it is band 3, 7, 10, 12 and 18, it is clear that they include a larger part of visual bands than for minced meat. This implies the assessment of the frying treatment is for a large part depended on the look of the meat, rather than the properties derived from the NIR bands. Common for the two is however that band 18 is included, this is also be expected as water has absorbance in this band, and water content is good indicator of the frying degree. Comparing the selected bands with the CDF for diced turkey, again it is observed that it is not necessarily the bands with the highest weight that has the highest impact. E.g. band 12 (870 nm) does not have a high weight in the CDF, but still seems to be rather important for the assessment of the frying degree.

Considering the issue of performing pre-processing, the originally proposed procedure was using band 2 and 13. However when examining the spectrums in Figure 11.2a it becomes clear that band 3 and 12 also would be able to do the job, as they have some of the same properties.

To further examine the correctness of the results using the reduced bands, histogram curves are derived for images transformed using the new five band transformation. The histograms are plotted in Figure 13.4.

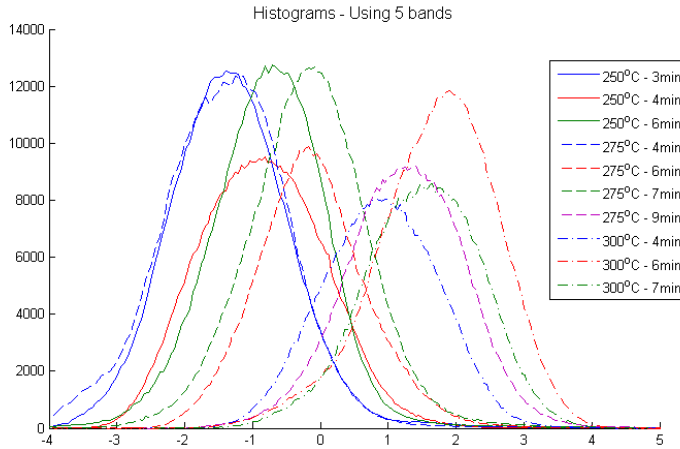


Figure 13.4 – Histogram curves - 5 bands used

Comparing Figure 13.4 to the original histogram curves in Figure 11.8a shows only minor differences, thus showing the 5 band reduction is a good approximation to the 18 band CDF. The differences observed are primarily more smooth curves, indicating a smaller deviation of the data giving a better approximation of the frying degree.

### 13.1.3 Sliced Diced Turkey

The process used for reducing bands for the sliced diced turkey images is the same as for the diced turkey images. All images were loaded, preprocessed and every 25 pixel were taken out to use for band reduction calculations. As with the other band reductions the RMSE and  $R^2$  value were recorded and plotted for each step. The plotted curves are shown in Figure 13.5 and the results are given in Table 13.3.

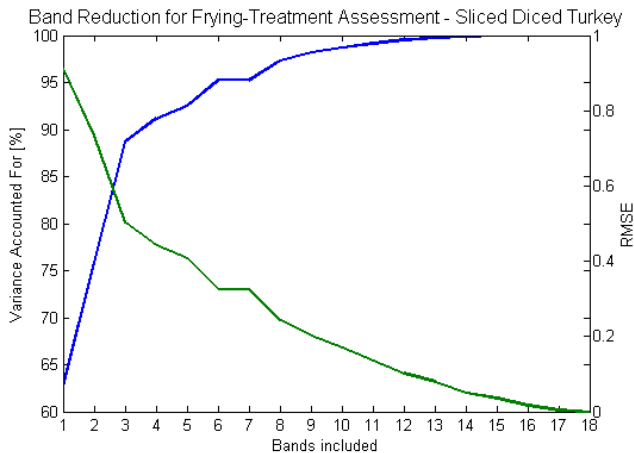


Figure 13.5 - RMSE & R2 for band reduction – Sliced Diced Turkey

Subset size	Bands included																		Root Mean Square Error	R <sup>2</sup>
	1	2	3	4	5	6	7	8	9	10	11	12	13	14	15	16	17	18		
1									█										0.9117	0.6268
2								█				█							0.7334	0.7585
3	█							█				█							0.5021	0.8868
4	█		█					█				█							0.4430	0.9119
5	█		█					█				█							0.4077	0.9254
6	█		█			█		█				█							0.3257	0.9524
7	█		█			█		█				█						█	0.3257	0.9524
8	█		█			█		█		█		█						█	0.2434	0.9734
9	█		█			█		█				█						█	0.2020	0.9816
10	█		█			█		█			█							█	0.1695	0.9871
11	█		█			█		█				█							0.1368	0.9916
12	█		█			█		█				█						█	0.1019	0.9953
13	█		█			█		█				█						█	0.0795	0.9972
14	█		█			█		█				█						█	0.0492	0.9989
15	█		█			█		█				█						█	0.0362	0.9994
16	█		█			█		█				█						█	0.0164	0.9999
17	█		█			█		█				█						█	0.0043	0.9999
18	█		█			█		█				█						█	0.0000	1.0000

Table 13.3 - Band reduction results - Sliced Diced Turkey

Examining Figure 13.5 shows the rapid increase in variance accounted for, slows down after adding the fourth variable. This motivates the use of the four band solution. It should be noted that the root mean square error seems somewhat high using this solution, but to get a large reduction in the root mean square error 2-4 extra variables must be included which is simply not worth the cost.

The bands to use for the solution are band 1, 3, 9 and 13. It is worth noticing that these bands except band 13 all are in the visual part of the spectrum, and that band 18 is not included as it was for the two prior band reductions. Furthermore it can be noted that these band all stands out in the CDF weights in Figure 12.9.

The pre-processing of the images for sliced diced turkey originally was designed using band 1 and 11; where only band 1 is included in the subset to use after reduction. However examining Figure 12.1, show that the preprocessing process could be redesigned using band 1 and 13, since the difference between band 11 and 13 are quite small. This leads to the conclusion that the preprocessing could be performed using only these bands.

To examine the solution further histogram curves has been derived from a number of images transformed with the new 4 band projection.

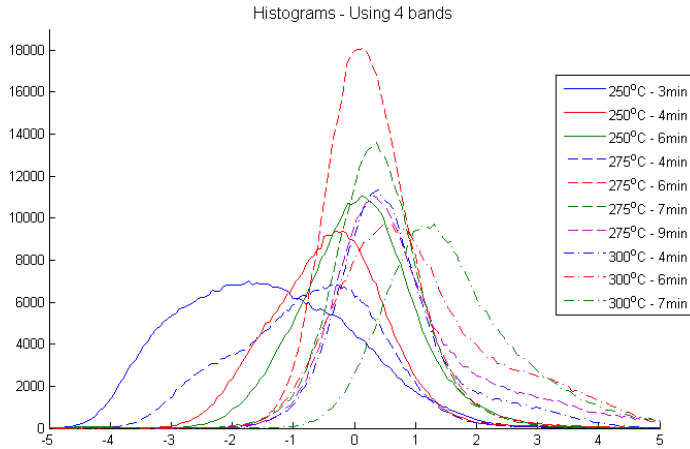


Figure 13.6 - Histogram curves - 4 bands used

The histogram curves are very like the ones in Figure 12.7a, the lower frying degrees still have a very wide bell shape since they contain meat with a variety of different frying degrees. Worth noticing is that the curves in Figure 13.6, generally have a more narrow shape, implying some kind of generalization was introduced by using only 4 bands. Fortunately the displacement of the tops still seems to be correct with regards to the frying degree, and the generalization only seems to be an advantage for assessing the frying degree.

## 13.2 Reducing for Agglutination Assessment

The reduction of bands for agglutination assessment of minced beef is somewhat different from the band reduction in relation to the frying degree. This is since the agglutination assessment focuses on the spatial properties of specific bands, and not the properties of all bands combined.

From Chapter 10 it can be concluded that the bands needed perform the agglutination assessment is the lower bands from 1 to 8, used to separate meat from the other objects in the image, and band 11 to perform the actual granule isolation. However as concluded in section 13.1.1 the separation of meat from the other objects could be performed using only band 3, thus leaving us with band 3 and 11 as the required for assessing agglutination.

Comparing this to the bands needed to assess frying treatment of minced beef (3, 11, 12 and 18), band 3 and 11 are both included, meaning it is possible to do both the frying treatment assessment and the agglutination assessment using only these four bands.

## 13.3 Discussion

This chapter shows how it is possible to reduce the bands needed for frying treatment assessment of minced beef, diced turkey and sliced diced turkey from eighteen to a maximum of five, without losing significant information regarding the frying treatment. Furthermore it shows that the agglutination assessment for minced beef, can be performed adding no additional bands than those needed for the frying treatment assessment of minced beef.

This significant reduction in bands decreases the complexity of implementing a system for production purposes. It not only decreases the space and time needed for image acquisition, but also reduces computation time.

Comparing the results of bands needed for frying treatment assessment of images containing the surface of different meat types, minced beef required band 3, 11, 12 and 18, and diced turkey required band 3, 7, 10, 12 and 18. Both meat types used band 3, 12 and 18 implying these generally are important for frying treatment assessment. Of these bands band 18 was expected, since this band gives an indication of water contents which is known to decrease due to increased heat treatment. Common for the two subsets are also a combination of both visual and NIR bands are used, showing that the appearance of the meat is not the only indicator of the frying degree, also features which are not normally visible to the human eyes plays an important role, thus proving the motivation of this project.



IV

Epilogue

## Chapter 14 Conclusion

---

The goal of this project was to examine the possibility of assessing various quality parameters, with regards to the frying process of a two meat products, namely minced beef and diced turkey. The quality parameters to assess for minced beef, was frying treatment and agglutination. The parameters assessed for diced turkey was the frying-treatment of two types of samples, namely whole (analyzing the surface) and sliced (analyzing the interior). A conclusion for each quality parameter is given below, along with some concluding remarks on the project.

### **Agglutination**

This thesis suggests a method for assessment for the agglutination in minced meat, based on the spatial properties of the image. Even though it is mainly the spatial properties which are utilized, the advantage gained through multi-spectral imaging is however still obvious, as band 11, a NIR band, plays an essential role in created the various measures of agglutination.

The spatial properties of the images are used to define a number of measures, such as meat pr. cm<sup>2</sup>, maximum granule size etc.. These measures are held against the physical measure of agglutination, the strainer loss. It was found that the mean granule size and the maximum granule size measures had a very high correlation with the strainer loss. These measures also

have the advantage of being more application independent, as these don't vary with the loading of meat in the image and the image area.

To further examine these spatial measures relation with the strainer loss, regression analysis is used to create a model of the strainer loss based on these measures, the model shows to be able to cover 56% of the variance in the strainer loss at a RMSE of 1.83. This seems like a fairly good approximation considering the differences between the measures. The results of the regression clearly show that the measures can be used to assess agglutination, perhaps not in the form of an estimation of the strainer loss, which also is not an optimal measure for the process operator. Instead another application could be to give direct feedback to the process operator, providing him with the current mean size of the granules on the belt, and the maximum granule size found, or simplified even further just sound an alarm when the agglutination has risen to certain level.

### **Frying Treatment Assessment**

The second quality parameter assessed is the frying treatment of two types of meat, minced meat and diced turkey. The frying-treatment to assess is not only based on if the meat is raw or fried, but rather on the quality of the frying-treatment assessed by experts. To assess frying treatment for these meat types, various multivariate statistical methods taking advantage of spectral properties of the multi-spectral images were examined. A common solution was found for assessing the frying treatment for all meat types, using canonical discriminant analysis.

The method finds the optimal linear combination, creating the largest separation of the image data at the various frying degrees using an extensive dataset. It should be noted that for obvious reasons it is required to derive a separate linear combination from meat type to meat type. From the linear combination a Frying-Treatment Score for each image can be derived, as the mean of the projected values of the pixels containing meat.

To examine the FTS relation with frying time and temperature, a model is created using regression. Using cross validation it was found that the optimal relation between FTS, and frying time and temperature is cubic. Using a cubic relation the parameters can be estimated to account for 65% to 98% of the variance in the FTS, using frying time and temperature.

The 65% percent was achieved for modeling the frying-treatment of minced meat, this is not an impressive results compared to the 98% from the turkey dices. The low amount of variance accounted for suggest other factors not examined to be influent. One of theses could be the quality of minced meat, as this known to vary. An example is the fat percentage which is known to be very varying ([22]). Another reason for the relatively low amount of variance accounted for could be the general larger variation over the minced meat samples.

For the diced turkey, two examinations were created one for examining the frying-treatment based on the surface, and one for the interior based on sliced turkey dices. Both show impressive results modeling the FTS by time and temperature, accounting for 95% and 98% respectively. Generally it was found the model for the surface of diced turkey seems to be the

most accurate based on the contours derived. The contours correctly show how the production window for adequately processed diced turkey narrows down for high and low temperatures, in the way that high frying times are required for low temperatures, and low frying times for high temperature.

In addition to the model of FTS by frying time and temperature, another application of the FTS is suggested, namely a visualization of the results. This visualization uses the FTS for each pixel value to create a false RGB image, with each color assigned to a specific frying degree. The visualization is done for minced beef and both types of diced turkey. The false RGB images seems to be a powerful tool for examining specific meat sample, giving a very good impression of the frying-treatment of each part / granule of the meat in question.

Having defined the FTS and shown how it could be used as an application, the linear combination leading to an FTS value is further examined, to investigate the possibility of reducing the bands used, thus decreasing the complexity and the implementation costs. It was found that the assessment of the FTS can be effectuated using only 4-5 spectral bands without losing considerable information. This 72% reduction in the bands required is very promising with regards to the implementation of such a system.

### **Concluding remarks**

Overall the thesis project proves that it is possible to assess certain quality parameters, with regards to the frying process of various meat products using multi-spectral imaging. The thesis shows how to take advantage of multi-spectral imaging, using both the spatial and spectral properties to extract an assessment of the quality parameters. Using the spatial information in the image given an edge, compared to conventional spectroscopy methods where only spectral information is used.

The results gained throughout this thesis is however not ready to be used in a production scenario without further research. Suggestions of future work are presented in Chapter 15.

---

## Chapter 15      Putting into perspective

---

The motivation for doing this thesis project was to examine the possibility to assess quality parameters using multi-spectral vision technology. This project proposes a method for assessment of frying-treatment of various types of meats and some measures for agglutination of minced beef. The methods proposed have been presented in two articles and one poster, of which the poster has been presented and the two articles are pending for publication.

Future work in this area could include maturing the method for production. The first step towards production is taken in Chapter 13, where it is shown how the number of spectral bands needed for assessing the quality parameters can be minimized. Aside from the band reduction more testing and research is still needed to better understand the nature of measures proposed in this thesis, and to adapt these to actual applications.

Also interesting could be to examine if / how the measures could be used in an automatic regulation system of the wok, maybe even enabling industry production of fried meat without being dependent on experienced process operators.

Another approach for future work, could be examining if the method for frying-treatment assessment can be transferred to other meat types, this is most likely the case as it is already shown it can be used for at least two types. Further interesting could be to investigate if the method is general enough to be transferred to other applications such as vegetables, which is one of the main application areas of the continuous wok.

## Bibliography

---

- [1] Jens Michael Carstensen (Ed.), *Image Analysis, Vision and Computer Graphics*, IMM – Informatics and Mathematical Modelling DTU, 2002
- [2] J. Adler-Nissen, “Continuous wok-frying of vegetables: Process Parameters Influencing scale up and product quality”, *Journal of Food Engineering*, 2006
- [3] Videometer, “VideometerLab2 – Data sheet”, [www.videometer.com](http://www.videometer.com)
- [4] Jørgen Slot, *Continuous Frying of minced beef*, Bachelor project, BioCentrum, Supervisor: J. Adler-Nissen 2004
- [5] J. Adler-Nissen, “A method of Frying Minced Meat”, Patent Application, 2006
- [6] J. Lattin J. D. Carrol, P. E. Green, *Analyzing Multivariate Data*, Brooks / Cole, 2003
- [7] M.C. Hunt, J.C. Acton, R.C. Benedict, C.R. Clakins, D.P. Comforth, L.E. Jeremiah, D.G. Olson, C.P. Salm, J.W. Saveil, S.D. Shivas, “Guidelines for Meat Color Evaluation”, American Meat Science Association, 1991
- [8] S. A. Skrydstrup, “Multi-spectral imaging for determine, onset and development of oxidation”, The Royal Veterinary and Agricultural University, 2006
- [9] J. R. Rasmussen L. H. Nikolajsen, “Multi-spectral Image Analysis in the Food Industry”, Master thesis, Supervisor: J. M. Carstensen, IMM – Informatics and

- Mathematical Modelling DTU, 2006
- [10] L. H. Clemmensen, “Estimation and Classification through Regression with Variable Selection amongst Features Extracted from Multi-Spectral Images”, IMM-Master thesis-2006-12, Supervisor: B. K. Ersbøll, IMM – Informatics and Mathematical Modelling DTU, 2006
- [11] J. Hawthorn, *Foundations of food science*, W.H. Freeman & Co. Ltd., 1981
- [12] S. B. Daugaard, “Oxidation of cheese”, Project paper, Supervisor: J. M. Carstensen, IMM- Informatics and Mathematical Modelling DTU, 2007
- [13] Jean Serra, “Introduction to mathematical morphology”, Computer Vision, Graphics, and Image Processing, Volume 35, Issue 3, Special Section on Mathematical Morphology, September 1986, Pages 283-305.
- [14] Luc Vincent, “Morphological Greyscale Reconstruction in Image Analysis: Applications and Efficient Analysis”, IEEE Transactions on image processing, Volume 2, Issue 2, April 1993, Pages 176-201.
- [15] Trevor Hastie, Robert Tibshirani, Jerome Freidman, *The Elements of Statistical Learning*, Springer 2001, Pages 9-39, 193-224.
- [16] Stanley R. Sternberg, “Greyscale Morphology”, Computer Vision and Image Processing, Volume 35, Issue 3, Special Section on Mathematical Morphology, September 1986, Pages 333- 355.
- [17] Peter Bajcsy and Peter Groves, “Methodology for Hypersepctral Band Selection”, Photogram-metric Engineering and Remote Sensing Journal, Vol. 70, Number 7, July 2004, Pages 793-802.
- [18] Marina Skurichina, Sergey Verzakov, Pavel Paclik and Robert P.W. Duin, “Effectiveness of Spectral Band Selection/Extraction Techniques for Spectral Data”, Lecture Notes in Computer Science, Issue 4109, 2006, Pages 541-550.
- [19] James Norman Sweet, “The Spectral Similarity Scale and its Application to the Classification of Hyperspectral Remote Sensing Data”, Conference Paper IEEE, 2003
- [20] R.M. Garcia-Rey, J Garcia-Olmo, E. De Pedro, R. Quiles-Zafra, M.D. Luque de Castro, “Prediction of texture and colour of dry-cured ham by visible and near infrared spectroscopy using a fiber probe”, Meat Science, Issue 70, 2003, Pages 357-363
- [21] Lindsay Smith, *A tutorial on Principal Components Analysis*, University of Otago, 2002.
- [22] Ina Clausen, *Stegning af kød – hvor fedt er det?*, Fødevaredirektoratet – Afdeling for ernæring, FødevareRapport 2002:08, Januar 2002

## Table of figures

---

Figure 4.1 - VideometerLab 2 Camera.....	23
Figure 4.2 - The continuous wok .....	25
Figure 5.1 - Matrix storage concept .....	29
Figure 5.2 - 2D transformation concept.....	30
Figure 5.3 - Example spectrum plot.....	30
Figure 5.4 - False color composition for identifying frying treatment .....	31
Figure 6.1 - Basic filter operation .....	34
Figure 6.2 - Dilation example.....	36
Figure 6.3 - Erosion example.....	36
Figure 6.4 - Opening example.....	37
Figure 6.5 - Closing example.....	37
Figure 6.6 – (a) The mask, (b) The marker, (c) Result of reconstruction .....	38
Figure 6.7 - (a) Original image, (b) Structural element, (c) Dilated image, (d) Eroded image....	39
Figure 6.8 – Reconstruction of the mask $f$ from the marker $g$ (Figure from [14]) .....	40
Figure 6.9 - H-Domes concept (From [14]).....	40
Figure 7.1 - Principal component and accounted variance .....	44
Figure 8.1 - Phases of the stir-frying process [2] .....	54
Figure 8.2 - Heme group .....	55
Figure 9.1 - Meat pieces before and after meat chopper.....	59
Figure 9.2 - a) Spectrum Background / Foreground, b) Histogram curves .....	62
Figure 9.3 - a) ROI before filtering, b) ROI after filtering, c) a-b.....	63
Figure 9.4 – a) Example image, b) After eradication of non-meat objects, c)Resulting pre-processing mask .....	63
Figure 9.5 - Preliminary spectra comparison .....	64

Figure 9.6 – a) Histogram curves PCA component 1, b) Histogram curves PCA component 2 .....	65
Figure 9.7 - PCA1 and PCA2 scatter plot .....	66
Figure 9.8 - Histogram – CDA .....	67
Figure 9.9 - Loadings Canonical Discriminant Function .....	67
Figure 9.10 - Frying-Treatment Score - Minced Meat .....	68
Figure 9.11 – ISO lines frying time .....	69
Figure 9.12 - FTS Contours, Time vs. Temperature .....	70
Figure 9.13 - FTS values to RGB .....	71
Figure 9.14 - a) 200°C - 160[s], b) 225°C – 200[s] c) 250°C – 160[s] .....	71
Figure 10.1 - Meat contained in plastic cups without cooling, and tray to use for cooling during frying .....	74
Figure 10.2 - Strainer .....	75
Figure 10.3 - Band 1 .....	78
Figure 10.4 - Band 2 .....	78
Figure 10.5 - Band 3 .....	78
Figure 10.6 - Band 4 .....	78
Figure 10.7 - Band 5 .....	78
Figure 10.8 - Band 6 .....	78
Figure 10.9 - Band 7 .....	79
Figure 10.10 - Band 8 .....	79
Figure 10.11 - Band 9 .....	79
Figure 10.12 - Band 10 .....	79
Figure 10.13 - Band 11 .....	79
Figure 10.14 - Band 12 .....	79
Figure 10.15 - Band 13 .....	80
Figure 10.16 - Band 14 .....	80
Figure 10.17 - Band 15 .....	80
Figure 10.18 - Band 16 .....	80
Figure 10.19 - Band 17 .....	80
Figure 10.20 - Band 18 .....	80
Figure 10.21 - Profile band 11 .....	81
Figure 10.22 - H-Domes image & profile .....	82
Figure 10.23 - H-Domes with threshold on 7 .....	82
Figure 10.24 - Threshold image w. median filter .....	82
Figure 10.25 - Ellipse area estimation .....	83
Figure 10.26 - Agglutination Measures .....	85
Figure 10.27 - Estimated Strainer Loss .....	86
Figure 10.28 - Estimated Strainer Loss .....	87
Figure 11.1 – a) Meat before lowering into boiling water, b) Meat after scalding .....	89
Figure 11.2 – a) Spectra of interesting objects, b) Histogram of interesting bands .....	92
Figure 11.3 - a) 890[nm] - 450[nm], b) histogram of 890[nm] - 450[nm] .....	92
Figure 11.4 - a) Mask without median filter, b) Mask after applying median filter .....	93
Figure 11.5 - Preliminary spectra analysis .....	93
Figure 11.6 - a) PCA component 1 histogram, b) PCA component 2 histogram .....	94
Figure 11.7 - Population means PCA1 vs. PCA2 .....	95
Figure 11.8 - a) CDF 1 Histograms, b) CDF 2 Histograms .....	95
Figure 11.9 - Loadings Canonical Discriminant Function .....	96
Figure 11.10 - Frying-Treatment Score - Diced Turkey .....	97

Figure 11.11 - Frying Time Contours .....	98
Figure 11.12 - FTS Contours Turkey Squares .....	98
Figure 11.13 - FTS values to RGB .....	99
Figure 11.14 - a) 250°C - 4min, b) 275°C - 7min, c) 300°C - 6min .....	100
Figure 12.1 - Pre-processing spectra comparison .....	103
Figure 12.2 – Pre-processing histogram curves .....	104
Figure 12.3 - a) Initial image (RGB), b) 850-430[nm], c) Threshold 47, d) Threshold + 5x5 median filter.....	105
Figure 12.4 - Preliminary spectrum comparison .....	105
Figure 12.5 - Histogram Curves, a) First principal component, b) Second principal component .....	106
Figure 12.6 – Histogram curves third component .....	107
Figure 12.7 - Histogram curves, a) CDF1, b) CDF2 .....	107
Figure 12.8 - CDF1 & CDF2 plot.....	108
Figure 12.9 - Loadings CDF 1 .....	108
Figure 12.10 - Frying-Treatment Score - Minced Meat.....	109
Figure 12.11 - Frying Time Contours .....	110
Figure 12.12 - FTS Contours Sliced Turkey Diced.....	111
Figure 12.13 - FTS values to RGB .....	111
Figure 12.14 - a) 250°C - 3min, b) 275°C - 6min, c) 300°C - 7min .....	112
Figure 13.1 - RMSE & R <sup>2</sup> for band reduction – Minced Beef .....	116
Figure 13.2 - Histograms curves - 4 bands used.....	117
Figure 13.3 - RMSE & R <sup>2</sup> for band reduction – Diced Turkey .....	118
Figure 13.4 – Histogram curves - 5 bands used .....	120
Figure 13.5 - RMSE & R <sup>2</sup> for band reduction – Sliced Diced Turkey .....	120
Figure 13.6 - Histogram curves - 4 bands used .....	122

V

Appendix

## Appendix A      VideometerLab 2 – Wavelength table

---

This table shows the wavelengths which the VideometerLab 2 camera is able to record, along with sample applications of the specific wavelength.

<b>Band</b>	<b>Wavelength [nm]</b>	<b>Color</b>	<b>Example application</b>
1	430	Ultra Blue	Chlorophyll A
2	450	Blue	Riboflavin
3	470	Blue	RGB, Blue
4	505	Green	RGB Green, Met-myoglobin
5	565	Green	RGB Green
6	590	Amber	Oxy-myoglobin
7	630	Red	RGB red
8	645	Red	Chlorophyll B
9	660	Red	Oxidation, Chlorophyll A
10	700	Red	Oxidation
11	850	NIR	Baseline
12	870	NIR	Baseline
13	890	NIR	Unsaturated fat
14	910	NIR	Protein

15	920	NIR	
16	940	NIR	Fat
17	950	NIR	Protein
18	970	NIR	Water

## Appendix B                      Experiment Design January (Danish)

---

**Jens Adler-Nissen**

**Forsøgsplan 29/1 07 – wokstegning af hakket kød**

***Tilberedning af råvaren:***

Det frosne kød knuses i stykker på ikke over 150 g. Mellem 0.5 og 1 kg. hakkes batchvis i hurtighakkeren (Kilia 57 cm diameter) på laveste hastighed indtil kødet er findelt til omkring 5 mm. stykker (tager et par minutter). Hakningen må ikke overdrives af hensyn til temperaturstigningen. Efter hakningen opsamles kødet (der er let som sne) i plastbægre med ca. 100g i hver.

Til hvert forsøg bruges 8 plast bægre = ca. 800g.

Der bør ikke hakkes og afvejes mere end hvad der kan bruges inden for ca. ½ time. Stil evt. bægerne i is eller koldt. Det skulle kunne lade sig gøre at nå 4 forsøg, svarende til en temperatur.

***Wokstegning:***

Når temperaturen har indstillet sig, tilsættes bægerne en af gange for hver omdrejning på sneglen. Produktet opsamles fra transportbåndet, således at de først ankomne 50-100g. og de sidste ca. 150-200 g. kasseres. Det totale udbytte er ca. 500-600 g. dvs. at der kan regnes med at der opsamles omkring 250-300 g. færdig kød per forsøg. Det opsamlede produkt anbringes i plastposer, der er mærket.

***Forsøgsparametre:***

200°C: tid: 120 s – 160 s – 200 s 240 s

225°C: tid: 120 s – 160 s – 200 s 240 s

250°C: tid: 120 s – 160 s – 200 s 240 s

Forsøgene køres med den laveste temperatur først.

***Videometer optagelse:***

Prøverne lægges i en petriskål i et så tykt lag, at man kan se bunden. Der laves 2 petriskåle for hvert forsøg således at man får dobbelt bestemmelser af billede-optagelsen (eller 3 petriskåle, så man får trippel-bestemmelser). Resten af prøverne gemmes (i køleskab til næste dag) til vandbestemmelse; evt. nedfrysning.

***Vandbestemmelse:***

Ca. 20 g. prøve homogeniseres i en miniblender. Vandbestemmelsen sker på ca. 2 g. prøve, som tørres ved 110°C i 24 timer i afvejede foliebægre – der laves trippel-bestemmelse.

# Appendix C      Results Moisture Contents January Experiment

---

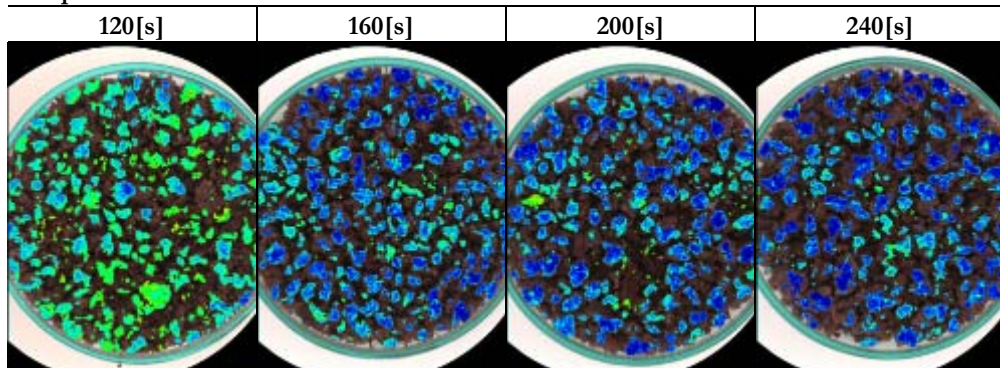
<b>Moisture content</b>		Weight		Cup weight: 0.3152 [g]		Moisture contents	
		Before [g]	After [g]	[g]	Percent	Std.	
<b>200 Degress</b>							
	<b>120 [sec]</b>			<b>Gns.</b>	<b>54.32574</b>	<b>0.216905</b>	
	I	2.2552	1.2018	1.0534	54.29897		
	II	2.3603	1.2446	1.1157	54.55479		
	III	2.3984	1.2709	1.1275	54.12346		
	<b>160 [sec]</b>			<b>Gns.</b>	<b>52.66065</b>	<b>0.440206</b>	
	I	2.5152	1.3455	1.1697	53.16818		
	II	2.2626	1.2425	1.0201	52.38266		
	III	2.3287	1.273	1.0557	52.43109		
	<b>200 [sec]</b>			<b>Gns.</b>	<b>51.49194</b>	<b>0.212021</b>	
	I	2.292	1.2735	1.0185	51.52266		
	II	2.2892	1.2689	1.0203	51.68693		
	III	2.4396	1.3505	1.0891	51.26624		
	<b>240 [sec]</b>			<b>Gns.</b>	<b>51.1633</b>	<b>0.424912</b>	
	I	2.65	1.4485	1.2015	51.46051		
	II	2.3924	1.3257	1.0667	51.35278		
	III	2.2587	1.2738	0.9849	50.67661		
<b>225 Degress</b>							
	<b>120 [sec]</b>			<b>Gns.</b>	<b>53.16467</b>	<b>0.150364</b>	
	I	2.2983	1.244	1.0543	53.16424		
	II	2.4538	1.3136	1.1402	53.31525		
	III	2.5527	1.3665	1.1862	53.01453		
	<b>160 [sec]</b>			<b>Gns.</b>	<b>53.96302</b>	<b>0.136475</b>	
	I	2.5732	1.3533	1.2199	54.02569		
	II	2.7768	1.4523	1.3245	53.80647		
	III	2.2095	1.1855	1.0240	54.05691		
	<b>200 [sec]</b>			<b>Gns.</b>	<b>52.55215</b>	<b>0.411431</b>	
	I	2.3866	1.3076	1.0790	52.09037		
	II	2.1817	1.1947	0.9870	52.87972		
	III	2.2081	1.2108	0.9973	52.68635		
	<b>240 [sec]</b>			<b>Gns.</b>	<b>51.27254</b>	<b>0.239858</b>	
	I	2.1957	1.2304	0.9653	51.33209		
	II	2.3231	1.2989	1.0242	51.00852		
	III	2.4445	1.3484	1.0961	51.47701		
<b>250 Degress</b>							
	<b>120 [sec]</b>			<b>Gns.</b>	<b>51.00601</b>	<b>0.185106</b>	
	I	2.2633	1.2657	0.9976	51.20887		
	II	2.3871	1.3312	1.0559	50.96288		
	III	2.4599	1.3694	1.0905	50.84627		
	<b>160 [sec]</b>			<b>Gns.</b>	<b>46.28823</b>	<b>0.206039</b>	
	I	2.3025	1.3821	0.9204	46.31409		
	II	2.4745	1.4797	0.9948	46.07049		
	III	2.6846	1.5833	1.1013	46.48012		
	<b>200 [sec]</b>			<b>Gns.</b>	<b>49.70203</b>	<b>0.272753</b>	
	I	2.3971	1.3666	1.0305	49.49805		
	II	2.4202	1.3762	1.0440	49.5962		
	III	2.4265	1.3706	1.0559	50.01184		
	<b>240 [sec]</b>			<b>Gns.</b>	<b>48.27531</b>	<b>0.225915</b>	
	I	2.5683	1.4854	1.0829	48.06267		
	II	2.459	1.4246	1.0344	48.25077		
	III	2.332	1.3536	0.9784	48.5125		

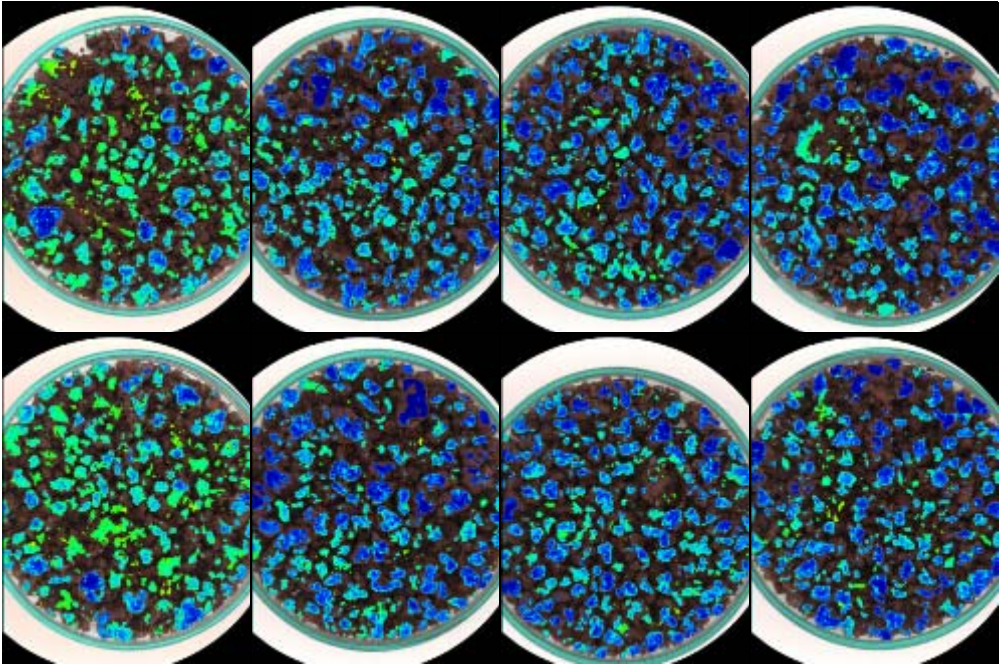
## Appendix D      Visualization Results – Minced Meat

---

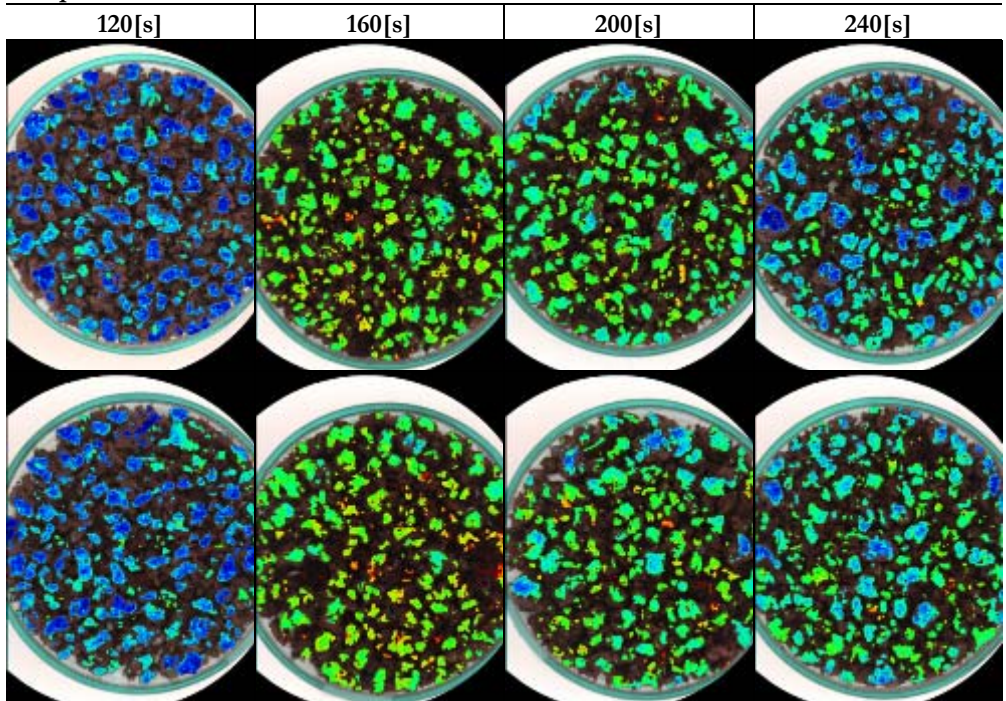
This appendix includes all images acquired of minced meat, each have been transformed for ease of inspection using the visualisation method from section 9.6 for minced meat.

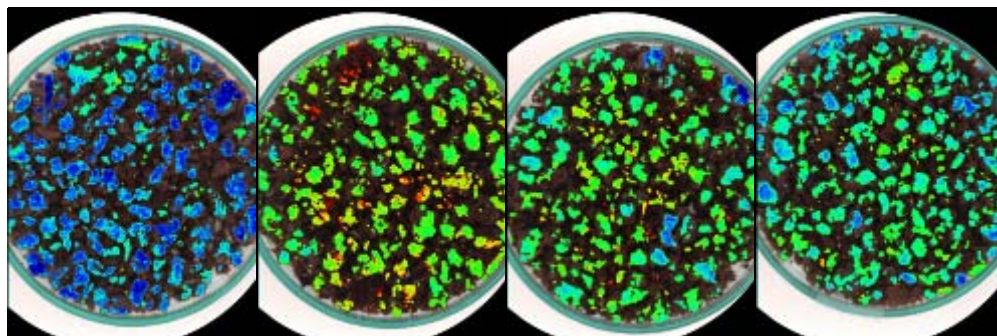
Temperature 200°C



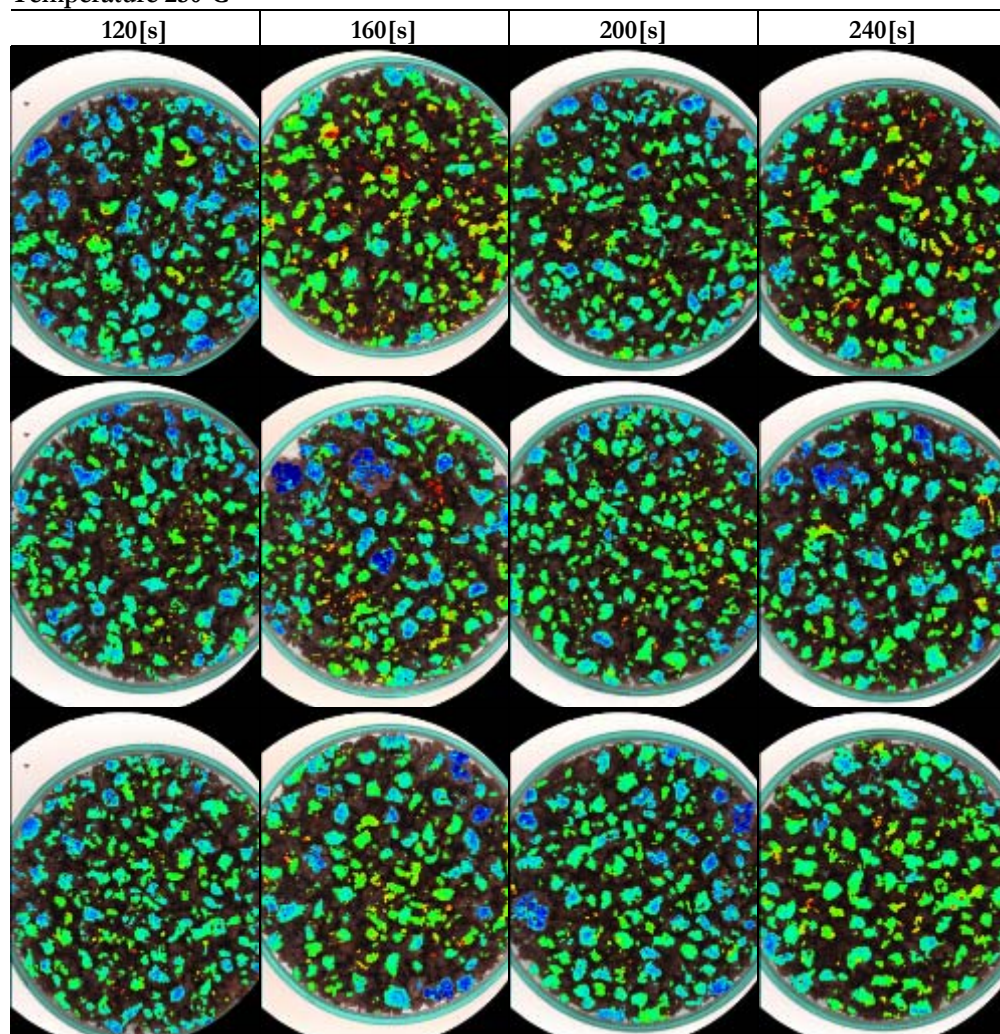


Temperature 225°C





Temperature 250°C



## Appendix E      Experiment Design March (Danish)

---

**Søren Blond Daugaard**  
**Forsøgsplan 14/3 07 – Wok stegning af hakket kød**

***Formål:***

Formålet med disse forsøg er at undersøge klumpning i hakket kød, afhængig af temperaturen før stegning, temperaturen under stegning og stege tid.

***Tilberedning af råvaren:***

Det frosne kød knuses i stykker på ikke over 150 g. Mellem 0.5 og 1 kg. hakkes batchvis i hurtighakkeren (Kilia 57 cm diameter) på laveste hastighed indtil kødet er findelt til omkring 5 mm. stykker (tager et par minutter). Hakningen må ikke overdrives af hensyn til temperaturstigningen. Efter hakningen opsamles kødet (der er let som sne) i plastbægre med ca. 100g i hver. Til hvert forsøg bruges 8 plast bægre = ca. 800g.

Alt kød klargøres fra starten af forsøget, når tiden fra hakning til stegning er opnået stilles plast bægerne i is for at stoppe optøningen indtil disse skal i wokken.

### **Wokstegning:**

Når temperaturen har indstillet sig, tilsættes bægerne en af gangen for hver omdrejning på sneglen. Produktet opsamles fra transportbåndet, således at de først ankomne 50-100g. og de sidste ca. 150-200 g. kasseres. Det totale udbytte er ca. 500-600 g. dvs. at der kan regnes med at der opsamles omkring 250-300 g. færdig kød per forsøg.

Det opsamlede produkt anbringes i foliepakker eller poser, der er mærket og der laves si måling efter hver gennemgang.

### **Forsøgsparametre:**

Tid fra hakning til stegning	Steketemperatur	Tid i wok	Hz for wok
~30 min			
For at stoppe optøningen bør bægerne stilles i is når de 30 min er opnået.	200°C	160s	44,32
	200°C	240s	29,55
	225°C	160s	44,32
	225°C	240s	29,55
~1t 30min			
For at stoppe optøningen bør bægerne stilles i is når de 1t 30 min er opnået.	200°C	160s	44,32
	200°C	240s	29,55
	225°C	160s	44,32
	225°C	240s	29,55
~2t 30min			
For at stoppe optøningen bør bægerne stilles i is når de 2t 30 min er opnået.	200°C	160s	44,32
	200°C	240s	29,55
	225°C	160s	44,32
	225°C	240s	29,55

Forsøgene køres kronologisk i overensstemmelse med ovenstående tabel.

### **Si tab:**

Der bruges en si med kvadratiske huller på 1,1 – 1,2 cm.

For hver prøve afvejes en tom foliebakke og vægten noteres. Herefter afvejes kød prøven og vægten noteres. Produktet tilsættes si'en, opsamles i den tomme foliebakken, vejes og vægten noteres.

Vægtene noteres ved hjælp af en printet version af regnearket Si-tab-Marts-070312.xls.

### **Videometer optagelse:**

Prøverne lægges i en petriskål i et så tykt lag, at man ikke kan se bunden. Der laves 2 petriskåle for hvert forsøg således at man får dobbelt bestemmelser af billede optagelsen (eller 3 petriskåle, så man får trippel bestemmelser).

Billederne gemmes i HIPS formatet efter følgende navne konvention:  
[TidFørWok]\[Temp]\_[Tid]\_[#].hips

Resten af prøverne gemmes (i køleskab til næste dag) til vandbestemmelse; evt. nedfrysning.

***Vandbestemmelse:***

Ca. 20 g. prøve homogeniseres i en miniblender. Vandbestemmelsen sker på ca. 2 g. prøve, som tørres ved 110°C i 24 timer i afvejede foliebægre – der laves trippel-bestemmelse.

# Appendix F      Results Moisture Contents March Experiment

---

**Moisture content - March Experiment**

	Weight Cup [g]	Weight		Moisture contents		
		Before [g]	After [g]	[g]	Percent	Std.
<b>~30 min</b>						
<b>200C - 160 S</b>				<b>Gns.</b>	<b>50.29219</b>	<b>0.4006</b>
I	0.3166	2.4739	1.3846	1.0893	50.49367	
II	0.315	2.7244	1.5064	1.2180	50.552	
III	0.315	2.4735	1.3979	1.0756	49.8309	
<b>200C - 240 S</b>				<b>Gns.</b>	<b>46.55977</b>	<b>0.2452</b>
I	0.3171	2.3497	1.4015	0.9482	46.64961	
II	0.3167	2.287	1.3751	0.9119	46.28229	
III	0.3172	2.497	1.478	1.0190	46.74741	
<b>225C - 160 S</b>				<b>Gns.</b>	<b>45.27876</b>	<b>1.8283</b>
I	0.3145	2.5059	1.4674	1.0385	47.3898	
II	0.3138	2.3687	1.4596	0.9091	44.2406	
III	0.3144	2.4476	1.5046	0.9430	44.20589	
<b>225C - 240 S</b>				<b>Gns.</b>	<b>46.03677</b>	<b>0.0799</b>
I	0.3148	2.7729	1.6412	1.1317	46.03962	
II	0.3151	2.4365	1.4616	0.9749	45.9555	
III	0.3153	2.4634	1.4728	0.9906	46.11517	
<b>~1t 30 min</b>						
<b>200C - 160 S</b>				<b>Gns.</b>	<b>43.38688</b>	<b>0.1889</b>
I	0.3174	2.2935	1.4395	0.8540	43.21644	
II	0.3171	2.5012	1.5543	0.9469	43.35424	
III	0.3178	2.622	1.6176	1.0044	43.58997	
<b>200C - 240 S</b>				<b>Gns.</b>	<b>48.13233</b>	<b>0.6723</b>
I	0.3151	2.7089	1.558	1.1509	48.07837	
II	0.3163	2.5402	1.4841	1.0561	47.48865	
III	0.3143	2.498	1.4317	1.0663	48.82997	
<b>225C - 160 S</b>				<b>Gns.</b>	<b>47.5126</b>	<b>3.0361</b>
I	0.3161	2.5419	1.446	1.0959	49.23623	
II	0.3162	2.6694	1.5094	1.1600	49.29458	
III	0.3159	2.3174	1.4366	0.8808	44.00699	
<b>225C - 240 S</b>				<b>Gns.</b>	<b>45.04778</b>	<b>0.2705</b>
I	0.3154	2.5917	1.5632	1.0285	45.18297	
II	0.3152	2.3632	1.447	0.9162	44.73633	
III	0.3153	2.5159	1.5207	0.9952	45.22403	
<b>~2t 30 min</b>						
<b>200C - 160 S</b>				<b>Gns.</b>	<b>48.8079</b>	<b>0.2093</b>
I	0.316	2.3366	1.3459	0.9907	49.02999	
II	0.3158	2.3271	1.346	0.9811	48.7794	
III	0.317	2.3629	1.3683	0.9946	48.6143	
<b>200C - 240 S</b>				<b>Gns.</b>	<b>49.23749</b>	<b>0.1167</b>
I	0.3164	2.5687	1.4568	1.1119	49.36731	
II	0.3172	2.5473	1.4514	1.0959	49.14129	
III	0.317	2.4146	1.3825	1.0321	49.20385	
<b>225C - 160 S</b>				<b>Gns.</b>	<b>53.80139</b>	<b>0.2608</b>
I	0.3156	2.4282	1.2858	1.1424	54.07555	
II	0.3161	2.2394	1.2052	1.0342	53.77216	
III	0.3155	2.3681	1.2688	1.0993	53.55646	
<b>225C - 240 S</b>				<b>Gns.</b>	<b>50.51604</b>	<b>0.3248</b>
I	0.3162	2.5641	1.4208	1.1433	50.8608	
II	0.3163	2.4373	1.3668	1.0705	50.47148	
III	0.3153	2.6317	1.4685	1.1632	50.21585	

## Appendix G      Results measures of agglutination

---

Wait time / Temperature	Frying time [s] / Measurement	Image Sample I	Image Sample II	Image Sample III	Average	Std.
<i>30 min</i>						
<i>200°C</i>	<i>160</i>					
	<i>Meat pr. cm<sup>2</sup></i>	6.43	6.81	5.88	6.37	0.4676
	<i>Mean size</i>	0.0549	0.0494	0.0615	0.0553	0.0060
	<i>Std. dev. size</i>	0.0889	0.0885	0.1072	0.0949	0.0107
	<i>Max. size</i>	0.5293	0.4663	0.6894	0.5616	0.1150
<i>200°C</i>	<i>240</i>					
	<i>Meat pr. cm<sup>2</sup></i>	7.71	7.96	6.48	7.38	0.7922
	<i>Mean size</i>	0.0459	0.0441	0.0528	0.0476	0.0046
	<i>Std. dev. size</i>	0.0704	0.0726	0.0801	0.0744	0.0050
	<i>Max. size</i>	0.4342	0.5486	0.5046	0.4958	0.0577
<i>225°C</i>	<i>160</i>					
	<i>Meat pr. cm<sup>2</sup></i>	6.03	6.59	5.92	6.18	0.3593
	<i>Mean size</i>	0.0574	0.0512	0.0601	0.0562	0.0045
	<i>Std. dev. size</i>	0.0941	0.0829	0.1081	0.0950	0.0126

Wait time / Temperature	Frying time [s] / Measurement	Image Sample I	Image Sample II	Image Sample III	Average	Std.	
225°C	<i>Max. size</i>	0.7216	0.4890	0.7023	0.6376	0.1290	
	240						
	<i>Meat pr. cm<sup>2</sup></i>	5.46	5.33	5.90	5.56	0.2987	
	<i>Mean size</i>	0.0648	0.0653	0.0614	0.0638	0.0021	
	<i>Std. dev. size</i>	0.1069	0.1057	0.1041	0.1055	0.0014	
	<i>Max. size</i>	0.6680	0.6144	0.7880	0.6901	0.0889	
	<i>Avg. meat pr. cm<sup>2</sup></i>					6.38	
	<i>Avg. size</i>					0.0557	
	<i>Avg. std. dev. size</i>					0.0925	
	<i>Avg. max. size</i>					0.5963	
<b>1h 30 min</b>							
200°C	160						
	<i>Meat pr. cm<sup>2</sup></i>	6.62	6.60	6.13	6.45	0.2768	
	<i>Mean size</i>	0.0529	0.0493	0.0585	0.0535	0.0046	
	<i>Std. dev. size</i>	0.0852	0.0834	0.1221	0.0969	0.0219	
	<i>Max. size</i>	0.6070	0.6164	1.2010	0.8081	0.3402	
200°C	240						
	<i>Meat pr. cm<sup>2</sup></i>	5.59	6.09	6.05	5.91	0.2749	
	<i>Mean size</i>	0.0642	0.0567	0.0596	0.0602	0.0038	
	<i>Std. dev. size</i>	0.1199	0.1113	0.0883	0.1065	0.0162	
	<i>Max. size</i>	1.1956	1.1653	0.4836	0.9482	0.4026	
225°C	160						
	<i>Meat pr. cm<sup>2</sup></i>	6.20	6.86	5.81	6.29	0.5303	
	<i>Mean size</i>	0.0557	0.0501	0.0607	0.0555	0.0053	
	<i>Std. dev. size</i>	0.0932	0.7514	0.1150	0.3199	0.3738	
	<i>Max. size</i>	0.9469	0.4540	1.1459	0.8489	0.3562	
225°C	240						
	<i>Meat pr. cm<sup>2</sup></i>	4.91	6.04	5.43	5.46	0.5638	
	<i>Mean size</i>	0.0689	0.0551	0.0662	0.0634	0.0073	
	<i>Std. dev. size</i>	0.1217	0.1083	0.1057	0.1119	0.0086	
	<i>Max. size</i>	0.6959	0.7567	0.6904	0.7143	0.0368	
<i>Avg. meat pr. cm<sup>2</sup></i>					6.03		
<i>Avg. size</i>					0.0582		
<i>Avg. std. dev. size</i>					0.1588		
<i>Avg. max. size</i>					0.8299		
<b>2h 30 min</b>							
200°C	160						
	<i>Meat pr. cm<sup>2</sup></i>	4.80	5.93	5.92	5.55	0.6466	

Wait time / Temperature	Frying time [s] / Measurement	Image Sample I	Image Sample II	Image Sample III	Average	Std.
	<i>Mean size</i>	0.0740	0.0600	0.0575	0.0638	0.0089
	<i>Std. dev. size</i>	0.1461	0.1291	0.1010	0.1254	0.0228
	<i>Max. size</i>	1.3014	0.8408	1.0547	1.0656	0.2305
200°C	240					
	<i>Meat pr. cm<sup>2</sup></i>	4.79	5.10	5.72	5.20	0.4743
	<i>Mean size</i>	0.0764	0.0747	0.0648	0.0720	0.0063
	<i>Std. dev. size</i>	0.1619	0.2037	0.1363	0.1673	0.0340
	<i>Max. size</i>	1.4465	2.7996	1.2549	1.8337	0.8419
225°C	160					
	<i>Meat pr. cm<sup>2</sup></i>	4.80	5.94	5.14	5.29	0.5853
	<i>Mean size</i>	0.0765	0.0603	0.0688	0.0686	0.0081
	<i>Std. dev. size</i>	0.0138	0.1210	0.1328	0.0892	0.0655
	<i>Max. size</i>	0.7897	1.1142	0.8028	0.9022	0.1837
225°C	240					
	<i>Meat pr. cm<sup>2</sup></i>	5.61	4.97	5.13	5.24	0.3289
	<i>Mean size</i>	0.0600	0.0743	0.0689	0.0677	0.0072
	<i>Std. dev. size</i>	0.1275	0.1643	0.1490	0.1469	0.0185
	<i>Max. size</i>	0.8468	1.4823	0.9581	1.0957	0.3393
	<i>Avg. meat pr. cm<sup>2</sup></i>				5.32	
	<i>Avg. size</i>				0.0680	
	<i>Avg. std. dev. size</i>				0.1322	
	<i>Avg. max. size</i>				1.2243	

## Appendix H

# Experiment Design April (Danish)

---

**Søren Blond Daugaard**  
**Forsøgsplan 16/4 07 – Wok stegning af kalkun kød**

***Formål:***

Formålet med disse forsøg er at undersøge stegnings graden af kalkun kød i tern, afhængig af temperaturen under stegning og stege tid.

***Tilberedning af råvaren:***

Kalkun brystet udskæres til stykker af ca. 10g. (ca. 2\*2\*2 cm). Der udtages 20 stykker til kontrol vejning, til vejningen bruges Tabel 1 – Vægt skema. For at undgå klæbning i starten af stegeprocessen, skal kødet skoldes. Dette gøres ved at nedsænke kødet i en gryde med kogende vand (som en frituregryde) i ca. 7 sekunder, alt kødet skal skoldes med udtagelse af ca. 600 g. der bruges til kontrol stegningen (Forsøg 2). Efter skoldning tilsættes en procent fedt til kødet og det blandes godt.

Efter udskæring og skoldning opdeles kødet i bægere med 10 stykker i hver (ca. 100g). Der skal bruges 6 kopper til hvert forsøg (ca. 600g).

Alt kødet kan klargøres før forsøgende da kødets temperatur før stegning ikke har indflydelse på stegeprocessen.

### ***Wok stegning:***

#### ***Forsøg 1***

Når temperaturen har indstillet sig, tilsættes bægerne en af gangen for hver omdrejning på sneglen. Produktet kan opsamles direkte fra samlebandet i foliebakker til nedkøling. Efter nedkøling skæres ca. halvdelen af kødet i halve. Kødet lægges herefter i markerede plast-posere (en til hele, og en til halve stykker) til VideometerLab optagelse.

#### ***Forsøgsparametre:***

<b>Stegetemperatur</b>	<b>Tid i wok</b>	<b>Forventet stegningsgrad</b>
250°C	3 min.	Tydlig rå., hvid overflade
250°C	4 min.	Stadig rå, hvid overflade
250°C	6 min.	Stegning ok, overflade bleg, saftig
275°C	4 min.	Rå, Ok overflade men bleg
275°C	6 min.	Fin stegning, saftig, overflade ok
275°C	7 min.	Fin stegning, saftig, overflade ok
275°C	9 min.	Fin stegning, saftig, overflade mørkere og sprødere.
300°C	4 min.	Tegn på rå, god overflade.
300°C	6 min.	Ok stegning, meget mørk overflade
300°C	7 min.	Ok stegning, meget mørk overflade

#### ***Forsøg 2***

For at kontrollere at skoldning ingen effekt har på stegningsgraden, laves en kontrol stegning med de 600g. kød der ikke blev skoldet. Disse steges ved 275°C 7 min., ca. halvdelen skæres igennem og prøverne ligges i to poser en til hele og en til halve stykker. Poserne skal tydeligt markeres som "Ikke skoldet" samt med temperatur og tid.

**Forsøg 3**

For at undersøge variationen i kødet ved overfyldning af wokken laves følgende forsøg.

Stegetemperatur	Tid i wok	Fyldning grad
275°C	6 min.	150 g. pr. kop * 4 kopper
300°C	6 min.	150 g. pr. kop * 4 kopper

Efter behandling skæres ca. halvdelen af prøverne over, og hver prøve pakkes i to poser, en til hele og en til halve, der er tydeligt markeret med fyldningsgrad, temperatur og tid.

**Videometer optagelse:**

Prøverne lægges i en petriskål med fire-fem kødstykker i hver. Der laves 3 petriskåle for hvert forsøg således at man får trippel bestemmelser af billede optagelsen. Ved de halve stykker er det vigtigt at stykkerne ligger med ”indersiden” opad.

Billederne gemmes i HIPS formatet efter følgende navne konvention:

**Forsøg 1**

[Temp]\[Tid]\[HEL/SNIT]\[#].hips

**Forsøg 2**

uSkoldning\[Temp]\[Tid]\[HEL/SNIT]\[#].hips

**Forsøg 3**

Fyldning\[Fyldning]\[Temp]\[Tid]\[HEL/SNIT]\[#].hips

Resten af prøverne gemmes (i køleskab til næste dag) til vandbestemmelse; evt. nedfrysning.

**Vandbestemmelse:**

Ca. 20 g. prøve homogeniseres i en miniblender. Vandbestemmelsen sker på ca. 2 g. prøve, som tørres ved 110°C i 24 timer i afvejede foliebægre – der laves trippel-bestemmelse.

**Skemaer:**

Tabel 1 – Vægt skema

Kød stykke	Vægt [g]	Kød stykke	Vægt [g]
1	[g]	12	[g]
2	[g]	13	[g]
3	[g]	14	[g]

---

4	[g]	15	[g]
5	[g]	16	[g]
6	[g]	17	[g]
7	[g]	18	[g]
8	[g]	19	[g]
9	[g]	20	[g]
10	[g]	<b>Gns.</b>	[g]
11	[g]	<b>Varians</b>	

# Appendix I      Results Moisture Contents April Experiment

---

<b>Moisture content - April Experiment</b>							
		Weight			Moisture contents		
		Cup [g]	Before [g]	After [g]	[g]	Percent	Std. Dev.
250C	<b>3min</b>				<b>Gns.</b>	<b>66.99612</b>	<b>0.0195</b>
	I	0.3165	2.3383	0.984	1.3543	66.98486	
	II	0.3159	2.338	0.9835	1.3545	66.98482	
	III	0.317	2.192	0.9354	1.2566	67.01867	
	<b>4min</b>				<b>Gns.</b>	<b>64.44339</b>	<b>0.3180</b>
	I	0.3151	2.5223	1.0945	1.4278	64.68829	
	II	0.3156	2.6349	1.1486	1.4863	64.08399	
	III	0.3152	2.231	0.9942	1.2368	64.55789	
	<b>6min</b>				<b>Gns.</b>	<b>64.93053</b>	<b>0.1523</b>
	I	0.3155	2.446	1.0658	1.3802	64.78291	
	II	0.3156	2.5734	1.1076	1.4658	64.92161	
	III	0.3153	2.3538	1.0270	1.3268	65.08707	
275C	<b>4min</b>				<b>Gns.</b>	<b>66.76658</b>	<b>0.0520</b>
	I	0.3161	2.2315	0.9538	1.2777	66.70669	
	II	0.3156	2.4573	1.0268	1.4305	66.79273	
	III	0.3152	2.4851	1.0356	1.4495	66.80031	
	<b>6min</b>				<b>Gns.</b>	<b>65.1227</b>	<b>0.2005</b>
	I	0.3159	2.4755	1.0653	1.4102	65.29913	
	II	0.3159	2.4877	1.0781	1.4096	64.90469	
	III	0.3157	2.4279	1.0515	1.3764	65.16428	
	<b>6min - 150 g fylgning</b>				<b>Gns.</b>	<b>65.26754</b>	<b>0.2971</b>
	I	0.3144	2.4686	1.0596	1.4090	65.40711	
	II	0.3142	2.3445	1.0263	1.3182	64.92637	
	III	0.3149	2.7449	1.154	1.5909	65.46914	
	<b>7min</b>				<b>Gns.</b>	<b>64.99262</b>	<b>0.0600</b>
	I	0.3162	2.6272	1.1247	1.5025	65.01514	
	II	0.3153	2.2966	1.008	1.2886	65.03811	
	III	0.3153	2.6631	1.1388	1.5243	64.92461	
	<b>7min - Uden skold</b>				<b>Gns.</b>	<b>68.1728</b>	<b>0.0547</b>
	I	0.3155	2.6478	1.058	1.5898	68.16447	
	II	0.3161	2.3316	0.9564	1.3752	68.23121	
	III	0.3153	2.4306	0.9896	1.4410	68.12272	
	<b>9min</b>				<b>Gns.</b>	<b>62.78468</b>	<b>0.0991</b>
I	0.3142	2.7338	1.2169	1.5169	62.69218		
II	0.3149	2.5165	1.1345	1.3820	62.77253		
III	0.3152	2.8452	1.2541	1.5911	62.88933		
300C	<b>4min</b>				<b>Gns.</b>	<b>66.39196</b>	<b>0.3344</b>
	I	0.3155	2.9995	1.2082	1.7913	66.73994	
	II	0.3147	2.4375	1.0349	1.4026	66.07311	
	III	0.3148	2.5858	1.0787	1.5071	66.36284	
	<b>6min</b>				<b>Gns.</b>	<b>63.70523</b>	<b>0.1020</b>
	I	0.3156	2.4352	1.0874	1.3478	63.58747	
	II	0.315	2.719	1.1861	1.5329	63.76456	
	III	0.3135	2.4561	1.0899	1.3662	63.76365	
	<b>6min - 150g fylgning</b>				<b>Gns.</b>	<b>64.22403</b>	<b>0.0760</b>

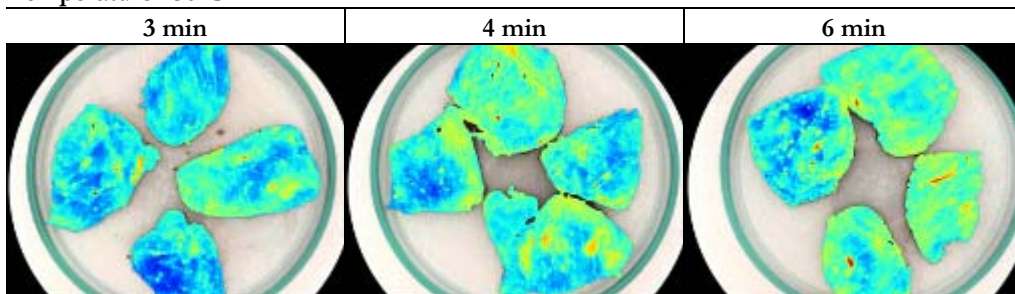
## Appendix J      Visualization results – Diced Turkey

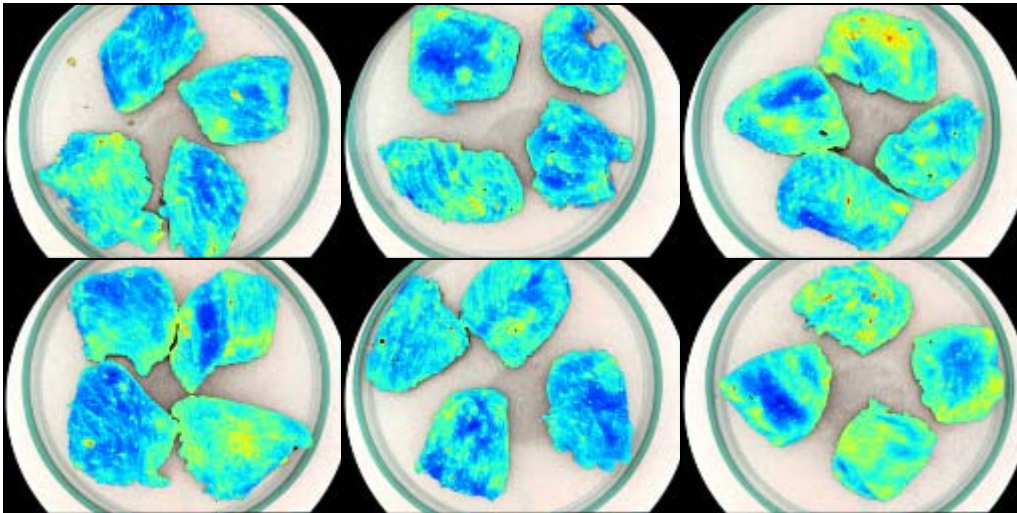
---

The appendix includes all images of the surface of the diced turkey meat, converted using the method described in section 11.6.

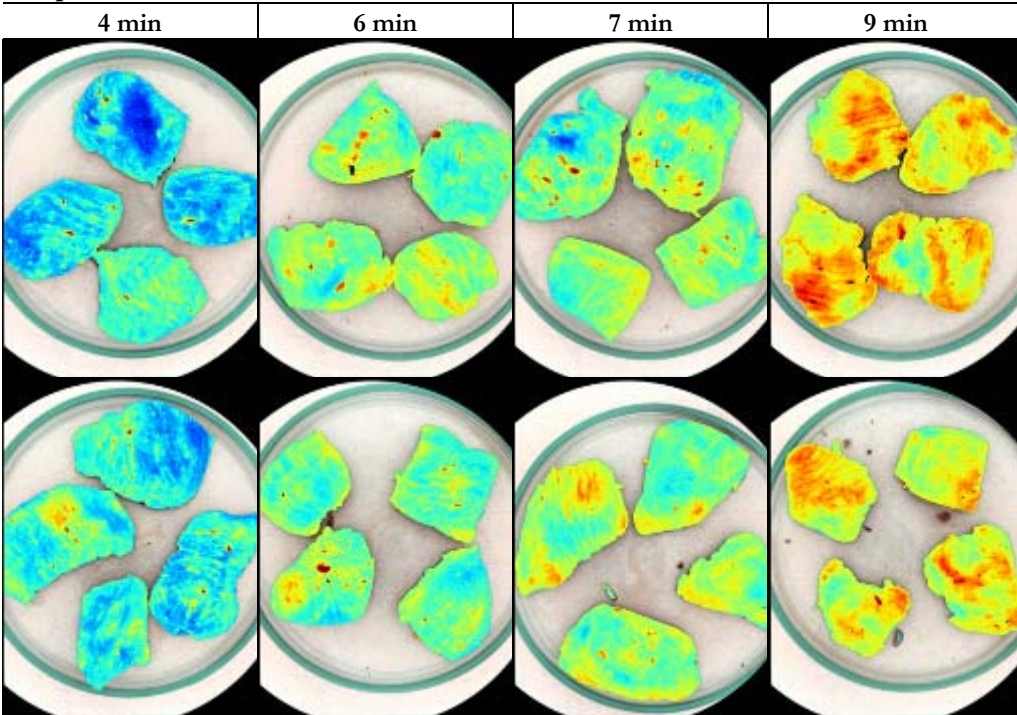
---

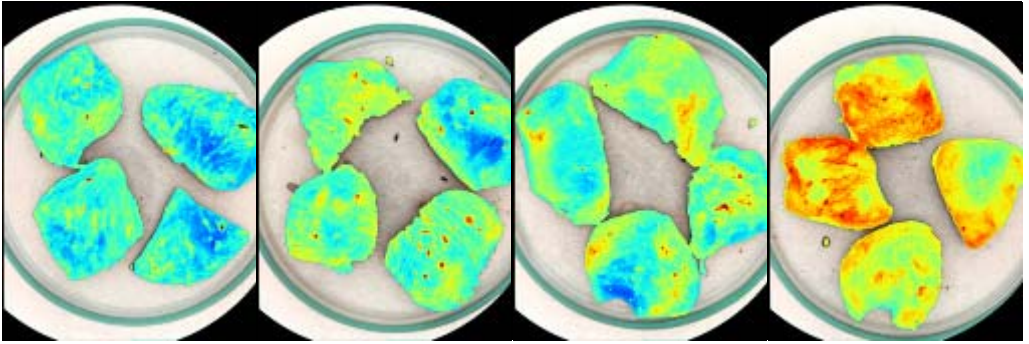
Temperature 250°C



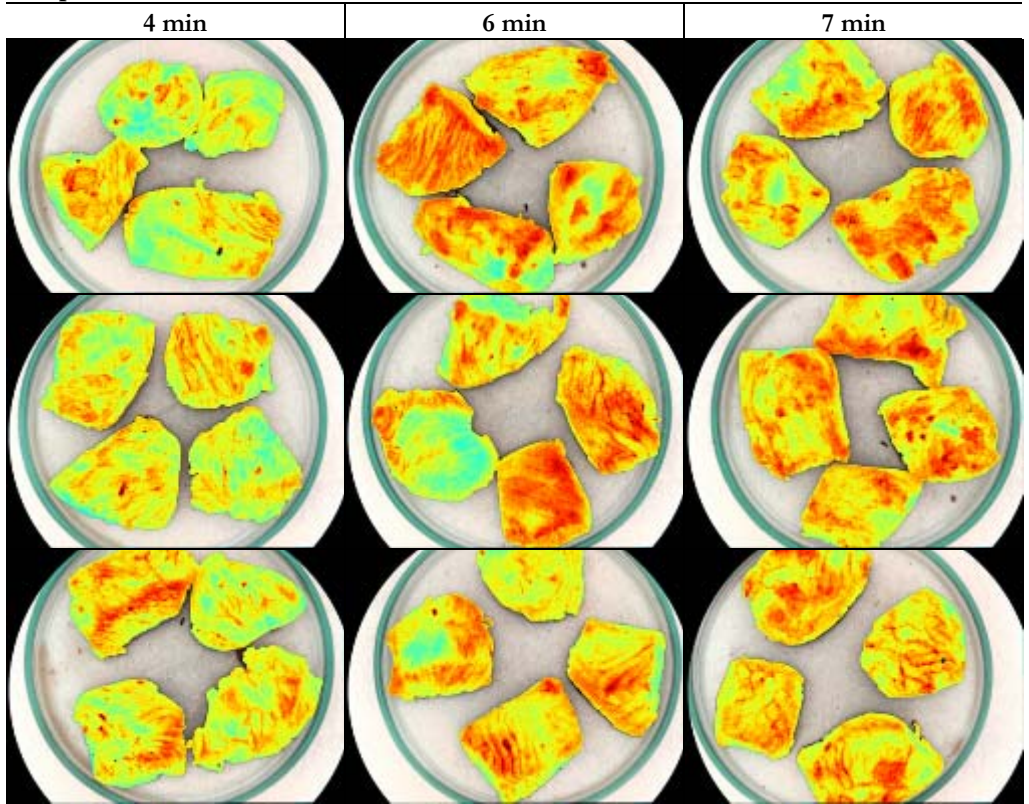


Temperature 275°C





Temperature 300°C



## Appendix K Visualization results – Sliced Diced Turkey

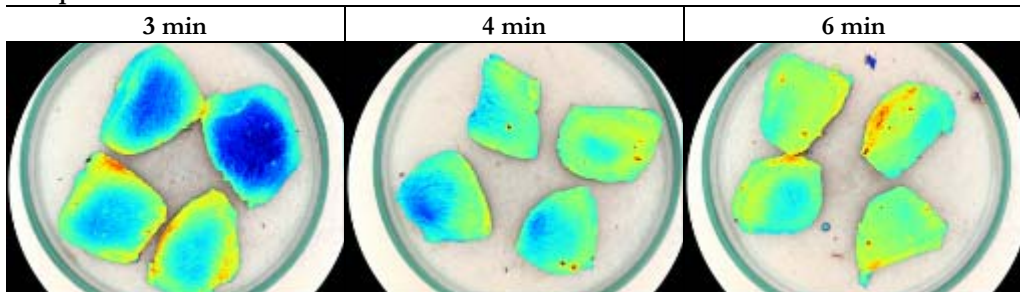
---

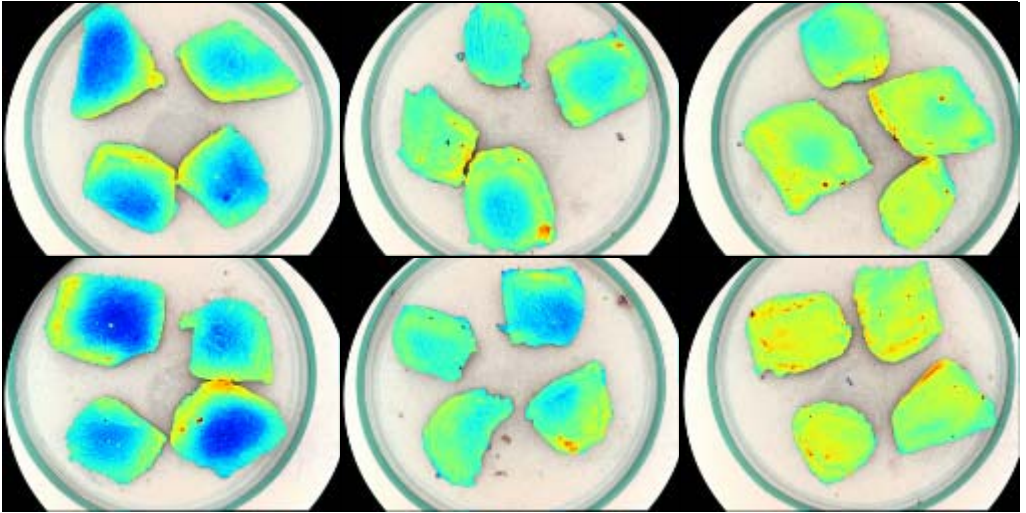
The appendix includes all images of the surface of the diced turkey meat, converted using the method described in section 12.6.

---

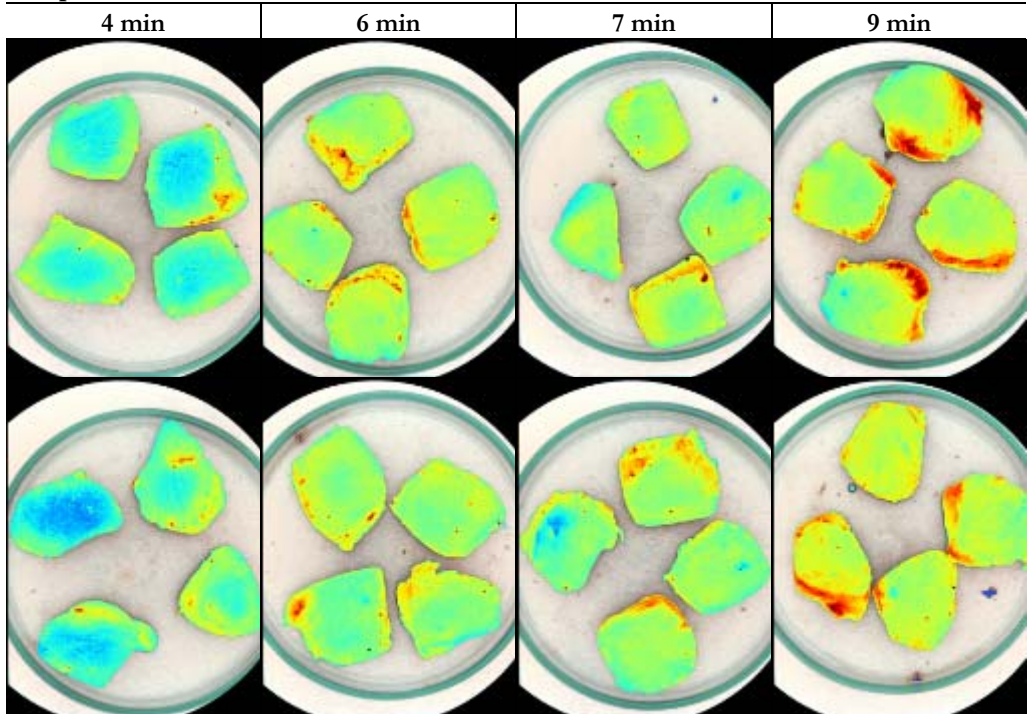
Temperature 250°C

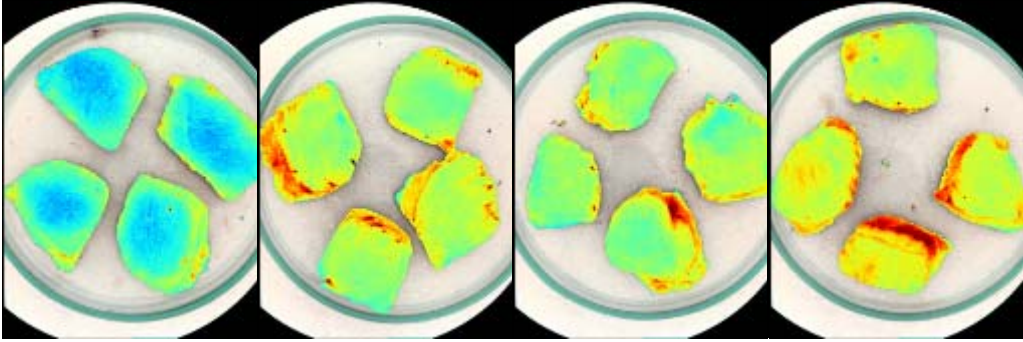
---



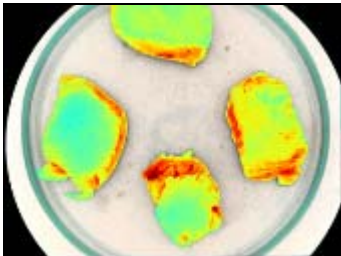
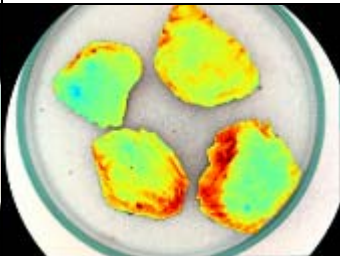
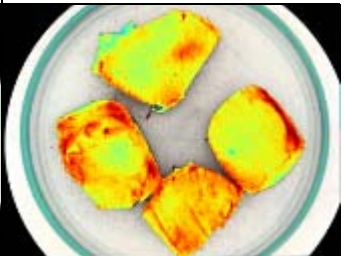
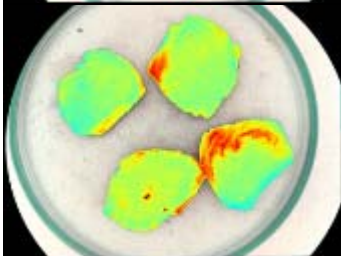
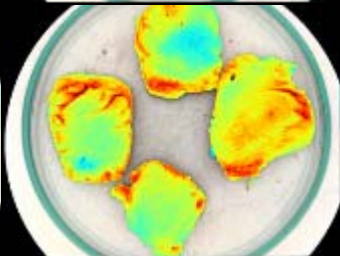
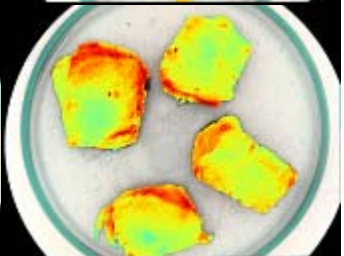
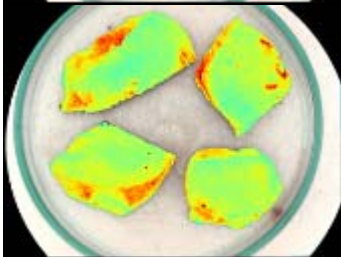
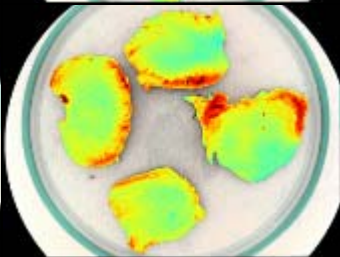


Temperature 275°C





Temperature 300°C

4 min	6 min	7 min
		
		
		

## Appendix L      Poster and presentation for 2007 Vision Day

---

The following poster “*A Method for Frying Treatment Assessment of Meat Using Multi-Spectral Vision Technology*” and accompanying slide show presentation was presented on the 2007 Industrial Vision Day, the 23<sup>rd</sup> of May at the Technical University of Denmark.



# A Method for Frying Treatment Assessment of Meat Using Multi-Spectral Vision Technology

Søren Blom Døuggaard  
 IMK, Informatics and Mathematical Modelling, Technical University of Denmark  
 Building 321, 352-8000 Ågø, Lyngby, Denmark  
 sbl@mat.dtu.dk



## 1. Motivation

Using the newly patented continuous wok developed at Biocen-tum-DTU, industry scale production of various fried meat products are easily achieved. Industry scale production of fried meat comes with the requirement of continuous monitoring of the product quality. This is achieved by using multi-spectral vision technology. Using the continuous wok to produce meat products, the potential of monitoring product quality using multi-spectral vision technology is examined. The work primarily focused on assessing the frying degree of the minced meat and turkey meat.

Using vision technology for quality testing of food production has the obvious advantage of being able to continuously monitor a production using non-destructive methods thus increasing quality and minimizing cost.

## 2. Sample preparation

Using the method for wok-frying of minced meat as described in [1] and the continuous wok described in [2], a number of samples was prepared having different characteristics such as under-, adequate and over-processed.

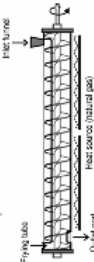


Figure 1 - Continuous Wok Concept

## 2.1. Minced Meat

The minced meat was prepared at combinations of time and temperature resulting in under- and adequately processed meat.

Temp / Time	120[s]	160[s]	200[s]	240[s]
205°C	Under	Under	Adequate	Adequate
225°C	Under	Adequate	Adequate	Adequate
250°C	Under	Adequate	Adequate	Adequate

The samples said to be under-processed is not necessarily under-processed in the sense that they cannot be served, but rather have the characteristics of being under-processed such as high levels of water and fat contents. Whereas the adequately-processed meat mainly represents the best quality meat as concluded in [4].

## 2.2. Squared Turkey Meat

The turkey meat was prepared at combinations of time and temperature resulting in under-, adequately- and over-processed meat.

Temp / Time	3 min	4 min	6 min	7 min	9 min
250°C	Under	Under	Adequate	Adequate	Over
300°C	-	-	Adequate	Over	-

## 3. Image Acquisition

Multi-spectral images were acquired using Interometrics 2, 2 multi-spectral camera for the acquisition of multi-spectral images. The camera acquires images in 18 bands (starting from ultraviolet blue to near-infrared, in a 90x1280 pixel resolution). The bands used are given in the table below.

For each combination of time and temperature 3 samples were taken out for imaging.

#	Wavelength [nm]	Color	#	Wavelength [nm]	Color
1	430	UV	10	705	Red
2	450	UV	11	705	Red
3	470	UV	12	875	NIR
4	505	Green	13	895	NIR
5	565	Green	14	915	NIR
6	590	Amber	15	930	NIR
7	630	Red	16	945	NIR
8	645	Red	17	950	NIR
9	660	Red	18	970	NIR

## 4. Pre-processing procedures

All images acquired contained objects not relevant to the assessment of meat quality such as metal detecting and pepper shiners. The pre-processing procedure is to isolate the meat in each image, removing the other objects.

## 4.1. Minced Meat

Fortunately the spectra for the meat and other objects vary significantly, enabling an dynamic threshold operation to eradicate the unwanted objects.

To further isolate the tops of the meat granules a histogram segmentation technique is used resulting in masks as the one given below.



Figure 2 - Minced meat image, 2) mask created

## 4.2. Squared Turkey Meat

To isolate the larger turkey meat pieces, the spectral properties of the turkey meat and the unwanted objects were used to make the meat stand out.

By subtracting the first band from band thirteen, the turkey meat stands out clearly leaving it up to a simple threshold to create the mask.

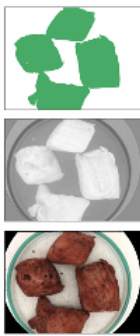


Figure 3 - a) Turkey meat, b) Band 13 - Band 1, c) Isolated Mask

## 5. Canonical Discriminant Analysis

To enhance the differences in the spectra when applying the best treatment, Canonical Discriminant Analysis (CDA) was applied with the group division given in the sample preparation.

CDA is used to find the linear combination which leads to the highest separation of the given groups  $X_1, X_2, \dots, X_k$ . Let  $W$  denote the within groups sum-of-squares and  $A$  denote the between group sum-of-squares. The problem can be described by the following eigen-value problem:

$$W^{-1} A k - \lambda k$$

The linear combination found are also called the canonical discriminant functions, for two groups one is found and for three groups two functions are found.

## 6. The Frying-Treatment Score

Applying CDA to both dataset, and deriving the histogram curves for the data applied with the first canonical discriminant function, it shows that the top point of the histogram curves are different based on the frying degree.

From this the Frying-Treatment Score (FTS) is defined as the mean value of the histogram curve.

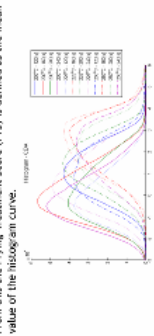


Figure 6 - Histogram over method: under-processed (OP) and adequately-processed (AP) meat. The same tendency is found with turkey meat thus enabling the same definition of the Frying-Treatment Score (FTS).

Using the FTS values and cubic regression the frying treatment can be measured using the variables: frying time (t) and temperature (T). This model is used to draw contour curves describing the frying treatment.

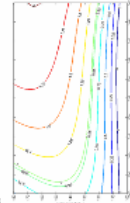


Figure 7 - Contour for Minced Meat, 0.50 out of the between under- and adequately-processed, 1.05 out of the adequately and over-processed

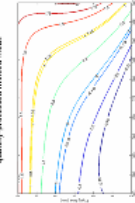


Figure 8 - Contour for Turkey Meat, 0.110 out of the between under- and adequately-processed, 1.05 out of the adequately and over-processed

## 7. Conclusion

Using data from the laboratory a method for assessment of frying treatment for two types of meat using multi-spectral imaging is developed. The frying treatment is assessed by applying a canonical discriminant function, derived from an extensive amount of test data, to the image and thereafter deriving the mean of the histogram denoted the frying-treatment score (FTS). The FTS values of the samples are used to approximate the coherence between the variables. This coherence are used to derive different temperature contours for various frying degrees.

The results obtained lead to the conclusion that an assessment of the frying treatment for meat, using non-destructive multi-spectral vision technology, is possible. Furthermore the contours increased the accuracy of the assessment by turning the contours into, to achieve higher quality Fried meat.

## References

- [1] J. Adler-Nissen, "A Method of Frying Minced Meat", Patent application, 8 September 2006.
- [2] J. Adler-Nissen, "Continuous wok frying of vegetables: Process parameters influencing scale up and product quality", Journal of Food Engineering, 30 November 2006.
- [3] Vidcometer, "VidcometerLab2 - Data sheet".
- [4] Jørgen Søl, "Continuous frying of minced beef", Bachelor project, BioCenterum, 11. June 2004.

Industrial Visionday, Wednesday May 23rd 2007

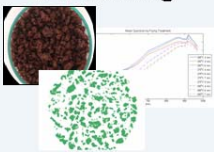
## A Method for Frying Treatment Assessment of Meat Using Multi-Spectral Vision Technology

**Søren Blond Daugaard**  
IMM, Informatics and Mathematical Modeling, Technical University of Denmark  
 Building 321, DK-2800 Kgs. Lyngby, Denmark  
 s053042@student.dtu.dk  
 Phone: +45 25 74 43 77

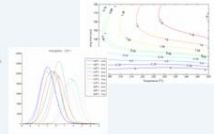
**Processing & Imaging**



**Analyzing & Modelling**



**Assessing Quality Parameters**



Industrial Visionday, Wednesday May 23rd 2007

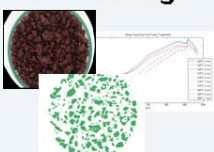
### A Method for Frying Treatment Assessment of Meat Using Multi-Spectral Vision Technology

Søren Blond Daugaard, IMM, Informatics and Mathematical Modeling, Technical University of Denmark, Building 321, DK-2800 Kgs. Lyngby, Denmark, s053042@student.dtu.dk

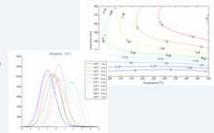
**Processing & Imaging**



**Analyzing & Modelling**



**Assessing Quality Parameters**



Minced Beef and Diced Turkey Meat

Samples created using on the continuous wok at BioCentrum

Multi-spectral image acquisition using the VideometerLab camera

18 bands spanning from 430 [nm] to 970 [nm] recorded in a 1280x1960 pixel resolution

All image are pre-processed to isolate relevant meat areas

Multi-variant statistical methods are applied to all datasets

Canonical Discriminant Analysis is found to be appropriate

The first Canonical Discriminant Function (CDF) shows large separation of frying degrees

A Frying Treatment-Score (FTS) can be defined from the first Canonical Discriminant Function

The FTS can be used to assess the meat quality with respect to the frying degree

The FTS is used to model the frying process based on frying time and temperature

## Appendix M      A Method for Frying Treatment Assessment of Minced Meat Using Multi-Spectral Imaging (Article)

---

The article was submitted for the 14<sup>th</sup> International Conference on Image Analysis and Processing (ICIAP), but rejected as it was out of scope of the conference.

The article is to be submitted to the 3<sup>rd</sup> International Symposium on Recent Advances in Food Analysis.

## A Method for Frying Treatment Assessment of Minced Meat Using Multi-Spectral Imaging

Soren Blond Daugaard<sup>1</sup>, Jens Michael Carstensen<sup>2</sup>

*IMM, Informatics and Mathematical Modeling, Technical University of Denmark  
Building 321, DK-2800 Kgs. Lyngby, Denmark  
s053042@student.dtu.dk<sup>1</sup>, jmc@imm.dtu.dk<sup>2</sup>*

### Abstract

*Using a newly developed method for frying minced meat for industry scale applications, a method for assessment of the frying treatment using multi-spectral vision technology is examined.*

*The method uses a combination of mathematical morphological segmentation and multi-spectral analysis techniques to find the optimal combination of the 18 multi-spectral bands that give a measure of the frying treatment. This measure is mapped against frying time and frying temperature to give an expression of how they should be combined to obtain an adequate frying treatment.*

*Keywords: canonical discriminant analysis, mathematical morphology, H-Domes, NIR, heat, oxidation, VideometerLab.*

### 1. Introduction

Industry scale production of fried minced meat for products as lasagna, chili con carne etc. where small discrete particles is preferred, has been very hard to produce since the meat tends to agglomerate, and exude water resulting in a boiled product [1]. A method for industry scale production of minced meat has been developed at BioCentrum, DTU. Using this method the potential of categorizing the produced meat as having under- or adequate-processed characteristics using multi-spectral vision technology is examined.

Using vision technology for quality testing of food production has the obvious advantage of being able to continuously monitor a production using non-destructive methods thus increasing quality and minimizing cost.

### 2. Dataset

#### 2.1. Sample preparation

Using the method for wok-frying minced meat as described in [1] and the continuous wok described in [2] a number of samples was prepared. The samples were prepared at the temperatures 200°C, 225°C and 250°C, and with the frying time changing from 120[s] to 240[s] in 40[s] intervals. These combinations of time and temperature provides us with samples that have characteristics of being under- and adequately-processed as well as a few samples which had the characteristics of being over-processed. These are categorized as adequately-processed in this context, since the samples mainly contains adequate-processed meat and only in smaller amounts meat granules of over-processed meat, which can be easily identified using the human eye due the it very characteristic black-brown burned color.

**Table 1. Meat samples and processing degree**

	120[s]	160[s]	200[s]	240[s]
200°C	Under	Under	Under	Under
225°C	Under	Adequate	Adequate	Adequate
250°C	Adequate	Adequate	Adequate	Adequate

The samples said to be under-processed is not necessarily under-processed in the sense that they cannot be served, but rather have the characteristics of being under-processed such as high levels of water and fat contents. Whereas the adequately-processed meat mainly represents the best quality meat as concluded in [4].

#### 2.2. Data acquisition

To acquire the multi-spectral image data the VideometerLab 2 camera was used. VideometerLab 2

is a multi-spectral camera for laboratory analysis [3], acquiring data in 18 bands spanning from Ultra-Blue to Near-Infrared in a 960x1280 pixel resolution; the wavelengths used are given in Table 2. Some of interesting wavelength are at 505[nm] and 590[nm] where met-myoglobin and oxy-myoglobin shows reflectance. Also interesting are the upper parts of the wavelengths where water, fat and protein have reflectance since the contents and structure of these are known to change during frying.

For each meat sample, 3 sub-samples were taken out for imaging. For each sub-sample a small dish was filled, and a finger was run over to remove the excess particles, leaving a somewhat homogenous surface. The resulting image-data were saved in the hips format to ease access from Matlab and the VideometerLab software, thus resulting in 2.94 GB image data.

**Table 2. VideometerLab bands**

Band #	Wavelength [nm]	Color
1	430	Ultra blue
2	450	Blue
3	470	Blue
4	505	Green
5	565	Green
6	590	Amber
7	630	Red
8	645	Red
9	660	Red
10	700	Red
11	850	NIR
12	870	NIR
13	890	NIR
14	910	NIR
15	920	NIR
16	940	NIR
17	950	NIR
18	970	NIR

### 3. Methods

To minimize the variation over the image data given, a pre-processing taking advantage of the spatial properties of the image is used to select the interesting areas. Further analysis of the relevant data is performed using canonical discriminant analysis, to find the optimal linear combination that gives a measure of the frying treatment.

#### 3.1. H-Domes

H-Domes is a morphologically segmentation technique for determining maximal structures in grey-scale images. The H-Domes method uses the original images as a mask, from the mask a marker is generated by subtracting a predefined value  $h$ . Using grayscale morphologically reconstruction the image is reconstructed from the marker. Subtracting the reconstructed image from the marker gives the h-domes of the original image. The h-domes are then structurally opened to remove any small grains present. Figure 1 shows the concepts of H-domes.

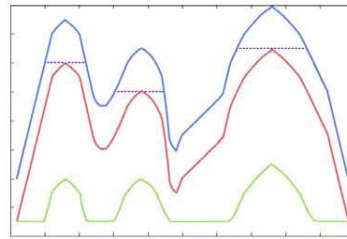


**Figure 1. H-Domes concept**

#### 3.2. Pre-processing procedure

In-order to remove unwanted objects and to reduce the immense data amount, the H-Domes segmentation technique was used. The segmentation was performed on band 10 since this band, independent of frying treatment, visually shows little variation from the fat/meat/frying product composition and thus more relates to the sample topography of the minced meat. After doing the H-Domes segmentation a threshold value was applied to the resulting image, leaving only the tops and the surrounding metal plate of the imaging device. The metal plate was removed from the mask manually. Figure 2 shows one of the sample images along with the mask generated by pre-processing.

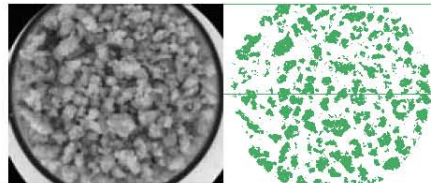


**Figure 2. Meat dish and mask**

**3.3. Canonical discriminant function**

Canonical discriminant analysis (also called Fisher’s discriminant analysis) is used to find the linear combination which leads to the greatest separation of two or more groups. Let  $x_{(1)}$  and  $x_{(2)}$  be two groups, and  $W$  denote the within group sum-of-squares matrix and  $A$  denote the between group sum-of-square matrix the problem can be written as:

$$\text{Find } k \text{ to maximize } \lambda = \frac{k'Ak}{k'Wk} \tag{1}$$

Taking the first derivative of this yields an eigen-value problem described by:

$$W^{-1}Ak = \lambda k \tag{2}$$

Having two groups this results in one optimal linear function  $k'x$  called the canonical discriminant function. The function can be used to categorize data using the decision rule:

$$k'(x - \mu) > 0 \tag{3}$$

Where  $\mu$  is the overall observation mean.

**4. Results and discussion**

**4.1. Preliminary spectrum comparison**

To determine if a basis for performing further analysis of the data exists, the spectrums of meat granules from various frying degrees is compared to find a visual coherence between the amount of frying and the spectrum.

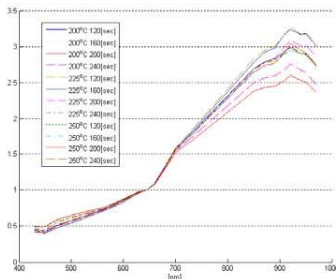


Figure 3. Meat spectrums

To clarify the coherence between the amount of frying and spectrum of the meat, the spectrums have been normalized around band 8. The normalized data shows a clear trend, as the amount of frying of the meat increases, it introduces a “break” on the curve around 950[nm], likely due to a change in fat and

water contents. Whereas the under-done meat which has a curve which is more smoothly descending in the last part of the spectrum due to higher amounts of fat and water.

Further interesting is that the spectrums do not show remarkable differences in the bands reflecting met-myoglobin and oxy-myoglobin. This is since all samples of the meat have undergone sufficient heat treatment, such that the by-far largest part of the myoglobin has been transformed into de-naturated met-myoglobin.

**4.2. Canonical discriminant analysis**

It was found that a basis for separating the various frying degrees based on their differences in spectral characteristics exists. In order to examine this further a canonical discriminant analysis (CDA) was performed on the preprocessed data, separating them into the classes as described in Table 1. The resulting grayscale images show a clear change in the insensitivity of the meat granules based on the frying time, the resulting images are shown in Figure 4 (The contrast of these images has been increased to clarify differences.).

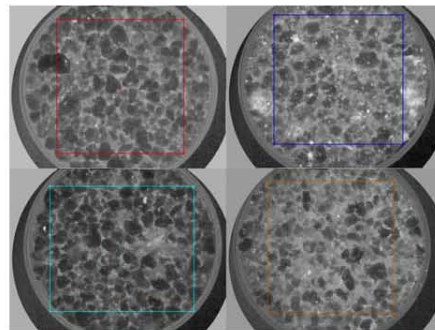


Figure 4. From upper-left – 200°C 160[sec], 250°C 160[sec], 225°C 120[sec], 225°C 160[sec]

To investigate these differences further the histogram of the marked regions of interest in the images are plotted. From the histogram it is clear that the mean value of histogram curves can prove as a tool for separating the meat into the classes needed. The mean value of the histogram is here from called the frying-treatment score (FTS).

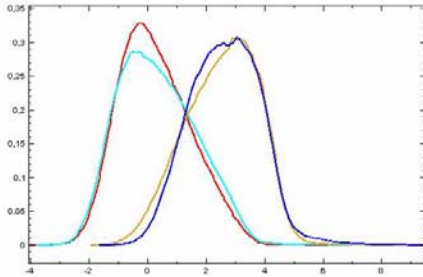


Figure 5. ROI histogram

Using the FTS scores from all samples, the cut-off score between under-processed and adequately processed meat is found to 1.1708. In-order to examine the coherence between temperatures, frying time and the FTS score, cubic regression was used to fit the results to the two variables, time and temperature. Having found the approximated polynomial, contours can be approximated to describe the various frying degrees as illustrated in Figure 6. In Figure 6 the term “score” directly applies to the frying degrees and the FTS score mentioned earlier. A frying degree above 1.17 or as named in Figure 6 the “Adequate-Processed Cut-Off Line” represents meat that are adequate processed, whereas a frying degree below naturally refers to insufficiently-processed meat.

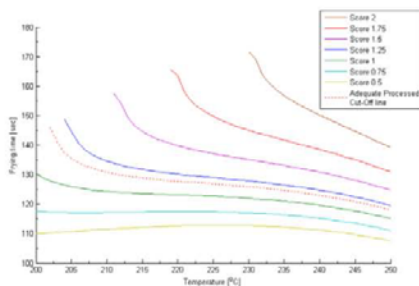


Figure 6. Contours and cut-off line

A number of contours other than the cut-off line are drawn to show how the frying degree evolves with relation to temperature and time. From the approximated cut-off line it is shown that meat processed at 120 seconds or less, regardless of temperature does not reach a frying degree which can be described as adequately processed, in addition to this the contours also shows that the same applies to temperatures of 200°C regardless of frying time.

## 5. Conclusion

Using data from the laboratory a method for assessment of frying treatment for minced meat using multi-spectral imaging is developed. The frying treatment is assessed by applying a canonical discriminant function the image, derived from an extensive amount of test data, and thereafter deriving the mean of image histogram called the frying-treatment score (FTS). The FTS values of the samples are used to approximate the coherence between the variables, this coherence are used to derive time-temperature contours for various frying degrees.

The results obtained leads to the conclusion that an assessment of the frying treatment for minced meat, using non-destructive multi-spectral vision technology, is possible. Furthermore the contours created in this article can be used as a guideline for tuning the continuous wok; to achieve higher quality fried minced meat.

## Acknowledgements

We would like to thank Professor Jens Adler-Nissen for help and guidance in the lab and for comments and suggestions on the manuscript.

## References

- [1] J. Adler-Nissen, “A Method of Frying Minced Meat”, Patent application, 8 September 2006.
- [2] J. Adler-Nissen, “Continuous wok-frying of vegetables: Process parameters influencing scale up and product quality”, *Journal of food Engineering*, 30 November 2006.
- [3] Videometer, “VideometerLab2 - Data sheet”, [www.videometer.com](http://www.videometer.com).
- [4] Jørgen Slot, “Continuous frying of minced beef”, Bachelor project, BioCentrum, 11. June 2004.
- [5] J. Lattin, J. D. Carroll, P. E. Green, “Analyzing Multivariate Data”, Brooks/Cole, 2003.
- [6] M.C. Hunt, J.C. Acton, R.C. Benedict, C.R. Calkins, D.P. Cornforth, L.E. Jeremiah, D.G. Olson, C.P. Salm, J.W. Saveil, S.D. Shivas, “Guidelines for Meat Color Evaluation”, American Meat Science Association, 1991.
- [7] Susan A. Skrydstrup, “Multi-spectral imaging for determine, onset and development of oxidation”, The Royal Veterinary and Agricultural University, Dec. 2006.

## **Appendix N      New Vision Technology for Multidimensional Quality Monitoring of Continuous Frying of Meat (Article) Draft**

---

The following article is currently in a draft form, but will be submitted to Elsevier's journal of Food Control when completed.

## New Vision Technology for Multidimensional Quality Monitoring of Continuous Frying of Meat

Søren Blond Daugaard, Jens Adler-Nissen, Jens Michael Carstensen

### 1. Introduction

Loose particles of fried minced meat or meat cut in small strips or dices are characteristic components of a wide range of popular dishes all over the world. Chili con carne, lasagne, hash, and a range of Oriental stir-fried dishes are some well-known examples. Many of these dishes are sold as ready-made meals in retail and also served in canteens and in fast food restaurants. The initial frying of the meat for these dishes is an important process step, since the frying gives the meat a desired flavour and colour which cannot be obtained by e.g. boiling, dielectric cooking or microwave cooking of the meat (Pearson & Gillett, 1996, 105-115).

Proper frying of minced and cut meat is not an easy operation to carry out in large scale, however. Deep-fat frying is the most widely used frying process for large scale productions, but deep-fat frying is not suitable for minced meat. Furthermore, deep-fat frying usually results in a high uptake of fat, depending on the product (Makinson, 1987), while the uptake of fat in plain meat after pan frying is quite low (Clausen & Ovesen, 2007). From visits paid to several industries producing ready-made meals we have observed that a common procedure is to fry minced meat batch wise by contact frying in large pans or vessels. The same applies to meat cut in small pieces; although deep-fat frying is possible in that case, contact frying in pans, on frying tables or on frying conveyor bands is preferred when a high sensory quality and low fat content is desired. In most cases the resulting quality of the fried meat is evaluated and controlled by trained operators who usually judge the progress of the process by visual inspection.

This situation that process control is effectuated through the subjective judgment of an experienced operator is not confined to frying processes; it is common in other food processes, too; for example in the baking industry and in the confectionary industry. However, the trust invested in the experienced human does not always live up to expectations when confronted with a statistical evaluation.

The visual judgment by a process operator can be supported by heuristic decision-making systems (Perrot, Ioannou, Gilles, Allais, Curt, Chevallereau, & Trystram, 2002) or substituted by different on-line measuring systems in combination with suitable control algorithms

(Haley & Mulvaney, 1995; Linko & Linko, 1998). The introduction of near-infrared reflection (NIR) spectroscopy for on-line measurements of water and fat was a break-through for such systems in the food industry (Hoyer, 1997; Schwarze, 1997), and NIR presents further potentials in quality monitoring and classification, such as distinguishing between fresh fish meat from frozen and thawed fish meat (Uddin, Okazaki, Turza, Yomiko, Tanaka, & Fukuda, 2005).

As a measuring principle NIR does not directly match visual quality monitoring, and different vision technologies are therefore also being investigated for on-line quality measurements, for example of fresh poultry, apples and other fruits (Chen, Chao, & Kim, 2002; Abdullah, Mohamad-Saleh, Fathinul-Syahir, & Mohd-Azemi, 2006). It is, however, still difficult with most vision technologies to reliably distinguish small differences in the appearance of food products, because the visual variation is typically within shades of red, shades of green, shades of yellow etc. A way to solve this and to combine the strengths of vision technology and spectroscopy is to use multispectral imaging in the visual and shortwave infrared range of wavelengths. This opens up for the possibility of using vision technology for surface chemistry mapping in addition to visual appearance mapping (Carstensen, Hansen, Lassen & Hansen 2006).

#### *1.1. The Videometer vision technology*

A new principle in vision technology researched and developed by the Technical University of Denmark and commercialised by [www.videometer.com](http://www.videometer.com) is based on the following principle (Carstensen & Folm-Hansen 2000): The product is placed under an Ulbricht sphere (a sphere painted white on the inside giving diffuse backscattering of the light) and illuminated with light-emitting diodes (LEDs) placed along the rim of the sphere. The LEDs cast light at specified wavelengths up into the sphere to be reflected as scattered light onto the product. This gives a uniform and reproducible illumination over a large area (50 cm<sup>2</sup>). The technology has proven its ability in difficult sorting tasks such as classification of molds, grading of skin lesions in psoriasis and quality assessment of sand (Hansen 2005; Maletti 2003; Gomez 2005; Hansen 2003, Clemmensen & Ersboll 2006). All these tasks normally require a visual assessment by trained personnel, and the results suggest that the Videometer technology may match the visual judgment of the experienced food process operator rather closely.

The present work aims at investigating the potential use of this new vision technology for quality monitoring of food processes in cases where small differences in colour, size and

shape are crucial. The frying of meat in a new continuous frying process to be described below presents an excellent case, since it is possible to make reproducible and not exaggerated variations in the sensory (taste) quality by changing the process conditions. The applied changes in process conditions also results in small, but noticeable changes in the visual appearance of the fried meat; thus simulating typical conditions facing the process operator.

### *1.2. The continuous frying process*

Heat treatment of meat causes the meat fibres and the collagen to contract, resulting in a considerable exuding of meat juice (Tornberg, 2005). If the juice is not evaporated instantaneously in the frying process, the well-known result is boiling rather than frying. A new continuous stir-frying process originally developed for stir-frying of vegetables (Adler-Nissen, 2002; Adler-Nissen, 2007) has proved to be able to give instantaneous evaporation of the exuded juice when small pieces of meat (5-20 g) are fried. The processed pieces have an attractive fried, brown crust and a juicy texture. Even minced meat can be fried, provided the meat is frozen and disintegrated in the frozen state by chopping immediately before frying (Adler-Nissen, 2006).

In the process frying takes place in a horizontal, thick-walled open frying tube equipped with a stainless steel conveyor helix with scrapers (Adler-Nissen, 2002). The heat source is natural gas. Measured portions of ingredients and oil are added at one end of the frying tube at each turning of the helix. The product is transported and tossed simultaneously by the helix and leaves the machine through a port at the other end.

The main process parameters in the continuous frying process are: temperature of the frying tube (this is regulated by feed back signals to the gas flow valves from temperature sensors in the tube wall) and process time (this is regulated by the rotational speed of the helix). Combinations of temperature and time define a process window within which the resulting product quality is optimal; outside these limits the product is either under-processed or over-processed.

## **2. Materials and methods**

### *2.1 Samples*

#### *2.1.1 Minced beef*

Frozen minced beef with 15-18% fat was purchased through a wholesale supplier, Inco

Danmark a.m.b.a, Copenhagen. The blocks of meat (2 kg) were stored at  $-30^{\circ}\text{C}$ . The blocks were crushed with a hammer in coarse pieces. Portions of about 1 kg were chopped at a time in an industrial bowel meat chopper (Kilia 57cm diameter) at the lowest speed step to prevent heating. The chopping was continued (about 2-3 min.) until the frozen meat was disintegrated with no large lumps left.

800 g of the disintegrated, frozen meat was fed in consecutive portions of 100g to the continuous frying machine described above at pre-selected temperatures and frying times. Samples were prepared at the temperatures  $200^{\circ}\text{C}$ ,  $225^{\circ}\text{C}$  and  $250^{\circ}\text{C}$ ; the frying time varied from 120[s] to 240[s] in 40[s] intervals. These combinations of frying time and temperature provided samples which had characteristics of being under and adequately processed, as sensory evaluated by the expert judgment of one of the authors (Adler-Nissen) together with a skilled meat technician. "Under processed" meant that the characteristic fried flavour was not adequately developed. The texture was firm but not dry in all cases. Visually, there was a slight tendency of the samples fried at  $200^{\circ}\text{C}$  being more grey and less brown than the other samples. None of the samples were over processed, which would have meant that they would have been dry and/or dark in colour.

The process conditions were chosen so to produce samples that would be acceptable or nearly acceptable. It is of no interest to include test conditions which would result in samples being clearly of unsatisfactory quality, since in this paper the vision technology is tested for its ability to distinguish *small* differences.

The division of meat into processing degree is given in Table 1.

Time / Temp	120[s]	160[s]	200[s]	240[s]
$200^{\circ}\text{C}$	Under	Under	Under	Under
$225^{\circ}\text{C}$	Under	Adequate	Adequate	Adequate
$250^{\circ}\text{C}$	Adequate	Adequate	Adequate	Adequate

To examine the effect of partial thawing of the minced beef before frying, samples were left to thaw for various specified times at room temperature. Excessive thawing may result in agglutination of the minced meat during the frying, giving rise to coarse lumps of fried meat (Adler-Nissen 2006). Three sample sets were thawed for 30 minutes, 1 hour and 30 minutes and 2 hours and 30 minutes, respectively. Each sample set included four samples processed at  $225^{\circ}\text{C}$  and  $250^{\circ}\text{C}$  and with frying times of 160[s] and 240[s]. To create a physical measure of agglutination all samples were run through a strainer with 1.1 cm square holes immediately

after frying. Strainer loss in percent of the total sample weight has previously been used as a measure of the degree of agglutination (Slot 2004).

### 2.1.2 Diced turkey meat

Turkey breasts were cut in dices of approximately 10[g]. 20 samples were taken out for control measurements, showing an average of 9.48[g] with a standard deviation of 2.09[g]; this is a typical and acceptable variation in size. Before frying the pieces were scalded for 7 seconds in a large pot of boiling water. The scalding coagulates the soluble meat proteins in the surface layer and prevents the meat from sticking to the walls of the cooking vessel – or in this case to the helix and frying tube of the continuous frying machine. Samples were prepared at 250°C, 275°C and 300°C, and frying times varying from 180[s] to 540[s]. These combinations of frying time and temperature provided samples characterised as being under-, adequately- and over-processed. The assessment was made by expert judgment as in the case of the minced meat. The categorization of samples into the processing classes is given in Table 2.

**Table 2 - Processing times and categorization of diced turkey**

Time / Temp	180[s]	240[s]	360[s]	420[s]	540[s]
250°C	Under	Under	Adequate	-	-
275°C	-	Under	Adequate	Adequate	Over
300°C	-	Adequate	Over	Over	-

### 2.1.3 Determination of water content

20g of meat was homogenized in a small Braun household blender with rotating knife. Three samples of approximately 2g were transferred to disposable aluminium pans taken and dried at 105°C for 24 hours in an oven. Water content was calculated from the difference between the weights of sample before and after drying.

### 2.2 Visible and near-infrared sample acquisition

For all combinations of times and temperature three sub-samples were taken out for imaging. The samples were placed in plastic petri dishes (10cm diameter). The multi-spectral images were acquired using the VideometerLab 2 camera, a multi-spectral camera for laboratory analysis acquiring images in 18 bands spanning from Ultra Blue (UB) to Near-Infrared (NIR) in a 960x1280 pixel resolution. The wavelengths used are given in Table 3.

**Table 3 - VideometerLab 2 Wavelengths**

#	Wavelength	Color	#	Wavelength	Color	#	Wavelength	Color
1	430 [nm]	UB	7	630 [nm]	Red	13	890 [nm]	NIR

#	Wavelength	Color	#	Wavelength	Color	#	Wavelength	Color
2	450 [nm]	Blue	8	645 [nm]	Red	14	910 [nm]	NIR
3	470 [nm]	Blue	9	660 [nm]	Red	15	920 [nm]	NIR
4	505 [nm]	Green	10	700 [nm]	Red	16	940 [nm]	NIR
5	565 [nm]	Green	11	850 [nm]	NIR	17	950 [nm]	NIR
6	590 [nm]	Amber	12	870 [nm]	NIR	18	970 [nm]	NIR

### 2.3 Image pre-processing

Due to the method of image acquisition, the images include objects not relevant to the analysis such as the metal sheeting from the camera, and the petri dish used to contain the meat. To ensure that these objects will not interfere with the analysis, a pre-processing step is included to remove the objects and isolate the meat pieces. The pre-processing is done by maximizing the contrast between the sample material and the other objects; thus enabling a threshold operation. Maximizing the contrast is done either by choosing a single appropriate wavelength or, in the case of the diced turkey, by subtracting two wavelengths and using the spectral differences as the image for further processing. The diced turkey meat samples needed no further pre-processing, while additional pre-processing was needed for the minced meat samples. For the images used for frying treatment assessment, this processing aimed at isolating the top part of the meat particles to minimise the spectral differences in the image from the rounded surface of the meat granules. The procedure used for this purpose is an h-domes segmentation technique (Vincent, 1993). This technique extracts the peaks of the image higher than a certain value  $h$ ; by carefully choosing the  $h$ -value it is possible to isolate the top of the meat granules.

The process of isolating meat objects for the agglutination assessment differs from the above procedure by focusing on the ability to separate and measure the *size* of the meat particles. In order to ensure a common separation of meat granules regardless of frying treatment, it is crucial to perform this separation using a spectral band which is practically independent of frying treatment. Examining spectra and profiles over the images revealed that band 11 was the best fit for the purpose. This band was used to perform an h-domes segmentation followed by a threshold, and various filter operations leaving a binary image clearly outlining the meat granules existing in the image.

### 2.4 Data analysis

#### 2.4.1 Canonical Discriminant Analysis

To enhance the differences in the spectra introduced by increased heat treatment, a

Canonical Discriminant Analysis (CDA) was applied. CDA is multivariate statistical method, used to find the largest possible separation of two or more classes based on a number of independent variables.

In this case the class division is based on the categorization of being under, adequately or over processed as given in section 2.1. The independent variables are the images of the 18 spectral bands acquired by the VideometerLab camera. From the groups of data, CDA finds the optimal linear combination of the 18 variables which create the largest possible separation, called the Canonical Discriminant Functions (CDF).

#### 2.4.3 Spatial Measurements

A connected component analysis using 4-connectivity is applied to the images; this analysis finds the number of non-connected components in the images, here representing a meat granule, and their corresponding pixel size. Knowing that ratio between pixel and millimetres in the VideometerLab camera are  $0.077 \left[ \frac{mm}{pixel} \right]$  conversion of the pixel size found in the image is straightforward. For each image the maximum granule size found and the mean granule size is extracted. These measures are chosen since they will be consistent regardless of the image size and amount of meat in the image.

### 3. Results and discussion

#### 3.1 Assessing Frying Treatment

The measured water contents are given in Table 4 and Table 5. The data show the expected tendency of decreasing water contents based on increased heat treatment.

Table 4 - Water contents - Minced Beef

Water contents	120 [sec]		160 [sec]		200 [sec]		240 [sec]	
	Mean	Std.	Mean	Std.	Mean	Std.	Mean	Std.
200°C	54.3%	0.217	52.7%	0.440	51.5%	0.212	51.5%	0.425
225°C	53.4%	0.150	54.0%	0.136	52.5%	0.411	52.5%	0.240
250°C	51.0%	0.185	46.3%	0.206	49.7%	0.273	49.7%	0.226

Table 5 - Water contents - Diced Turkey

Water contents	3 min		4 min		6 min		7 min		9 min	
	Mean	Std.								
250°C	66.9%	0.019	64.4%	0.318	64.9%	0.152	-	-	-	-
275°C	-	-	66.8%	0.052	65.1%	0.200	65.0%	0.060	62.8%	0.099
300°C	-	-	66.4%	0.334	63.7%	0.102	67.0%	0.310	-	-

Canonical Discriminant Analyses were performed on the data from minced beef and diced turkey separately. For the minced meat data set this results in a single Canonical Discriminant Function (CDF), which separates the under-processed meat from the adequately-processed. It is found that after applying the CDF to the 18 band images, the resulting greyscale images shows a displacement of the image histograms curve based on the frying degree. This is illustrated in Figure 1a where histogram curves are shown for selected interesting frying degrees. From this observation the Frying-Treatment Score (FTS) can be defined as the mean value of the image transformed with the derived CDF. Having defined the FTS it can be observed from Figure 1a, that a low FTS score relates to a low degree of heat treatment, whereas higher FTS scores relate to increased heat treatment. In this context it is further interesting to find the exact cut-off point between the meat categorized as under-processed and adequately-processed. This cut-off point is found to be a FTS of 0.95 for minced meat.

Because the diced turkey meat is divided into three classes, the CDA results in two discriminant functions. Examining the functions shows that the first CDF has the same property as for the minced beef; namely a displacement, based the on frying degree, of the image histograms after applying it. This enables a similar definition of the Frying-Treatment Score (FTS) as for minced meat, again it is observed that higher heat treatment leads to a higher FTS value. Following this observation the cut-off points are determined and found to be -0.118 for dividing the under-processed from adequately-processed meat and 1.05 for dividing adequately-processed from over-processed meat.

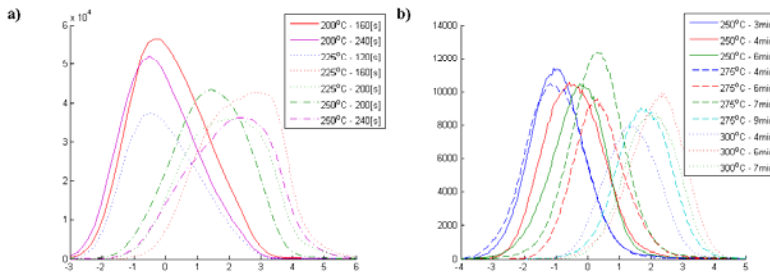


Figure 1 - Histogram curves for transformed images, a) minced beef, b) diced turkey

3.2 Modelling Frying-Treatment

The prior section shows how it is possible to measure the frying degree of minced meat

and diced turkey meat using multi-spectral images. Using the data derived from all images acquired it is possible to create a model of the frying process using least square regression. To select an appropriate model, several models (polynomials of different degrees) have been validated using 3-fold cross validation. The cross validation is performed by trying to determine the frying time in seconds based on the temperature and FTS value, the root mean square error is recorded along with the  $R^2$  given in Table 6.

**Table 6 – Cross Validation Results**

Polynomial degree	Minced Beef			Diced Turkey		
	RMSE <sub>Test</sub>	RMSE <sub>Train</sub>	R <sup>2</sup>	RMSE <sub>Test</sub>	RMSE <sub>Train</sub>	R <sup>2</sup>
1	44.78	44.71	0.00	70.75	70.09	0.55
2	39.58	32.97	0.43	47.75	41.92	0.83
3	30.97	26.85	0.62	44.62	34.22	0.88
4	120.34	24.10	0.67	48.34	32.97	0.89
5	122.51	23.57	0.68	186.45	25.16	0.92

From the results of the cross validation it can be observed that the optimal model for both minced beef and diced turkey meat is cubic. Using these models contours are created for the frying time based on FTS and temperature; the contour lines are shown in Figure 2a and Figure 2b.

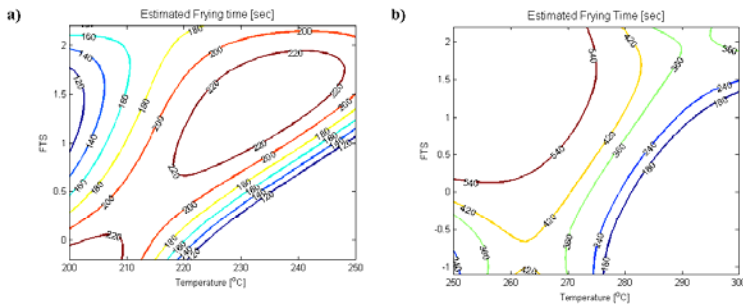


**Figure 2 - Frying time contour lines, a) minced beef, b) diced turkey**

Using the optimal polynomial degree found in the cross validation, models of the frying-treatment score based on frying -time and -temperature are created. The models created account for 65% and 98% percent of the variation respectively. The model derived for minced beef implies the lower boundary of the process window for adequately-processed minced beef is a temperature around 205°C, and a frying time higher than 130[sec] at any higher temperature.

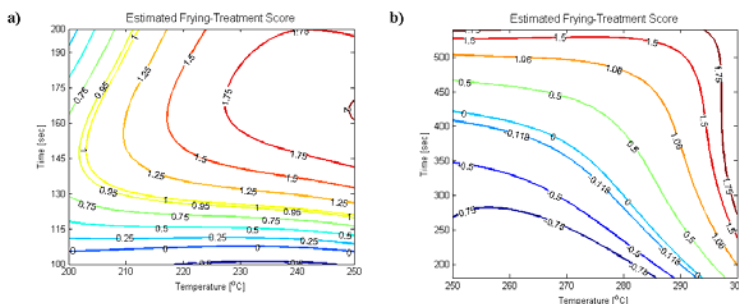


**Figure 3 - Frying-treatment score contour lines, a) minced beef, b) diced turkey**  
 For diced turkey the model shows a process window for obtaining adequately cooked meat that is widest time-wise around 280°C where it is possible to get adequately cooked meat at a large variety of times. Furthermore it does not suggest a minimum temperature within the range plotted, but rather narrows down the possible frying times at both low and high frying temperatures. It is obvious that at temperatures outside the tested range, the samples would be either inadequately fried on the surface or burnt on the surface.

3.3 Assessing agglutination

For each image the mean granule size and maximum granule size was recorded, all values are summarized in Table 7. The mean granule size and maximum granule size is shown as the average over the three images analysed for each combination of times and temperature.

**Table 7 - Agglutination measurements physical and spatial**

Thaw time	Frying time [s]	Temperature [°C]	Strainer Loss [%]	Avg. mean granule size [cm <sup>2</sup> ]	Std. mean granule size	Avg. max. granule size [cm <sup>2</sup> ]	Std. max. granule size	
30m	160	200	1.04	0.055	0.006	0.562	0.115	
		240	0	0.048	0.005	0.496	0.057	
	240	160	225	0.21	0.056	0.005	0.638	0.129
		240	225	0.94	0.064	0.002	0.690	0.088
1h 30m	160	200	1.88	0.054	0.005	0.808	0.340	
		240	200	5.09	0.060	0.004	0.948	0.402
	240	160	225	2.40	0.056	0.005	0.849	0.356
		240	225	2.22	0.063	0.007	0.714	0.036
2h 30m	160	200	6.59	0.064	0.009	1.066	0.230	
		240	200	6.65	0.072	0.006	1.834	0.842
	240	160	225	6.01	0.0686	0.008	0.902	0.184
		240	225	6.63	0.068	0.007	1.096	0.339

The strainer losses are very small (<1%) for the first sample set and increases to 6-7% after 2½ hours thawing. This is not a large proportion, but it is enough to consider the products in this sample set less satisfactory in quality. As expected the spatial measurements for mean granule size and maximum granule increase as the strainer loss increase. The deviations of the spatial measurements are in an acceptable scale, supporting these measures as a mean to assess agglutination. To further stress this, a model is created to predict strainer loss from the two spatial properties, this will show how much of the strainer loss variance can be accounted for by using these measurements. The results of a 3-fold cross validation to select the appropriate regression model are shown in Table 8.

**Table 8 - Cross Validation Results**

Polynomial degree	Spatial Properties		
	RMSE <sub>Test</sub>	RMSE <sub>Train</sub>	R <sup>2</sup>
1	2.04	1.80	0.48
2	1.83	1.67	0.56
3	106.47	1.50	0.58
4	687.11	1.09	0.72

The cross validation shows that a quadratic polynomial is the optimal model for modelling the strainer loss based on the spatial properties. 56% of the variance is accounted for by the spatial properties this is an acceptable results considering the deviations of the spatial measures. This also shows in contour lines which captures the expected tendencies.

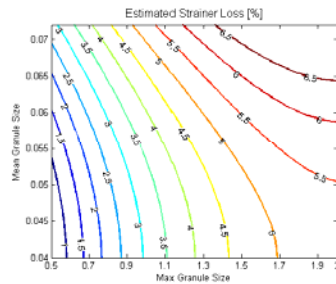


**Figure 4 - Estimated strainer loss**

The strainer loss model based on the spatial properties, show the expected tendency that higher mean and maximum size found results in higher strainer loss. Also it shows that the maximum size seems to have a somewhat higher influence than the mean size.

#### 4. Conclusion

The results obtained leads to the conclusion that multi-spectral vision technology can be used as a tool to assess quality parameters for a meat frying process, such as frying treatment assessment and assessment of agglutination for minced beef. Two widely different meat products, minced beef and diced turkey, have been tested. Using image analysis techniques and statistics a method for deriving a Frying-Treatment Score (FTS) is developed and may be used in process control. The FTS value range outlines a set of times and temperatures which constitute a process “window” for optimal processing. This process window, of course, depends on the nature of the product.

The vision technology cannot substitute the initial of experimentation with a new product and process, and this is also not the intention. Once, however, the optimal process conditions have been established, the vision technology can reliably test, if the product fulfils the criteria of being optimally processed or not.

The article also presents a method for detecting even small degrees of agglutination in fried minced meat, using a single NIR wavelength practically independent of heat treatment. This measurement is important, since agglutination is a severe fault.

The imaging has so far been an off-line technique, requiring the taking of samples. However, the method can reasonably easily be adapted to on-line measurements by placing the imaging sphere above the conveyor band transporting the fried meat products from the frying machine. The mechanical solution of this is fairly trivial and is not investigated in the present paper.

#### References

- Abdullah, M.Z., Mohamad-Saleh, J., Fathinul-Syahir, A.S. & Mohd-Azemi, B.M.N. (2006). Discrimination and classification of fresh-cut starfruits (*Averrhoa carambola* L.) using automated machine vision system. *Journal of Food Engineering*, 76, 506-523.
- Adler-Nissen, J., (2002). The Continuous Wok – A New Unit Operation in Industrial Food Processes. *Journal of Food Process Engineering*, 25, 435-453.
- Adler-Nissen, J. (2006). A method of frying minced meat. *International patent application* WO 2006/092139 A1.
- Adler-Nissen, J. (2007). Continuous wok-frying of vegetables, Process parameters influencing scale up and product quality. *J Journal of Food Engineering*, in print.
- Carstensen, J. M., Hansen, M. E., Lassen, N. K., Hansen, P. W. (2006). Creating surface chemistry maps using multispectral vision technology, 9th MICCAI - Workshop on Biophotonics Imaging for Diagnostics and Treatment.
- Carstensen, J. M., Folm-Hansen, J. (2000). An apparatus and a method of recording an image of an object,

- Patent EP1051660.
- Chen, Y-R, Chao, K. & Kim, M.S. (2002). Machine vision technology for agricultural applications. *Computers and Electronics in Agriculture*, 36, 173-191.
- Clausen, I. & Ovessen, L. (2005). Changes in fat content of pork and beef after pan-frying under different conditions. *Journal of Food Composition and Analysis*, 18, 201-201.
- Clemmensen, L.H and Ersbøll, B.K. (2006). Multi-spectral recordings and analysis of psoriasis lesions. Proceedings of the MICCAI (Medical Image Computing and Computer Aided Intervention) 2006 workshop on biophotonics imaging, Copenhagen, 6 Oct. 2006. ISBN 87-643-0116-8, pp. 15-18.
- Gomez, D. D. (2005). Development of an image based system to objectively score the severity of psoriasis (Ph.D. thesis), Informatics and Mathematical Modelling, Technical University of Denmark.
- Haley, T.A & Mulvaney, S.J. (1995). Advanced process control techniques for the food industry. *Trends in Food Science & Technology*, 6, 103-110.
- Hansen, M. E. (2003). "Color-Based Image Retrieval from High-Similarity Image Databases", 13th Scandinavian Conference on Image Analysis (SCIA), Gothenburg, Sweden.
- Hansen, M. E. (2005). Indexing and Analysis of Fungal Phenotypes Using Morphology and Spectrometry (Ph.D. thesis), Informatics and Mathematical Modelling, Technical University of Denmark.
- Hoyer, H. (1997). NIR on-line analysis in the food industry. *Process Control and Quality* 4, 143-152.
- Linko, S. & Linko, P. 1998. Developments in monitoring and control of food processes, *Transactions of the Institute of Chemical Engineering*, 76, Part C, 127-137.
- Mackinson, J.H., Greenfield, H., Womng, M.L., Wills, R.B.H. (1987). *Journal of Food Composition and Analysis*, 1, 93-101.
- Maletti, G. M. 2003. Novelty detection in dermatological images (Ph.D. thesis), Informatics and Mathematical Modelling, Technical University of Denmark.
- Pearson, A.M., Gillett, T.A. (1996). *Processed Meats*, 3<sup>rd</sup> ed., Chapman & Hall, New York.
- Perrot, N., Ioannou, I., Gilles, M., Allais, I., Curt, C., Chevallereau, V. & Trystram, G. 2002. Experiences about operator/technology cooperation using a fuzzy symbolic approach to decision support system design in food processes. *Proceedings of the IEEE International Conference on Systems, Man and Cybernetics*, 1, 94-99.
- Schwarze, H. (1997). Continuous fat analysis in the meat industry, *Process Control and Quality*, 4, 133-138.
- Slot, J. (2004). Continuous Frying of minced beef (Bachelor Thesis), BioCentrum, Technical University of Denmark.
- Tornberg, E. (2005). Effect of Heat on meat proteins – implications on structure and quality of meat products, *Meat Science*, 70, 493-508.
- Uddin, M., Okazaki, E., Turza, S., Yomiko, Y., Tanaka, M. & Fukuda, Y. (2005). Non-destructive visible/NIR spectroscopy for differentiation of fresh and frozen-thawed fish, *Journal of Food Science*, 70, C506-C510.
- Vincent, L. (1993). Morphological Grayscale Reconstruction in Image Analysis: Applications and Efficient Algorithms, *IEEE Transactions on Image Processing*, Vol. 2, Issue 3, 176-201

## Appendix O DVD

This DVD contains subsets of the datasets used throughout the project, all publications created and the Matlab source files created.

To use the DVD simply insert it into your DVD drive, if the DVD does not automatically start open the index.htm file on the DVD.

